05-12_di lena:Layout 1 4-09-2013 18:28 Pagina 5

A climatic perspective of the presence of the european grapevine moth (*Lobesia Botrana* Den. and Schiff) in the Abruzzo region, Italy

Bruno Di Lena[1], Domenico Giuliani[1], Antonio Zinni[1], Angelo Mazzocchetti[1], Emanuele Eccel[2]*

Abstract: *The European grapevine moth (*Lobesia botrana*) is probably the most important parasite of grapevine in Italy. This work analyzes the impact of climatic change on the development of* L. botrana *in the main viticultural areas of Abruzzo, central Italy. The calibration and validation of a mechanistic model based on Allen's thermal sums, allowed to estimate an advance of the flight dates of the carpophagous generations in two viticultural areas of the Adriatic coastal foothill. The higher bioclimatic availability, calculated by thermal sums from 1st January to 30th September, in the period 1951-2011, suggests that in some areas a third carpophagous generation could develop. In fact, a positive trend was calculated for thermal sums in the period. However, the harmfulness of this lepidopter might be decreased by the concomitant advance of the vintage times.*
Keywords: *grapevine, Lobesia Botrana, European grapevine moth, Abruzzo, climate.*

Riassunto: *La tignoletta dell'uva (*Lobesia botrana*) è probabilmente il parassita dell'uva di maggior rilievo in Italia. Il lavoro analizza l'impatto dei cambiamenti climatici sullo sviluppo della* L. botrana *nelle principali aree vitate della regione Abruzzo. La calibrazione e validazione di un modello meccanicistico basato sulle sommatorie termiche secondo Allen hanno permesso di stimare un anticipo delle date di inizio voli delle generazioni carpofaghe in due aree vitate della collina litoranea adriatica. La maggiore disponibilità bioclimatica, valutata con il calcolo delle sommatorie termiche dal 1° gennaio al 30 settembre, nel periodo 1951-2011, suggerisce che le condizioni possano essere adatte allo svolgimento, in alcune zone, di una terza generazione carpofaga. Il trend delle sommatorie termiche è risultato infatti positivo nel periodo. Tuttavia la dannosità del lepidottero potrebbe essere limitata dal concomitante anticipo della data di vendemmia.*
Parole chiave: *vite,* Lobesia Botrana*, tignoletta dell'uva, Abruzzo, clima.*

INTRODUCTION

The increase in thermal values that affected Europe in the late 80s was ascertained by Werner *et al.* (2000), who considered this phenomenon as a result of a sharp phase shift of the North Atlantic Circulation Index (NAO). In that period, the latter assumed positive values, enhancing the zonal, westerly circulation, consequently decreasing the incidence of the other circulation patterns. The study of time series of the ISPRA report (2009), based on the temperature anomalies of the period 1961-2008, with respect to the averages of 1961-1990, highlights, for Italy, a moderate decrease of mean temperature from 1961 to 1981, and an eventual quick increase until 2008, with an overall increase of about 1°C.

As stated by Laštůvka (2009), despite a general concern for the negative effects of climate change on the autoecology of many single species – and on biodiversity in general – in the case of insect pests, the effects of temperature increase on the presence and spread of such noxious species are thought to increase the threat to host plants (Estay *et al*., 2009; Quarles, 2007; Porter *et al.*, 1991). Future climatic warming will affect temperate annual and multivoltine species in different ways and to differing degrees, according to the species (Bale *et al*., 2002; Pollard and Yates, 1993). In general, a temperature increase associated to climate change could determine the increase of the number of generations of multivoltine insects and a widening of the distributional areas of some species (Tobin *et al*., 2008; Gutierrez *et al*., 2008a). Stange and Ayres (2010) report that insects could benefit from a temperature increase above all at middle and high latitudes thanks to a quicker development rate and to the increase of survival during cold seasons. Gutierrez *et al.* (2008b) modelled the effects of climate change on phytofagous insects, highlighting a multitrophic complexity, which involves also the antagonists.

* Corresponding author: Bruno Di Lena (dilenab@arssa-mail.it)
[1] Regione Abruzzo – Direzione Politiche Agricole e di Sviluppo Rurale – Pescara (I)
[2] Sustainable Agro-ecosystems and Bioresources Department, IASMA Research and Innovation Centre, Fondazione Edmund Mach, San Michele all'Adige, Trento (I)
Received 28 June 2012, accepted 6 December 2012.

05-12_di lena:Layout 1 30-08-2013 11:59 Pagina 6

For European viticulture, it is particularly interesting to study the interactions with the biological cycle of the European grapevine moth (*Lobesia botrana*, Den. and Schiff., Lepidoptera: Tortricidae). For the period 1984-2006 Martin-Vertedor *et al.* (2010) found, in six vine-growing areas in south-westerly Spain, an increase of 0.9°C and 3°C in the annual and spring mean temperature, respectively. Such increase would have induced an advance of more than 12 days in *L. botrana*'s phenology, and its voltinism to produce one fourth generation in 2006. In 2003 the lepidopter completed four generations in northern Italy, thanks to exceptionally high temperatures (Marchesini and Dalla Montà, 2004). Moleas (2006) stated that in southern Italy a fourth flight usually takes place, peaking in late September. Damages brought by this third carpophagous generation (the first one in the season is antophagous) are fortunately limited by both zoophagous fauna and by the incipient diapause (Anfora *et al.*, 2007).

In general, mathematical models that predict the phenological development of insect populations can be successfully adopted in defence strategies (Cossu *et al.*, 1999). Caffarra *et al.* (2012) analyzed several climate change scenarios, assessing the effects on grapevine and on the development of *L. botrana* in a viticultural area in the eastern Italian Alps. The authors found that possible greater impacts, due to the higher probability of the development of one more generation, would be reduced by the expected advance of vintage timing.

In this work, the thermal sums, relative to the beginning of flight, were first calculated by a mechanistic model based on the method of Allen (1976), for the carpophagous generations of *L. botrana*, in the viticultural areas of Scerni and S. Maria Imbaro (Abruzzo region, central Italy). Aiming to the assessment of the impact of the temperature increase in the period 1951-2011, thermal sums were eventually used to look for time trends in the simulated dates of the beginning of flight for the sites of Scerni and Lanciano. The analysis also concerned the trend of the bioclimatic availability (1st January – 30th September) as well as thermal sums in the same period, both in the abovementioned area, and in others, of viticultural interest in the Abruzzo region.

MATERIALS AND METHODS

The climate in Abruzzo goes from full Mediterranean on the Adriatic coast, to more continental conditions in the inner areas, where geography – and hence climatic conditions – are influenced by the presence of the highest Apennine mountain massif of Gran Sasso. Mean annual temperatures are around 15°C on the coast, decreasing with altitude toward the hill or mountain areas, where annual thermal range remarkably increases, bringing cold winters and hot summers. Precipitation is conditioned by mountain effects; the annual cumulative values in the viticultural areas range between about 700 and 1000 mm. Most of the annual rainfall usually falls in autumn-winter, while important rain events are much less frequent in the summer.

Daily temperatures from the weather stations of Scerni and S.Maria Imbaro (Abruzzo, central Italy) were used to simulate, by a mechanistic model, the time of the onset (beginning of flight) of the adult carpophagous generations of *L. botrana* in the decade 2002-2011. Two vineyards were chosen near the abovementioned stations, to optimize the match between the field and the station-site meteorological conditions. The monitoring of adults was carried out by feromone traps fed with the attractive synthesis molecule *trans*7,*cis*9 dodecadienil acetate; the date of beginning of flight was set in correspondence of a sudden rise of catches. The series of catches in the same decade (2002 – 2011), referring to the second and third generations, were taken from the database of the Decision Support System *"Agroambiente. Abruzzo"* (Mazzocchetti and Zinni, 2005). For each year, the monitoring of adults was carried out weekly from early April to mid September.

For the modelling of *L. botrana*'s flights, the algorithm proposed by Arca *et al.* (1993) was used. It cumulates degree days according to Allen's model (Allen, 1976) starting from 1st January. This model evaluates the contribution of temperature according to one lower and one upper thermal thresholds of development. The thresholds of minimum and maximum daily temperature, according to previous works (Del Rio *et al.*, 1989), were set to, respectively, 8°C and 28°C. The calculation of the thermal sum contribution of one day is based on the simulation of the daily cycle of temperature according to a sine wave, where the minima of the two consecutive nights can be different. Allen describes six different cases, from those with no effect on the thermal sum (when temperatures are below the lower threshold at any time of the day), to those where the temperature crosses one or both thresholds, giving rise to different rates of thermal sum. The maximum effect is attained when the temperature does not drop below the lower threshold upper threshold; the contribution of "heating degree days" (HDD in the original paper) of such a case is $HDD = \frac{1}{2}(T_u - T_l)$, where T_u and T_l are the upper and lower temperature thresholds, respectively.

05-12_di lena:Layout 1 30-08-2013 11:59 Pagina 7

The model calibration was carried out by calculating the thermal sums of the model for the five odd years of the period 2002 – 2011. The averages of the thermal sums over the calibration years, corresponding to the measured dates of beginning of each flight, were used to assess the onset of the carpophagous generations at the different sites in each year. The model validation was done for the corresponding five even years of the same period. The observed dates were compared to the simulated ones by the following indices:

- Root mean square error (RMSE; minimum and optimal value = 0; maximum = +∞; Fox, 1981):

$$RMSE = \sqrt{\frac{\sum_{i=1}^{n}(S_i - O_i)^2}{n}} \quad \text{where:} \quad \begin{array}{l} S_i = \text{estimated dates} \\ O_i = \text{observed dates} \\ n = \text{number of data pairs} \end{array} \qquad (1)$$

- Modelling Efficiency (EF; minimum = -∞; maximum and optimal value = 1; Nash and Sutcliffe, 1970)

$$EF = 1 - \frac{\sum_{i=1}^{n}(S_i - O_i)^2}{\sum_{i=1}^{n}(O_i - \overline{O})^2} \quad \text{dove:} \quad \begin{array}{l} S_i = \text{estimated dates} \\ O_i = \text{observed dates} \\ n = \text{number of data pairs} \\ \overline{O} = \text{mean of observed dates} \end{array} \qquad (2)$$

The averages of thermal sums calculated in the decade 2002-2011 were used to simulate the dates of the beginning of flight of the carpophagous generations in the period 1951-2011 at the following sites, where the long-term series of temperature were available by the Hydrographic Service of the Abruzzo Region:

– Scerni

– Lanciano (weather station of Santa Maria Imbaro).

The trend analysis for the times of beginning of flight was done by a t-test. The null hypothesis (H_0) is the absence of trends in the sample, and is tested against the alternative hypothesis of presence of either a growing or a decreasing trend. In the present work, *p-values* < 0.05 were considered as significant.

Having verified the reliability of the phenological model of *L. botrana*, the occurrences of the forth flight (third carpophagous generation) was assessed according to the calculated thermal sums. So, for the period 1951-2011, the t test was applied to assess the trends of thermal sums, calculated from 1st January to 30th September, in the stations of Scerni and S. Maria Imbaro, but also for other viticultural areas of the region: Nereto, Pescara, Chieti, Penne, and Sulmona (Fig.1).

RESULTS AND DISCUSSION

Tab. 1 shows negligible differences in the average date of beginning of flight between Scerni and S. Maria Imbaro - Lanciano; the dates fall at about half of the second week of June for the first carpophagous generation, and at the end of July for the second.

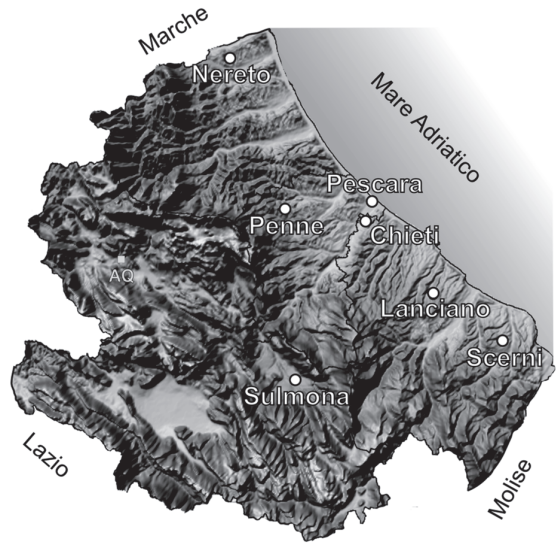

Site	Altitude m a.s.l.	Distance from the sea (km)
Scerni	220	12.0
Lanciano	283	10.0
Chieti	320	12.5
Pescara	5	0.1
Nereto	163	9.5
Penne	438	19.4
Sulmona	420	51.0

Fig. 1 - The sites for analysis of the thermal sums accumulated in the period 1st January – 30th September

Fig. 1 - Localizzazione delle sette stazioni utilizzate per le analisi delle sommatorie termiche accumulate nel periodo 1 gennaio- 30 settembre.

05-12_di lena:Layout 1 30-08-2013 11:59 Pagina 8

Site	Second flight		Third flight	
	Date	GDD	Date	GDD
Scerni	June 11	826 (± 58.4)	July 31	1630 (± 89.34)
Santa Maria Imbaro	June 12	773 (± 41.71)	July 30	1504 (± 70.26)

Tab. 1 - Mean dates of the beginning of flight of the two carpophagous generations of *L. botrana* and of the corresponding thermal sums (GDD – Growing Degree Days). Standard error is reported in brackets
Tab. 1 - Date medie dell'inizio dei voli delle due generazioni carpofaghe di L. botrana *e delle sommatorie termiche (GDD – gradi giorno). L'errore standard è indicato tra parentesi.*

Site	Second flight			Third flight		
	RMSE (d)	Obs. σ^2 (d^2)	EF (-)	RMSE (d)	Obs. σ^2 (d^2)	EF (-)
Scerni	3.63	23.3	0.29	6.09	33.7	-0.38
Lanc. / S. M. Imb.	1.73	15.2	0.75	5.42	52.3	0.29

Tab. 2 - Model validation: accuracy indices of the thermal-sum model for the estimate of time of beginning of flights of the carpophagous generations of *L. botrana*.
Tab. 2 - Validazione del modello: indici di accuratezza del modello basato sulle sommatorie termiche per la stima dell'inizio dei voli delle generazioni carpofaghe di L. botrana.

The mechanistic model, based on the Allen method, yielded the best results in the estimate of the date of beginning of flight of the first carpophagous generation, for which moderate RMSE values were recorded, and a positive Efficiency Index (EF). As regards to the second carpophagous generation, the best results were obtained at S. Maria Imbaro - Lanciano, where the lowest RMSE was found, with a positive value for EF. If the two generations are considered together, the model performed best at S. Maria Imbaro - Lanciano than at Scerni (Tab. 2). However, at this site RMSE is very close to the value at S. Maria Imbaro - Lanciano (difference is less than 1 day); hence, the low performance in EF at Scerni is in large parte due to a much lower value of the denominator in eq. (2) than at S. Maria Imbaro – Lanciano, thanks to the more regular series recorded at the former site (see Tab. 2, where variances of the observations are reported). The observations at Scerni, less scattered with respect to the average, would make the mean a more precise estimator at this site. However, a lower value of EF does not really invalidate the model because the RMSE remains similar to that of S. Maria Imbaro – Lanciano, so, for the sake of homogeneity, we preferred to apply the model to both sites.
The series of the deviations from the means of the estimated dates at Lanciano and Scerni highlights a remarkable trend of advance in the last 15 years of the period (Fig. 2). The trend analysis shows the advance of the estimated flight dates for both sites and both flights (Tab. 3). Nevertheless, the phenomenon, which can be ascribed to the thermal increase, assumes a significant extent only at Scerni, where the advance in 60 years is about 9 days for the first carpophagous generation, and about 11 for the second.
The analysis of the thermal sums accumulated in the period 1st January – 30th September was aimed at simulating the bioclimatic availability for the parasite cycles during the development season, in order to assess possible trends. Thermal sums show a minor variability among the different sites, even despite the elevation ranges between 5 and 438 m a.s.l., with distances from the coast from 0 to 51 km

Site	2nd flight β (d yr^{-1})	3rd flight β (d yr^{-1})
Scerni	-0.16 **	-0.21 ***
Lanc. / S. M. Imb.	-0.05 ns	-0.11 ns

Tab. 3 - Results of the t-test applied to the estimated dates of beginning of flight of the carpophagous generations in the period 1951-2011 (ns = non-significant, * p0.05, ** p0.01, *** p0.001). β = advance rate (dyr^{-1}).
*Tab. 3 - Risultati del test t sui trend applicato alle date stimate di inizio volo delle generazioni carpofaghe nel periodo 1951-2011 (ns = non significativo, * p0.05, ** p0.01, *** p0.001). β = tasso di anticipo (dyr^{-1}).*

05-12_di lena:Layout 1 30-08-2013 11:59 Pagina 9

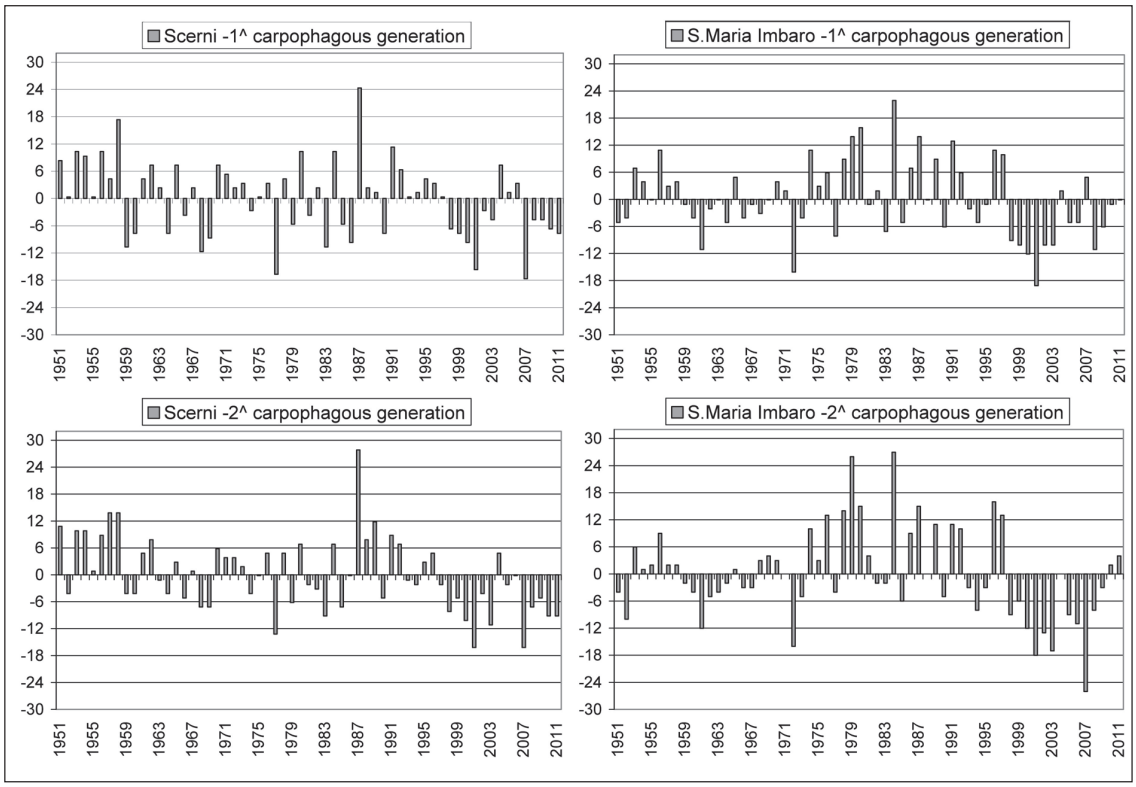

Fig. 2 - Trend of the deviations from the means of the estimated initial flight dates for the carpophagous generations of *L. botrana* at the sites of Scerni (left panel) and Lanciano (right panel) during the period 1951-2011.
Fig. 2 - Andamento degli scarti dalle medie delle date stimate di inizio volo per le generazioni carpofaghe di L. botrana nelle località di Scerni (grafici di sinistra) e Lanciano (grafici di destra) durante l'arco temporale 1951-2011.

(Fig.1). The lowest mean value of the thermal sum was estimated for Sulmona (2230 GDD), the highest for Chieti (2243 GDD) (Fig. 3).
At five sites out of seven, the last decade showed the highest thermal sums, with an often remarkable increase from the previous period (Fig. 4). The t test, applied to the time series of the thermal sums of 1951-2011, shows inhomogeneous changes among relatively close sites. At Scerni, Pescara and Sulmona a significant increase of thermal sums was recorded, whereas at Lanciano and Chieti the increase was lower, statistically non-significant. The stations of Penne and Nereto, unlike the others, recorded a decrease, even if statistically non-significant (Tab. 4).
An increased thermal availability in some Abruzzo viticultural areas could enhance the development of a third carpophagous generation of *L. botrana*, which could be responsible for damages to the ripening berries. However, the potential impacts of the additional generation could be limited by the advance of harvest, which is a fact in Abruzzo, as

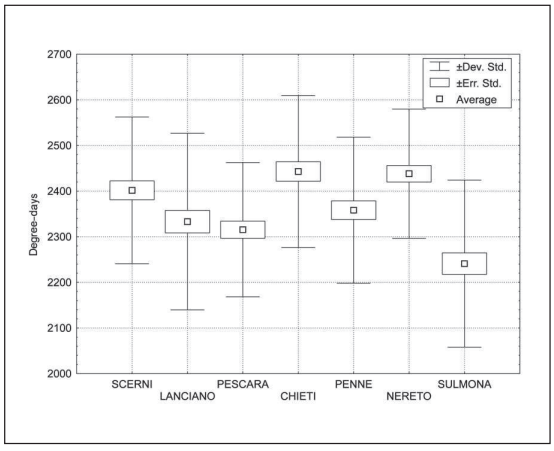

Fig. 3 - Descriptive statistics of thermal sums accumulated in the period 1st January – 30th September during the period 1951-2011 for the sites of Scerni, Lanciano Sulmona, Penne, Pescara, Chieti, and Nereto.
Fig. 3 - Statistiche descrittive delle sommatorie termiche accumulate nel periodo 1° gennaio – 30 settembre durante l'arco temporale 1951-2011 per le località di Scerni, Lanciano Sulmona, Penne, Pescara, Chieti e Neret.

05-12_di lena:Layout 1 30-08-2013 11:59 Pagina 10

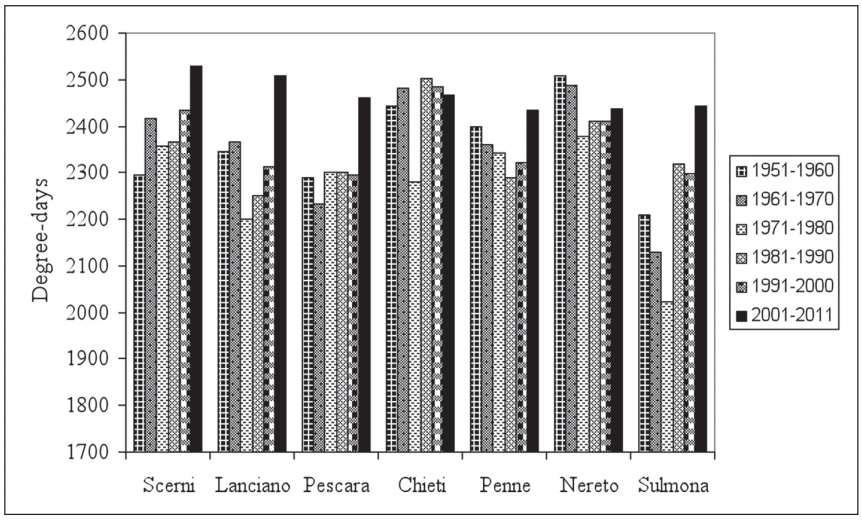

Fig. 4 - Trend of the thermal sums accumulated in the period 1st January – 30th September during the period 1951-2011 at Scerni, Lanciano, Sulmona, Penne, Pescara, Chieti, and Nereto.
Fig. 4 - Andamento delle sommatorie termiche calcolate nel periodo 1° gennaio - 30 settembre durante l'arco temporale 1951-2011 per le località di Scerni, Lanciano, Sulmona, Penne, Pescara, Chieti e Nereto.

Site	trend (d yr^{-1})
Scerni	3.57 **
Lanciano	1.74 ns
Pescara	2.80 *
Chieti	1.29 ns
Penne	-0.01 ns
Nereto	-1.87 ns
Sulmona	4.95 ***

Tab. 4 - Results of the t-test on time trends, applied to the thermal sums accumulated in the period 1st January – 30th September for the sites of Scerni and Lanciano (1951-2011) and for Sulmona, Penne, Pescara, Chieti, and Nereto (1951-2009) (ns = non-significant, * p0.05, ** p0.01, *** p0.001).
*Tab. 4 - Risultati del test t sui trend temporali, applicato alle sommatorie termiche accumulate nel periodo 1° gennaio – 30 settembre durante l'arco temporale 1951-2011 per le località di Scerni e Lanciano e 1951-2009 per quelle di Sulmona, Penne, Pescara, Chieti e Nereto (ns = non significativo, * p0.05, ** p0.01, *** p0.001).*

well as in other European regions (Jones *et al.*, 2005b; Caffarra *et al.*, 2012), and which is expected to advance further, due to a persistent climate heating (Caffarra and Eccel, 2011). As an example, Fig. 5 shows the trend of advance of the beginning of vintage, cv *Montepulciano*, in the area of Scerni, in the period 1974-2011 (data from the register of conveyance of the local cooperative winery).

CONCLUSIONS

The study highlighted the effectiveness of the mechanistic model based on Allen's method for the estimation of the onset time of adult generations of *Lobesia botrana*, above all for the first carpophagous one. The simulation of the following generation, when estimated independently from the first one by a unique thermal sum beginning from 1st January, obviously suffers from a larger inaccuracy, arising from a sum of errors over a longer period. However, errors are still acceptable for the proposed model to be adopted for simulations.

Climatic change is having different effects at sites even quite close one another, but a general trend of advance can be detected for the date of beginning of flight of the two carpophagous generations, at least at one site (Scerni) among the two that were analyzed. A general trend of increase of the thermal sums from 1st January to 30th September is evident in most of the viticultural sites analyzed in Abruzzo; this can give rise, in particularly warm years, to one more generation. When assessing the true impacts of this possibility, it should be considered that also vintage time is going to experience a parallel advance, thanks to the expected, continuous increase in temperature. In order to simulate at best the matching between grapevine and insect timing, a phenological model should be adopted. An aspect that was not considered in this work is the effective consistence of the populations of *L. botrana* in vineyards. Indeed, the effect of climate change on the abundance of herbivorous insects remains unknown until parallel investigations on the responses of their natural enemies is carried out (Davis *et al.*, 1998). And the interactions between plant, pest, and the environment is generally complex, and impossible to trace back to general, simple rules (Grulke, 2011; Gregory *et al.*, 2009).

05-12_di lena:Layout 1 30-08-2013 11:59 Pagina 11

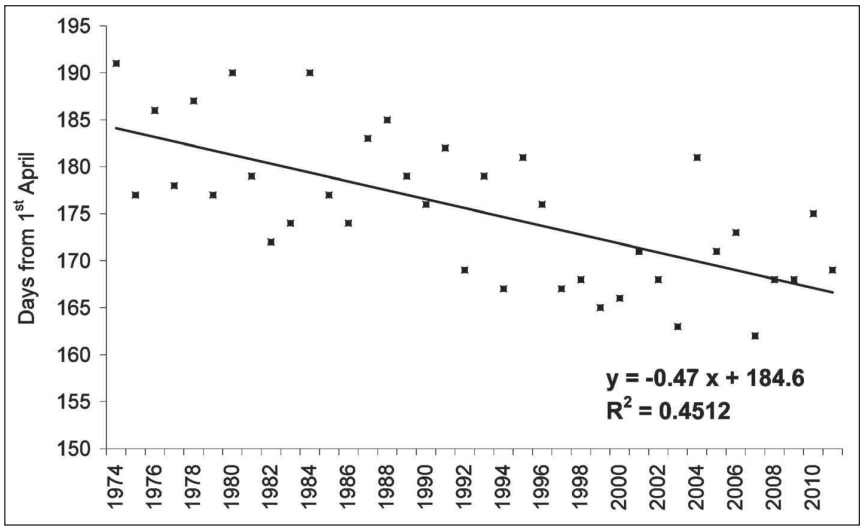

Fig. 5 - Trend of the beginning of vintage, cv *Montepulciano*, at Scerni, in the period 1974-2011.
Fig. 5 - Andamento delle date di inizio vendemmia per la cv. Montepulciano nell'areale di Scerni durante l'arco-temporale 1974-2011.

REFERENCES

Allen, J. C., 1976. A modified sine wave method for calculating degree-days. Env. Entomol. 5:388-396.

Anfora, G., Angeli, G., Baldessari, M., Ioriatti, C., Marchesini, E., Mattedi, L., Menke, F., Mescalchin, E., Schmidt, S., Tasin, M., Varner, M. Le tignole della vite. Serie "Agricoltura Integrata". Istituto Agrario di San Michele all'Adige, S. Michele, 86 pp.

Arca, B., Cossu, A., Delrio, G., Locci, L., 1993. Individuazione dei gradi giorno relativi allo sviluppo della Lobesia botrana (Den. et Schiff.) in Sardegna. Atti Convegno Nazionale "Protezione delle colture: osservazioni, previsioni, decisioni", Pescara 7-8 Ottobre, 325-334.

Bale, J., Masters, G., Hodkinson, I., Awmack, C., Bezemer, T., Brown, V., Butterfield, J., Buse A., Coulson, J., Farrar, J., et al., 2002. Herbivory in global climate change research: direct effects of rising temperature on insect herbivores. Glob. Chang. Biol. 8:1-16.

Caffarra, A., Eccel, E., 2011. Projecting the impacts of climate change on the phenology of grapevine in a mountain area. Australian Journal of Grape and Wine Research, 17(1):52-61. DOI: 10.1111/j.1755-0238.2010.00118.x.

Caffarra, A., Rinaldi, M., Eccel, E., Rossi, V., and Pertot, I., 2012. Modelling the impact of climate change on the interaction between grapevine and its pests and pathogens: European grapevine moth and powdery mildew. Agriculture Ecosystems & Environment, 148:89-101.

Davis, A.J., Jenkinson, L.S., Lawton, J.H., Shorrocks, B., and Wood, S., 1998. Making mistakes when predicting shifts in species range in response to global warming. Nature, 39:783-786.

Estay, S.A., Lima, M., Labra, F.A., 2009. Predicting insect pest status under climate change scenarios: combining experimental data and population dynamics modelling. J. Appl. Entomol. 133: 491-499.

Fox, D.G., 1981. Judging air quality model performance: a summary of the AMS workshop on disperision model performance. Bull. Am. Meteorol. Soc. 62:599-609.

Gregory, P.J., Johnson, S.N., Newton, A.C., and Ingram, J.S.I., 2009. Integrating pests and pathogens into the climate change/food security debate. J. Exp. Bot. 60: 2827-2838.

Grulke, N.E., 2011. The nexus of host and pathogen phenology: understanding the disease triangle with climate change. New. Phytol. 189:8-11.

Gutierrez, A.P., Daane, K.M., Ponti, L., Walton, V.M., Ellis, C.K., 2008a. Prospective evaluation of the biological control of vine mealybug: retuge effects and climate. Journal of Applied Ecology, 45:524-536.

Gutierrez, A.P., Ponti, L., d'Oultremont, T., Ellis, C.K., 2008b. Climate change effects on poikilotherm tritrophic interactions. Climatic Change 87 (Suppl. 1):S167-S192.

ISPRA, 2009. Gli indicatori del clima in Italia nel 2008. Rapporto Serie Stato dell'Ambiente n. 12/2009. Anno IV.

Jones, G.V., Duchene, E., Tomasi, D., Yuste, J., Braslavka, O., Schultzh, H., Martinez, C., Boso, S., Langellier, F., Perruchot, C., Guimberteau, G.,

05-12_di lena:Layout 1 30-08-2013 11:59 Pagina 12

2005. Change in Euopean winegrape phenology and relationship with climate. GESCO, August 2005, Geisenheim (D): proceedings, Vol.1:55-62.

Laštu˚vka, Z., 2009. Climate change and its possible influence on the occurrence and importance of insect pests. Plant Protection Science, 45, spec. iss. S53-S62.

Marchesini, E., Dalla Montà, L., 2004. Nel Veneto quattro generazioni di di tignoletta della vite. L'informatore Agrario, 18:75-78.

Martin Vertedor, D.M., Ferrero- García, J.J., Torres-Vila, L.M., 2010. Global warming affects phenology and voltinism of Lobesia botrana in Spain. Agricultural and Forest Entomology, 12(2): 169-176.

Mazzocchetti, A., Zinni, A., 2005. "Agroambiente. Abruzzo: sistema integrato per la gestione dei dati biologici e per l'applicazione di modellistica previsionale" – AIAM congress 2005 "Agrometeorologia, risorse naturali e sistemi di gestione del territorio" - Book of Extended abstract - Rivista Italiana di Agrometeorologia, 9(1):14-15.

Moleas, T., 2006. Le tignole della vite: notizie bioetologiche e tecniche di controllo. Atti convegno La difesa della vite dagli artropodi dannosi – Università degli studi di Palermo. Marsala 10-11/10/2005- 85-96.

Nash, J.E., Sutcliffe, J.V., 1970. River flow forecasting through conceptual models, Part I - A discussion of principles. J. Hydrol. 10:282-290.

Pollard, E., and Yates, T.J., 1993. Monitoring Butterfies for Ecology and Conservation. Chapman & Hall, London, 292 pp.

Porter, J.H., Parry, M.L., Carter, T.R., 1991. The potential effects of climatic change on agricultural insect pest. Agric. For. Meteorol. 57:221-240.

Quarles, W., 2007. Global warming means more pests. The IPM Practitioner 29:1-8.

Stange, E.E, Ayres, M.P., 2010. Climate change impacts: Insects. John Wiley & Sons.

Tobin, P.C., Nagarkatti, S., Loeb, G., Saunders, M.C., 2008. Historical and projected interactions between climate change and insect voltinism in a multivoltine species. Global Change Biology, 14: 951-957.

Werner, P. C., Gerstengarbe, F.W., Fraedrich, K., Oesterle, K., 2000. Recent climate change in the North Atlantic/European sector. International Journal of Climatology. Vol. 20. Issue 5:463-471.

13-24_terranova:Layout 1 4-09-2013 18:43 Pagina 13

Stima dell'erosività annua delle piogge in Calabria tramite analisi di frequenza regionale

Oreste G. Terranova[1], Antonella Bodini[2], Roberto Coscarelli[1], Stefano Luigi Gariano[3], Pasquale Iaquinta[3]*

Riassunto: *Ad una breve disamina delle principali metodologie per la stima dell'aggressività della pioggia, seguono formulazioni e metodi originali per: (I) la stima, con una nuova formula, dell'aggressività del singolo evento piovoso adeguata all'ambito climatico dell'Italia meridionale; (II) la valutazione accurata dell'aggressività media annua del singolo sito, grazie all'analisi di oltre 45000 eventi erosivi con dettaglio temporale di 5 minuti; (III) la stima della aggressività sulla base di analisi di regressione di frequenza con osservazioni pluviometriche di facile reperimento; (IV) la caratterizzazione dell'aggressività in termini probabilistici, anche nei siti sprovvisti di osservazioni, mediante gli strumenti dell'analisi regionale. La variabile oggetto dell'analisi di frequenza regionale è l'indice di Fournier modificato, FF, le cui osservazioni sono disponibili in un numero elevato di siti per lunghi periodi di osservazione, e che risulta ben correlato con l'aggressività della pioggia. Dall'analisi sono state ottenute 4 aree omogenee per l'indice FF e, conseguentemente, per l'indice di aggressività della pioggia R. All'interno di tali aree sarà possibile ottenere una stima, per diversi tempi di ritorno, dell'aggressività della pioggia.*
Parole chiave: *aggressività della pioggia, analisi regionale, Calabria, erosività.*

Abstract: *First a brief critical review of the main methods used in estimating rain aggressiveness is proposed, followed by original formulations and methods that aim to: (I) estimate the aggressiveness of the single rainstorm, by means of a new formula, adequate to the climate of southern Italy; (II) accurately assess, the at site mean annual erosivity, R, through the analysis of more than 45000 rainfall erosive events having 5-minutes time detail; (III) estimate the rainfall erosivity, R, based on regressive analysis with easily available rainfall characteristics; (IV) characterize R in terms of probability, even in sites without data, by regional frequency analysis. In this last regard, the observations of a variable of interest, collected within a homogeneous region, have been used in order to estimate the probability distribution of the variable. The analysed variable is the modified Fournier index, FF, that is well correlated with mean annual erosivity R. For estimating FF, data are available in a large number of rain gauges and for long observation periods. As a result of the analysis, 4 homogeneous regions for FF and consequently for R, have been obtained. In these regions, it will be possible to obtain an estimate, for different return times, of the rainfall erosivity, even in sites where rainfall observations are unavailable.*
Keywords: *Calabria, erosivity, rainfall aggressiveness, regional analysis.*

1. INTRODUZIONE

L'entità di erosione idrica di un suolo dipende, a parità di altri fattori, dalla capacità del suolo di "resistere" al distacco delle particelle, nel corso di un evento di pioggia, e dalle caratteristiche dello stesso evento.

Il concetto di aggressività della pioggia è stato introdotto da Wischmeier e Smith (1958), secondo i quali la potenziale capacità di un evento pluviometrico a causare erosione del suolo è quantificabile ed è in proporzione diretta con l'erosione stessa, allorché gli altri fattori erosivi siano costanti. La stima dell'erosività della pioggia (*R*) viene fatta dipendere (si vedano, fra gli altri, Wischmeier e Smith, 1978; Brown e Foster, 1987; Van Dijk *et al.*, 2002) dalla energia cinetica (*KE*) che le gocce di pioggia acquisiscono precipitando sul suolo. Questa energia viene dissipata per staccare le particelle del suolo, romperne gli aggregati, spostarli e trasportarli con lo scorrimento superficiale, che, a sua volta, provoca la rimozione di altro suolo. Vista l'impossibilità pratica di valutare l'energia cinetica per un generico evento di pioggia, sono state proposte relazioni fra l'intensità di pioggia e l'energia cinetica: (*I*) in forma di potenza (Uijlenhoet e Stricker, 1999), che stima bene i valori bassi di *KE* ma sovrastima quelli alti; (*II*) in forma logaritmica (Wischmeier e Smith, 1958), che, essendo illimitata, risulta irrealistica; (*III*) in forma logaritmica ma con limite superiore costante, che porta a stimare bene sia i valori bassi di KE sia quelli alti, ma introduce una discontinuità fisicamente discutibile; (*IV*) in forma espo-

* Corresponding author: e-mail: terranova@irpi.cnr.it
[1] Ricercatore, CNR-IRPI, U.O.S. di Cosenza, Rende (CS)
[2] Ricercatore, CNR-IMATI, U.O.S. di Milano
[3] Assegnista di ricerca, CNR-IRPI, U.O.S. di Cosenza, Rende (CS)
Received 14 January 2013, accepted 01 March 2013.

13-24_terranova:Layout 1 30-08-2013 12:00 Pagina 14

nenziale (Kinnell, 1981), che stima bene i valori alti di *KE* ma tende molto lentamente al proprio minimo per basse intensità di pioggia.
Perché un evento di pioggia sia in grado di causare erosione, la sua energia cinetica deve superare un valore critico di soglia (KE_C) caratteristico del suolo (Park *et al.*, 1982; Sharma *et al.*, 1991). Kinnell (2005) ha proposto una relazione che lega il peso del suolo distaccato dalla goccia di pioggia alla soglia di energia cinetica e ad un coefficiente di "distaccabilità" del suolo.
Altri esempi delle relazioni che valutano l'effetto dell'impatto delle gocce di pioggia sul suolo e del conseguente ruscellamento, sono quelli proposti da Hudson (1971), Lal (1976), Arnoldus (1977, 1980) e Onchev (1985).
Sicuramente, fra le relazioni più applicate rimane quella proposta da Wischmeier e Smith (1978), secondo la quale vengono considerati come singoli eventi di pioggia quelli separati da almeno 6 ore con pioggia nulla ed eventi erosivi quelli che totalizzano almeno 12.7 mm nell'evento oppure almeno 6.35 mm in 15 minuti. Secondo gli stessi Autori per il calcolo accurato dell'aggressività della pioggia, R, occorrono lunghe serie di dati pluviometrici a piccolo passo temporale (≤15 minuti), che spesso, però, non sono disponibili.
Per ovviare alla frequente indisponibilità di dati ad alto dettaglio temporale, sono state proposte relazioni basate su aggregazioni a scala temporale maggiore (si vedano fra gli altri Arnoldus, 1977; Richardson *et al.*, 1983; Ferro *et al.*, 1991; Renard e Freimund, 1994; Zhang *et al.*, 2002).
In particolare, facendo riferimento a studi e relazioni proposte per territori prossimi all'area oggetto della presente indagine, si cita la proposta di D'Asaro e Santoro (1983), per le aree coperte da apparecchi non registratori, che permette di stimare l'aggressività dall'altitudine del pluviometro e dalla media annua del numero di giorni piovosi.
Ferro *et al.* (1991) propongono, per la stima dell'aggressività annua della pioggia, una relazione, tarata sui dati della Sicilia, in cui compare il valore medio annuo dell'indice di Fournier modificato (*FF*), nel caso in cui non ci sia apparecchio registratore, ed una espressione, per le aree dove sono presenti i pluviografi, funzione dei massimi annuali delle intensità di pioggia di durata 1 ora, 6 ore e 24 ore e tempo di ritorno pari a 2 anni.
Aronica e Ferro (1997), sulla base di studi sugli estremi idrologici in Calabria (Versace *et al.*, 1989), caratterizzano in termini probabilistici l'erosività sul territorio della Calabria assumendo valida la forma della relazione fra indice di Fournier modificato e aggressività annua, proposta per la Sicilia.
Diodato (2004), con riferimento a 12 stazioni dell'Italia peninsulare, ciascuna con 8 anni di osservazioni, caratterizzate da regime mediterraneo delle piogge, propone una relazione in cui compare la pioggia annua, il massimo annuale di pioggia giornaliera e il massimo annuale delle piogge di durata 1 ora.
Sorrentino (2001) ha, invece, considerato 3120 eventi erosivi registrati, con passo di tempo 5 minuti, fra il 1997 ed il 1999, relativi a 56 stazioni ben distribuite sul territorio calabrese. In tal modo sono state ricavate due relazioni per la stima dell'aggressività annua: la prima, funzione della pioggia media annua, della quota sul livello del mare e del numero medio annuo di giorni piovosi; la seconda, funzione della media dei massimi annuali delle intensità di pioggia di 1 ora e 24 ore.
Terranova *et al.* (2009) hanno considerato 226 stazioni calabresi, con almeno 15 anni di osservazione fino al 2001, proponendo una mappa delle isoerodenti, di maggior dettaglio rispetto a quella di Sorrentino (2001).
Niccoli *et al.* (2008), utilizzando le serie storiche, con almeno 20 anni di registrazione, relative a 24 pluviografi in Calabria, propongono una relazione, caratterizzata da un elevato coefficiente di correlazione, che permette la stima dell'aggressività della pioggia annua dal solo calcolo dell'indice di Fournier modificato.
Il presente studio propone una metodologia per la stima dell'indice annuo di aggressività della pioggia, in qualunque area di studio del territorio calabrese, per prefissati valori del tempo di ritorno, in maniera indiretta, tramite cioè un'analisi di frequenza regionale dell'indice climatico FF che, come sopra riportato, sulla base di altre analisi di letteratura, è abbastanza correlato con l'aggressività della pioggia. Il calcolo dell'indice climatico, infatti, necessita dei valori mensili di precipitazione, che sono sicuramente disponibili, sia a livello spaziale sia a livello temporale, in misura notevolmente maggiore rispetto ai dati necessari per la stima dell'indice di aggressività.
Sono stati utilizzati i dati di pioggia registrati dal Centro Funzionale Multirischi della Regione Calabria. Per le piogge giornaliere, i dati utilizzati per il calcolo dell'indice climatico *FF* sono quelli relative a 189 stazioni, con almeno 30 anni di dati nel periodo 1916-2007. Per le piogge con passo temporale di 5 minuti, necessari per la stima dell'indice di aggressività della pioggia *R*, i dati sono disponibili dal 1989 e sono relativi a 155 stazioni:

13-24_terranova:Layout 1 30-08-2013 12:00 Pagina 15

la banca dati presenta mediamente 12 anni di osservazione con frequenti problemi di discontinuità (Fig. 1).

2. CARATTERI PLUVIOMETRICI DELLA CALABRIA

In Calabria l'orografia gioca un ruolo fondamentale nella localizzazione e nell'energia dei movimenti convettivi delle masse d'aria che investono la regione. In tutte le stagioni, condizioni di bassa pressione causano piogge spesso intense e durature, portate da fronti di aria calda provenienti da Sud-Est. Nella stagione invernale, invece, piogge molto intense vengono causate dai fronti freddi che arrivano da Nord Ovest; le frequenti piogge autunnali, invece, sono determinate dall'aria fredda proveniente da Nord Est. La primavera è caratterizzata da un clima molto instabile con piogge di più bassa intensità rispetto a quelle autunnali; nella stagione estiva, invece, non sono rari i forti temporali di natura convettiva.

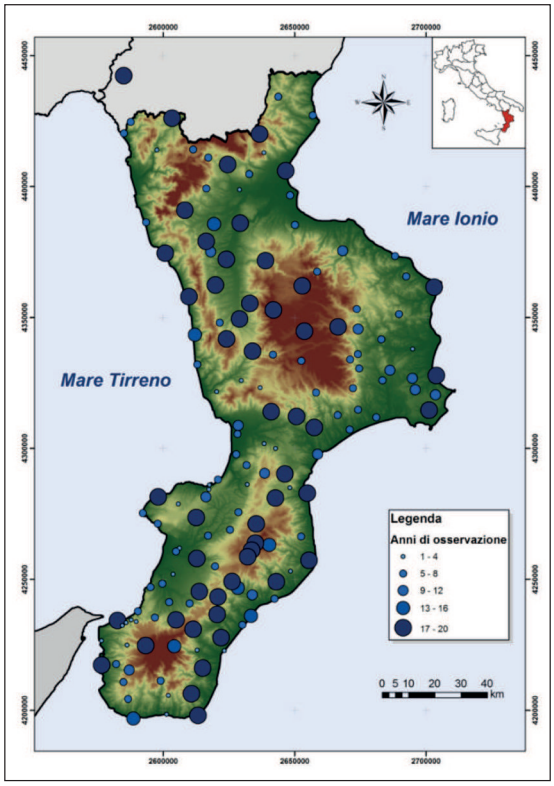

Fig. 1 - Localizzazione delle stazioni pluviografiche con disponibilità di osservazioni a scala temporale di 5 minuti e numero di anni di osservazione disponibili.
Fig. 1 - Localization of examined rain gauges (with 5-minutes observation) and valid years of observation.

La pioggia media annua in Calabria è pari a circa 1150 mm. In Aspromonte e sulla Catena Costiera si verificano i totali annui di pioggia maggiori (fra i 1200 e i 2000 mm). Sul versante ionico settentrionale e all'estremità meridionale della regione, a bassa quota, sono presenti le aree con le precipitazioni annue minori (circa 500 mm).
Il versante orientale è meno piovoso di quello occidentale. La Catena Costiera e le Serre Calabresi sono più piovose rispetto all'Altopiano Silano che è parzialmente schermato ad Ovest dalla Catena Costiera. Nel semestre caldo, le stazioni situate sulla costa Ionica centro-meridionale mostrano precipitazioni inferiori rispetto alle stazioni situate sulla costa Tirrenica, essendo meno esposte alle perturbazioni, anche se complessivamente Terranova (2004) ha mostrato come gli eventi eccedenti soglie elevate, in termini di "giorno piovoso normale", siano più frequenti sul versante ionico della regione.

3. METODOLOGIA

3.1 Fasi applicative dell'analisi di frequenza regionale

Un'analisi di frequenza regionale ha come obiettivo la stima che un dato valore di una variabile casuale, distribuita nello spazio, si verifichi con assegnata probabilità, utilizzando i dati che rappresentano osservazioni della variabile di interesse, raccolte in siti diversi, all'interno di una regione omogenea. Indicando con q la variabile casuale di interesse, misurabile ad intervalli di tempo regolari, con $G(x)$ la probabilità che q non superi il valore x, o probabilità di non superamento, è noto che il quantile z_T, corrispondente al periodo di ritorno T, è un valore della variabile q che ha probabilità $1/T$ di essere superato:

$$z_T = G^{-1}\left(1 - T^{-1}\right) \qquad (1)$$

La stima di z_T in una data località è spesso resa difficoltosa per valori di T significativamente maggiori del periodo di osservazione. Obiettivo dell'analisi di frequenza regionale è trovare stime di z_T, anche in presenza di un numero non adeguato di dati, incrementando detti dati con quelli misurati in siti con distribuzione di frequenza simile a quella della località di interesse. La procedura, detta della grandezza-indice (index-flood), originariamente proposta per l'analisi di frequenza regionale delle piene (Dalrymple, 1960) e poi estesa anche ad altri tipi di dato, ha come assunto fondamentale che i siti in una regione *"omogenea"*, abbiano distribuzioni di fre-

13-24_terranova:Layout 1 30-08-2013 12:00 Pagina 16

quenza identiche a meno di un parametro di scala m_i caratteristico di ogni sito, detto grandezza indice.
Indicando con G_i^{-1} la funzione dei quantili nell'*i*-esimo sito, sulla base di quanto indica il metodo della grandezza indice, si può scrivere:

$$G_i^{-1} = m_i G^{-1} \quad (2)$$

dove G^{-1} è *la curva di crescita regionale*, ossia una funzione dei quantili adimensionale comune a tutti i siti. La curva di crescita regionale può esprimersi come funzione dei quantili della distribuzione di frequenza regionale, che è la distribuzione comune delle variabili standardizzate q_{ij}/m_i essendo q_{ij} la *j*-esima osservazione dell'*i*-esimo sito.
Tornando quindi all'espressione (1), per ogni sito *i*, può scriversi

$$z_{Ti} = G_i^{-1}\left(1-T^{-1}\right) = m_i \cdot G^{-1}(1-T^{-1}) \quad (3)$$

In altre parole, i quantili relativi tempo di ritorno *T*, nel sito *i*, possono essere calcolati a partire dalla curva di crescita regionale G^{-1}, tramite moltiplicazione per il valore indice m_i. Usualmente m_i è stimato con la media dei dati al sito *i*. Il problema, quindi, si risolve con la stima della curva di crescita regionale, che, utilizzando l'approccio di Hosking e Wallis (1993, 1997), si suppone nota, a meno di un numero finito di parametri incogniti, stimabili secondo il metodo degli L-momenti introdotti da Hosking (1990). Questi producono stime robuste ed accurate dei quantili di una distribuzione ed individuano univocamente la distribuzione di probabilità, purché questa abbia media.
La metodologia può essere schematizzata nei seguenti step:

A. Screening dei dati: Per valutare se nei dati esistano errori o inconsistenze, viene utilizzata una misura di discordanza *D*, che identifica le stazioni con L-momenti campionari molto differenti rispetto a quelli degli altri siti nella medesima regione.

B. Identificazione di sotto-regioni omogenee: Dopo aver eventualmente eliminato le stazioni discordanti, viene decisa l'appartenenza delle stazioni a sotto-regioni diverse. A tal proposito, è usuale adottare tecniche di *cluster analysis* (Ward, 1963) e la conoscenza delle caratteristiche geografiche e climatiche locali. Di tali sotto-regioni viene testata l'omogeneità, cioè l'ipotesi che per le stazioni della regione sia ammissibile una unica distribuzione di frequenza, a meno di un parametro di scala. L'omogeneità di un gruppo di stazioni, comunque scelto, viene valutata confrontando la variabilità campionaria degli L-momenti con quella che ci si aspetterebbe se la regione fosse omogenea. Quest'ultima è stimata attraverso ripetute simulazioni di regioni omogenee con campioni estratti da una distribuzione Kappa a quattro parametri. Una misura dell'omogeneità è fornita dalla statistica *H*, funzione degli L-momenti campionari (coefficienti di L-*variazione*, L-*skewness*, L-*kurtosis*) e degli L-momenti della regione simulata come omogenea (Hosking e Wallis, 1993): se $H < 1$, la regione viene considerata "accettabilmente omogenea"; se $1 \leq H < 2$, "eventualmente eterogenea"; se $H \geq 2$, la regione è "eterogenea".

C. Stima della curva di crescita regionale: Per le regioni di cui sia stata stabilita l'omogeneità, diverse distribuzioni possono essere utilizzate per simulare la curva di crescita regionale. Nell'ottica di adottare distribuzioni che risultino "parsimoniose" per quanto riguarda il numero di parametri, viene data preferenza alle distribuzioni a tre parametri, quali la logistica generalizzata (GLO), degli eventi estremi generalizzata (GEV), di Pareto generalizzata (GPA), log-normale generalizzata (GNO) e la distribuzione Pearson di tipo III (PE3). Si noti che le distribuzioni GLO, GEV e GPA sono casi particolari della distribuzione Kappa a quattro parametri (Hosking, 1994). Le distribuzioni menzionate presentano flessibilità sufficiente per adattarsi alle "pesanti" code tipiche dei dati di pioggia. In appendice vengono riportate le espressioni delle funzioni dei quantili G^{-1}, o quelle delle funzioni di distribuzione *G*, qualora le prime non abbiano forma analitica esplicita, delle distribuzioni utilizzate nel presente studio. La stima dei parametri di una data distribuzione viene effettuata col metodo degli L-momenti, imponendo cioè l'uguaglianza tra gli L-momenti teorici della distribuzione e quelli regionali campionari.

D. Scelta della distribuzione: La scelta della distribuzione che meglio si adatta ai dati viene effettuata, appunto, sulla base della statistica *Z* di "bontà di adattamento", che confronta quanto i momenti L-skewness ed L-kurtosis, stimati a livello regionale, sono prossimi a quelli teorici (Hosking e Wallis, 1997).

13-24_terranova:Layout 1 30-08-2013 12:00 Pagina 17

3.2 Relazione tra indice climatico e indice di aggressività della pioggia

La variabile oggetto di analisi di frequenza regionale è l'indice climatico *FF*, che risulta essere ben correlato con l'indice di aggressività della pioggia (POR Calabria 2000-2006 – Lotto 2).

L'indice climatico annuo, *FF* (mm), come proposto da Ferro *et al.* (1991), è definito, per ogni stazione, come media dei valori annui dell'indice di Fournier, modificato secondo Arnoluds (1980):

$$FF = \frac{1}{N}\sum_{i=1}^{N} F_{a,i} \tag{4}$$

essendo:

$$F_{a,i} = \frac{\sum_{1}^{12} P_{j,i}^{\ 2}}{\sum_{1}^{12} P_{j,i}} = \frac{\sum_{1}^{12} P_{j,i}^{\ 2}}{P_{a,i}} \tag{5}$$

dove $P_{j,i}$ e $P_{a,i}$ rappresentano la precipitazione rispettivamente del mese j e quella annua entrambe del generico anno i.

Secondo Ferro *et al.* (1991), la relazione tra l'indice climatico e l'indice di aggressività della pioggia è ben descritta da un'espressione del tipo:

$$R = a \cdot FF^{b} \tag{6}$$

Per stimare i coefficienti a, b che compaiono nella citata formula occorre stimare l'indice climatico *FF* e l'indice di aggressività per quelle stazioni le cui serie presentano i dati necessari per il calcolo dei due indici.

L'indice di aggressività viene calcolato come media su un periodo di N anni degli indici di aggressività annuali R, somma degli indici di aggressività relativi agli eventi erosivi R_{ej} verificatisi in ciascun anno. Le sequenze di pioggia intervallate da almeno 6 ore di tempo di asciutto, vengono assunte essere eventi di pioggia distinti; fra questi, gli eventi erosivi sono quelli con pioggia cumulata P almeno pari a 12.7 mm. Fra gli eventi di pioggia erosivi vengono inoltre inclusi quelli con almeno 6.35 mm in 15 minuti (Wischmeier e Smith, 1978).

L'indice di aggressività R_{ej} del singolo evento erosivo j è definito come prodotto dell'energia totale dell'evento di pioggia E_j, relativa all'unità di area, per la massima intensità I_{30j} in 30 minuti raggiunta dall'evento, secondo l'espressione:

$$R_{ej} = E_j \cdot I_{30\,j} \left(MJ/ha \cdot mm/h\right) \tag{7}$$

L'energia totale di un evento E_j di durata D_j è valutabile come sommatoria delle singole energie cinetiche KE_k dei k intervalli di pioggia ad intensità costante in cui si suppone suddivisa la pioggia dell'evento j:

$$E_j = \sum_{k=1}^{Dj} KE_k \cdot P_k \tag{8}$$

Al fine di ottenere una stima dell'energia cinetica adeguata alle regioni caratterizzate da clima di tipo mediterraneo, nel presente studio viene proposta l'adozione di una relazione, limitata superiormente, che non presenta brusche variazioni di *KE* in corrispondenza di qualche intensità di pioggia. La relazione è intermedia fra quelle di Zanchi e Torri (1980), Cerro *et al.* (1998) e di Coutinho e Tomas (1995), da un lato, e quelle di Brown e Foster (1987) e Foster (2004), dall'altro. Il limite superiore, consistente con i valori di letteratura relativi all'ambito climatico mediterraneo, è posto pari a 30.7 (J m^{-2} mm^{-1}); questo valore corrisponde al massimo della funzione che si verifica per I ≃ 111.9 mm h^{-1}. L'equazione ha la seguente espressione:

$$\begin{aligned} KE &= 2\cdot 10^{-2}\Big(1962 + 2250\cdot Log_{10} I + 19.19\cdot I - \\ &\quad -11.25\cdot Log_{10} I^{I} - 20.88\cdot I\cdot e^{-0.082\cdot I}\Big) \qquad per\ I \le 111.9\,mm\,h^{-1} \\ KE &= 30.7 \qquad per\ I > 111.9\,mm\,h^{-1} \end{aligned} \tag{9}$$

Come si può evincere dalla Fig. 2, per qualunque valore di I, questa relazione rimane al di sotto di quelle di Cerro *et al.* (1998) e di Coutinho e Tomas (1995); essa è molto vicina a quella proposta da Zanchi e Torri (1980) per I<50 mm h^{-1} , mentre, per I > 50 mm h^{-1}, ne rimane al di sotto con valori maggiori di quelli relativi alle relazioni di Brown e Foster (1987) e di Foster (2004).

In definitiva, l'intera metodologia proposta può condurre alla stima dell'indice di aggressività della pioggia per un fissato tempo di ritorno e per un qualsiasi sito della Calabria tramite i seguenti passi:

1) si identifica la regione omogenea cui appartiene il sito di interesse;
2) si determina il valore indice di *FF*, sulla base della stazione più vicina o interpolando fra quelle più vicine appartenenti alla stessa regione omogenea;
3) si applica la curva di crescita valida per la regione omogenea di interesse, al fine di determinare il valore di *FF* corrispondente al tempo di ritorno fissato T;
4) si calcola il valore di R_T dal corrispondente valore di FF_T utilizzando la regressione preventivamente stimata.

13-24_terranova:Layout 1 30-08-2013 12:00 Pagina 18

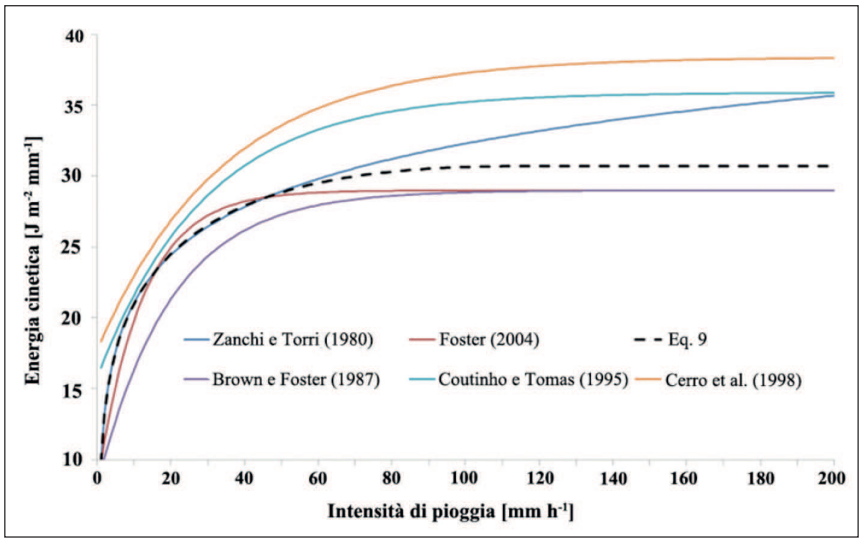

Fig. 2 - Confronto fra alcune stime dell'energia cinetica, *KE*.
Fig. 2 - Comparison among some kinetic energy, KE, estimations.

4. RISULTATI

Utilizzando i valori di precipitazione mensile e di pioggia annua, sono stati calcolati, per ciascuna stazione, i valori annui dell'indice climatico ed il suo valore medio. La distribuzione di *FF* sul territorio regionale evidenzia valori più elevati sui rilievi (specie in quelli centro-meridionali) e valori più bassi lungo le coste, specialmente quelle ioniche settentrionali.

Per poter determinare la relazione fra *FF* e indice di aggressività *R*, per gli anni in cui si hanno a disposizione sia i dati a 5 minuti sia quelli mensili, è stata effettuata la stima dell'indice *R*, estrapolando per le 155 stazioni utili 152575 eventi di pioggia. Detti eventi sono stati distinti in eventi erosivi, pari a 45533 eventi, e in eventi non-erosivi, pari a 107042, secondo la definizione di Wischmeier e Smith (1978). I 45533 eventi erosivi sono stati così caratterizzati: (*I*) la pioggia media di evento, P_{ev}, è pari a 23.5 mm; (*II*) 18033 eventi hanno una pioggia di evento compresa fra 6 e 12.7 mm, ma eccedenti 6.35 mm in 15 minuti; (*III*) 27501 eventi hanno una pioggia d'evento superiore a 12.7 mm; (*IV*) la durata degli eventi, D_{ev}, è compresa tra 10

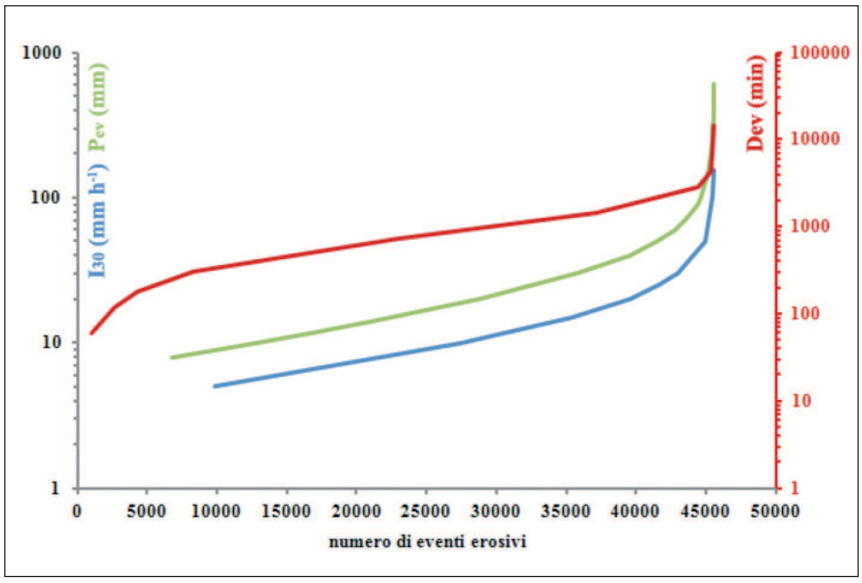

Fig. 3 - Curve di frequenza di pioggia cumulata (P_{ev}), intensità massima in 30 minuti (I_{30}) e durata (D_{ev}) degli eventi erosivi analizzati.
Fig. 3 - Frequency curves of cumulated rainfall (P_{ev}), maximum intensity in 30 minutes (I_{30}) and duration (D_{ev}) of erosive events.

e 13390 minuti; (*V*) la durata media d'evento è di circa 15 ore; (*VI*) la massima intensità in 30 minuti, I_{30}, varia da 0.4 a 154.8 mm h^{-1}; (*VII*) la media della massima intensità in 30 minuti è risultata pari a 11.6 mm h^{-1}. Queste caratteristiche sono riassunte nelle curve di frequenza mostrate nella Fig. 3. Ulteriori dettagli, relativi soprattutto alla struttura temporale di questi eventi, sono descritti in Terranova e Iaquinta (2011).

I dati prima esposti sono stati utilizzati per il calcolo dell'aggressività *R* in corrispondenza delle stazioni e per determinare la relazione con l'indice climatico medio *FF*, utilizzando il modello di equazione (6). Utilizzando per *FF* ed *R* i valori medi ottenuti per ciascuna stazione – cfr. Ferro et al. (1991, 1999) e Angulo-Martínez e Beguería (2009) – è stata ottenuta la nuvola di punti sperimentali di Fig. 4. Nella regressione che è stata effettuata, alla coppia di valori (*FF*, *R*) di ciascuna stazione è stato associato il peso corrispondente al numero di anni di osservazione disponibili, ottenendo la relazione

$$R = 7.52 \cdot FF^{1.227} \qquad (10)$$

avente coefficiente di correlazione $\rho = 0.90$.

Tale relazione ha permesso di ottenere la mappa dei valori medi annui di *R* (Fig. 5), realizzata utilizzando la tecnica di interpolazione geostatistica del *Kriging*. Per l'analisi di frequenza regionale dell'indice climatico *FF* è stato utilizzato il software libero ***R*** ed, in particolare, il pacchetto ***lmomRFA*** (Hosking, 2009). Delle 189 stazioni originarie, ne sono state scartate 8 in base al test di discordanza (misura *D*) che identifica le stazioni con L-momenti campionari molto differenti rispetto a quelli degli altri siti nella medesima sotto-regione. Inizialmente, sono state considerate le tre sotto-regioni individuate da Versace *et al.* (1989) e prese in considerazione anche da Aronica e Ferro (1997), le quali sono state sottoposte al test di eterogeneità *H*. I risultati di questo primo tentativo mostrano come soltanto la sotto-regione Ionica possa considerarsi omogenea. In un secondo tentativo, le stazioni esterne alla sotto-regione Ionica sono state suddivise in tre sotto-regioni, indicate come Centro-Ionio, Centro e Tirreno (nei due tentativi le sotto-regioni, pur mantenendo la stessa denominazione, sono ovviamente diversamente delimitate), sia usando tecniche di *cluster analysis* (avendo come uniche variabili le coordinate e la pioggia media annua) sia considerando la prossimità territoriale. Infine, un'ulteriore analisi ha portato a scartare le stazioni di Gallico Marina

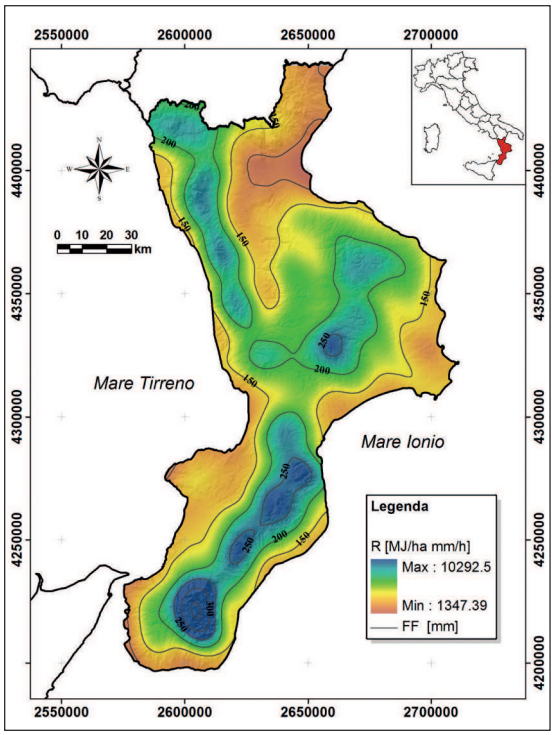

Fig. 5 - Mappa dei valori dell'indice di aggressività della pioggia *R* (Eq. 10) e isolinee rappresentanti i valori dell'indice climatico *FF*.
Fig. 5 - Map of R (Eq. 10) and FF isolines.

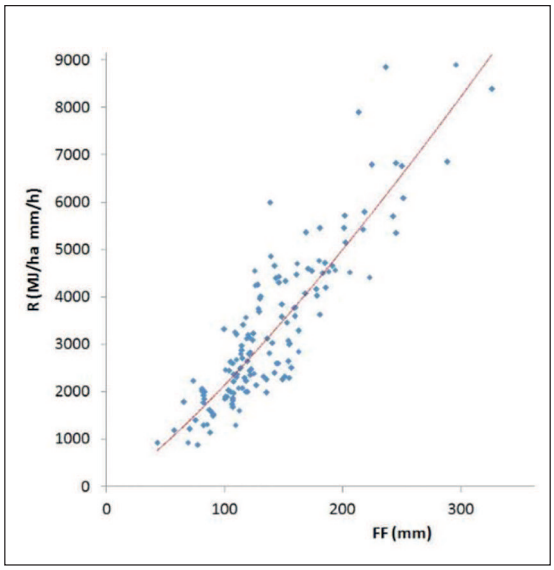

Fig. 4 - Regressione fra l'indice climatico *FF* e l'indice di aggressività della pioggia *R*.
Fig. 4 - Regression between the climatic index, FF, and the rainfall erosivity index, R.

Sotto-regione	Numero stazioni	Anni disponibili (media)	Quota media [m s.l.m.]	P_{annua} [mm]		FF	
				μ	σ	μ	σ
Tirreno	39	56.0	235.6	1023.5	178.9	143.8	26.9
Centro	44	50.8	530.6	1274.6	284.1	185.7	42.5
Centro-Ionio	35	49.5	511.2	1016.5	296.6	172.9	48.0
Ionio	60	54.3	305.7	902.2	280.8	161.5	47.3

Tab. 1 - Principali caratteristiche delle sotto-regioni omogenee. Legenda: P_{annua} = pioggia annua; *FF* = indice climatico (Eq. 4); μ = valor medio; *s* = deviazione standard.
Tab. 1 - Main information about the homogeneous sub-regions. Key: P_{annua} = annual rainfall; FF = climatic index (Eq. 4); μ = average value; s = standard deviation.

Z	Tirreno	Centro	Centro/Ionio	Ionio
Stazioni discordanti	2860 (San Tommaso)	1150 (S. Sofia d'Epiro)	1140 (Tarsia) 2540 (S. Cristina d'Aspr.)	1760 (Botricello) 2140 (Mammola)
GLO ξ, α, k	2.31	4.90	2.40	**1.58** 0.9001, 0.2251, -0.2505
GEV ξ, α, k	-3.18	**-0.40** 0.8609, 0.2508, 0.02313	**-1.21** 0.8096, 0.3063, -0.04332	-2.02
GNO ξ, α, k	-3.13	**-0.80** 0.9526, 0.2892, -0.3193	-2.03	-3.73
PE3	-4.05	-2.23	-3.77	-6.83
Kappa ξ, α, k, h	* 0.9292, 0.1690, -0.02767, -0.3576			

* È stata usata una distribuzione Kappa a 4 parametri; aumentando di uno il numero dei parametri è stato ottenuto un buon adattamento ai dati che non ha necessitato del calcolo del valore di Z.

Tab. 2 - Risultati del test di adattamento per le 4 sotto-regioni individuate, sulla base di 1000 simulazioni. In grassetto sono i valori di Z indicanti la accettabilità (|Z| < 1.64) della distribuzione ipotizzata, per la quale sono riportate le stime dei parametri. Nel primo rigo sono riportate, per ogni sotto-regione, le stazioni discordanti.
Tab. 2 - Goodness-of-fit test for the 4 homogeneous sub-regions based on 1000 simulations. Bold values indicate acceptable distributions (|Z| < 1.64), for which estimated parameters are reported. In the first line, the discordant rain gauges are also listed.

e di Umbriatico, che sono sembrate classificate in modo anomalo, e quella di Rosarno, in quanto non rientrante in nessuna delle sotto-regioni identificate.
La Tab. 1 riporta le principali caratteristiche medie delle quattro sotto-regioni.
Per la stima della funzione di crescita in ciascuna sotto-regione, sono state considerate le distribuzioni elencate nella sottosezione 3.1. I risultati di verifica dell'adattamento del modello ai dati per ciascuna delle precedenti distribuzioni sono riportati in Tab. 2: si può notare che, in riferimento solo alla sotto-regione "Tirreno", per nessuna delle distribuzioni a tre parametri risulta |Z|<1.64. Conseguentemente, per questa sotto-regione si è ipotizzata una distribuzione Kappa a 4 parametri.
In Fig. 6 sono riportati i valori di L-skewness ed L-kurtosis per ciascuna sotto-regione omogenea, confrontati con i valori teorici delle distribuzioni utilizzate. La Fig. 7 riporta le curve di crescita della variabile *FF* stimate per le quattro sotto-regioni ed i relativi quantili regionali (rapportati al valor medio) corrispondenti ad alcuni valori del tempo di ritorno.
Al fine di effettuare la delimitazione delle quattro zone, sulla base dei risultati ottenuti per le singole stazioni, come primo passo, sono stato tracciati i poligoni di Thiessen, al fine di determinare l'area di influenza di ciascuna stazione. Si è quindi proceduto raggruppando i poligoni delle stazioni afferenti a ciascuna zona omogenea. Il risultato della perimetrazione così effettuata, anche se palesa chiaramente il criterio adottato, segue, con discreta approssimazione, la morfologia del territorio regionale. Al fine di ottenere però una zonazione più "fedele" alla morfologia del territorio, sono state effettuate piccole correzioni della perimetrazione, cercando di ri-

13-24_terranova:Layout 1 30-08-2013 12:00 Pagina 21

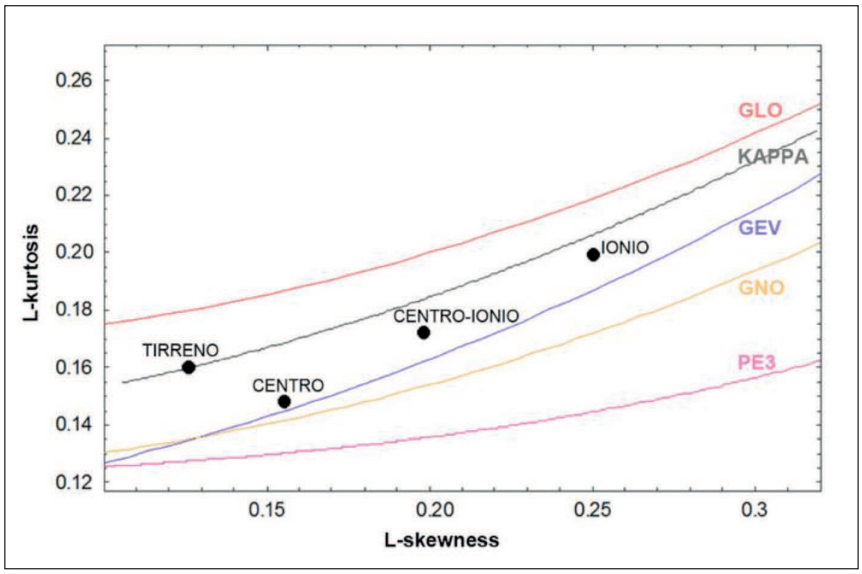

Fig. 6 - Valori medi di *L-skewness* e *L-kurtosis* delle 4 sotto-regioni e curve relative alle 5 distribuzioni considerate.
Fig. 6 - Average values of "L-skewness" and "L-kurtosis", related to the 4 homogeneous sub-regions, compared to the curves of the 5 considered probability distributions.

spettare l'andamento delle linee di spartiacque e, quindi, l'integrità dei bacini idrografici (Fig. 8).

5. CONCLUSIONI

La stima dell'erosività della pioggia su base statistica rimane sicuramente un problema di non immediata risoluzione, in quanto necessita di dati pluviometrici a passo temporale basso, le cui serie temporali risultano non particolarmente lunghe.
La metodologia proposta nel presente studio cerca di ovviare a dette difficoltà, utilizzando per la stima dell'aggressività della pioggia in Calabria, per diversi tempi di ritorno, l'indice climatico medio *FF*, per la cui stima sono disponibili osservazioni in numero maggiore e quindi più idonei per le valutazioni statistiche.
L'utilizzo di un considerevole numero di eventi (oltre 45000) di pioggia erosivi, ad elevata definizione temporale, nonché la proposta per la stima dell'energia cinetica di una relazione adeguata all'ambito delle aree con clima mediterraneo e che non presenta incongruenze da un punto di vista fisico, rende sicuramente affidabile e corretta la relazione che permette di stimare l'aggressività media

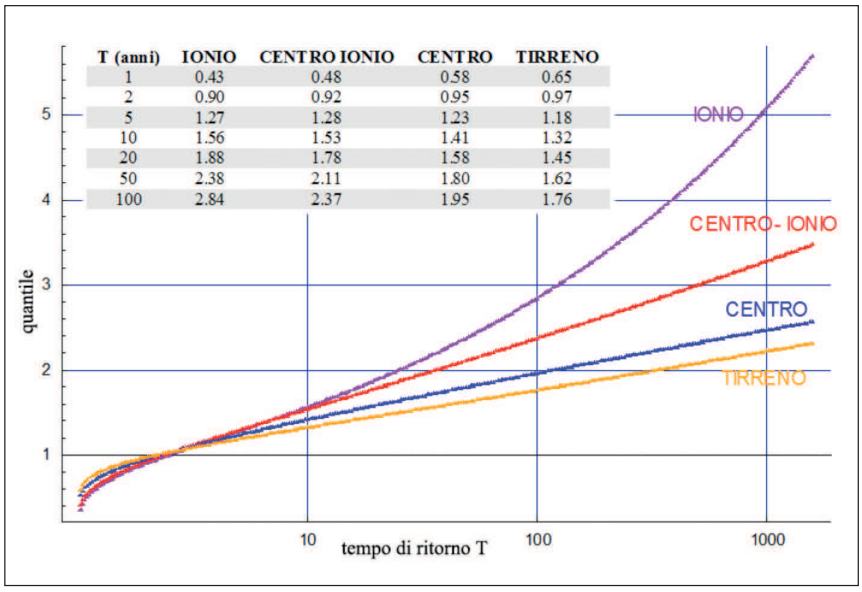

Fig. 7 - Curve di crescita regionali per le quattro sotto-regioni omogenee e quantili adimensionali della variabile FF rapportati al valore medio, per diversi tempi di ritorno.
Fig. 7 - Regional growth curves related to the 4 homogeneous sub-regions. In the table, some significant quantiles of FF index are shown (as a ratio of the mean value).

13-24_terranova:Layout 1 30-08-2013 12:00 Pagina 22

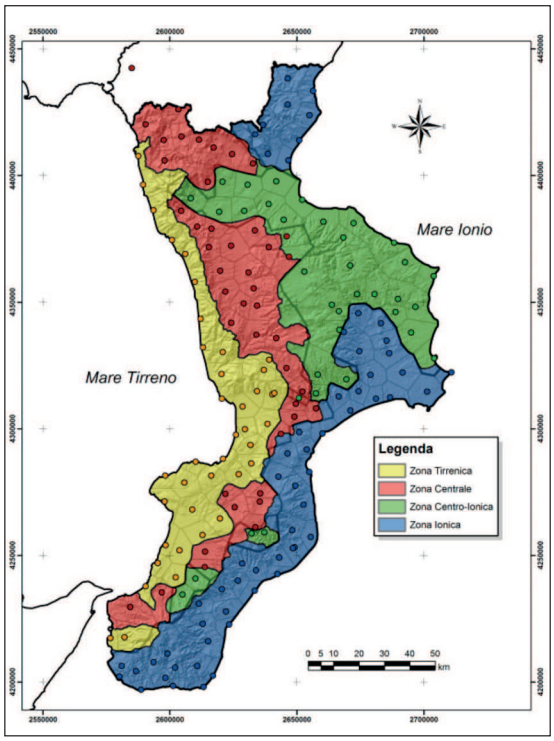

Fig. 8 - Delimitazione delle sotto-regioni omogenee in base ai poligoni di Thiessen ed alla morfologia del territorio.
Fig. 8 - Homogeneous sub-regions based on "Thiessen" polygons and morphological evidences.

annua dall'indice climatico. Inoltre, l'individuazione di sottozone omogenee rende possibile ottenere, per qualsivoglia tempo di ritorno, i valori dell'indice climatico *FF*, e quindi quelli di aggressività della pioggia, in qualsiasi punto del territorio calabrese, prescindendo dalla presenza di un pluviografo.
I risultati conseguiti in questo lavoro, attraveso l'analisi delle serie degli eventi di pioggia erosivi, la regressione con l'indice climatico medio *FF* e l'analisi regionale statistico-probabilistica di quest'ultimo, risultano particolarmente importanti e utili per il territorio regionale calabrese. Infatti, questa regione presenta alta variabilità climatica, sia nel tempo sia nello spazio, dovuta alla morfologia notevolmente complessa ed accidentata. Il trasferimento *tout court* di misure da un'area, magari coperta da strumento, ad altre aree risulta pertanto un'operazione di particolare delicatezza. Inoltre, l'applicazione della procedura proposta può essere estesa, con i dovuti adattamenti e le necessarie tarature, ad altre regioni presenti nel bacino del Mediterraneo, essendo la Calabria rappresentativa di più estesi ambiti territoriali caratterizzati da peculiarità climatiche simili.

APPENDICE

Espressioni delle funzioni dei quantili, $G^{-1}(p)$, $0 < p < 1$, o delle funzioni di distribuzione, $G(x)$, $x > 0$, utilizzate:

- Generalized Logistic (GLO):

$$G^{-1}(p) = \xi + \alpha \cdot \left[1 - \left\{(1-p)/p\right\}^k\right]/k \qquad (11)$$

- Generalized Extreme Value (GEV):

$$G^{-1}(p) = \xi + \alpha \cdot \left\{1 - \left(-\log(p)\right)^k\right\}/k \qquad (12)$$

- Generalized Normal o Log-normal (GNO):

$$G(x) = \Phi\left(\sigma^{-1}\left[\log(x-\xi) - \mu\right]\right) \qquad (13)$$

dove Θ è la distribuzione normale standard

- Pearson type III (PE3):

$$G(x) = \Lambda \cdot \left[(x - \mu + 2\sigma/\gamma)/|\sigma\gamma/2|, 4/\gamma^2\right], \; se\,\gamma > 0$$
$$G(x) = 1 - \Lambda \cdot \left[-(x - \mu + 2\sigma/\gamma)/|\sigma\gamma/2|, 4/\gamma^2\right], \; se\,\gamma < 0 \qquad (14)$$

dove $\Lambda(x,\alpha) = \left[\Gamma(\alpha)\right]^{-1}\int_0^x t^{\alpha-1}e^{-t}dt$

- Generalized Pareto (GPA):

$$G^{-1}(p) = \xi + \alpha\left\{1 - (1-p)^k\right\}/k \qquad (15)$$

- Distribuzione Kappa a 4 parametri:

$$G^{-1}(p) = \xi + \alpha\left[1 - \left\{\left(1 - p^h\right)/h\right\}^k\right]/k \qquad (16)$$

BIBLIOGRAFIA

Angulo-Martínez, M., Beguería, S., 2009. Estimating rainfall erosivity from daily precipitation records: A comparison among methods using data from the Ebro Basin (NE Spain). Journal of Hydrology 379: 111-121

Arnoldus, H.M.J., 1977. Methodology used to determine the maximum potential average annual soil loss due to sheet and rill erosion in Morocco, FAO Soils Bulletin, 34: 39-51.

Arnoldus, H.M.J., 1980. An approximation of the rainfall factor in the Universal Soil Loss Equation. In: Assessment of Erosion, De Boodt, M. and Gabriels, D. (Eds). John Wiley and Sons, Ltd, Chichester: 127-132.

Aronica, G., Ferro, V., 1997. Rainfall erosivity

13-24_terranova:Layout 1 30-08-2013 12:00 Pagina 23

over the Calabrian region. Hydrol. Sci. J., 42: 35-48.

Brown, L.C., Foster, G.R., 1987. Storm erosivity using idealized intensity distributions. Transactions of the American Society of Agricultural Engineers, 30: 379-386.

Cerro, C., Beck, J., Codina, B., Lorente, J., 1998. Modeling rain erosivity using disdrometric techniques. Soil Sci. Soc. Amer. J., 62: 731-735.

Coutinho M.A., Tomas P.P., 1995. Characterization of raindrop size distributions at the Vale Formoso Experimental Erosion Centre, Catena, 25: 187-197.

Dalrymple, T., 1960. Flood frequency analyses. U.S. Geological Survey Water Supply Paper, 1543-A.

D'Asaro, F., Santoro, M., 1983. Aggressività della pioggia nello studio dell'erosione idrica del territorio siciliano. CNR Progetto Finalizzato Conservazione del Suolo, Sottoprogetto: Dinamica dei versanti. Publ. no. 130.

Diodato, N., 2004. Estimating RUSLE's rainfall factor in the part of Italy with a Mediterranean rainfall regime. Hydrol. Earth Syst. Sc., 8(1): 103-107.

Ferro, V., Giordano, G., Iovino, M., 1991. Isoerosivity and erosion risk map for Sicily. Hydrological Sciences Journal 36: 549-564.

Ferro, V., Porto, P., Yu, B., 1999. A comparative study of rainfall erosivity estimation for southern Italy and southeastern Australia. Hydrological Sciences Journal 44, 3-24.

Foster, G.R., 2004. User's reference guide. Revised Universal Soil Loss Equation, Version2. National Sedimentation Laboratory, USDA–Agricultural Research Service Oxford, Mississippi.

Hosking, J.R.M., Wallis, J.R., 1990. L-moments: analysis and estimation of distributions using linear combinations of order statistics. Journal of the Royal Statistical Society, Series B, 52: 105-124.

Hosking, J.R.M., 1994. The four-parameter kappa distribution. IBM Journal of Research and Development, 38: 251-258.

Hosking, J.R.M., 2009. Regional frequency analysis using L-moments". R package, version 2.1. URL: http://CRAN.R-project.org/package=lmomRFA,.

Hosking, J.R.M., Wallis, J.R., 1993. Some Statistics Useful in Regional Frequency Analysis. Water Resources Research, 29: 271-281.

Hosking, J.R.M., Wallis, J.R., 1997. Regional Frequency Analysis. Cambridge University Press.

Hudson, N., 1971. Soil Conservation. Batsford, London.

Kinnell, P.I.A., 1981. Rainfall intensity–kinetic energy relationships for soil loss prediction. Soil. Sci. Soc. Amer., 45: 153–155.

Kinnell, P.I.A., 2005. Why the universal soil loss equation and the revised version of it do not predict event erosion well Hydrological Processes. Special Issue: SWAT 2000, Development and Application, Vol. 19, Issue 3: 851-854.

Lal, R., 1976. Soil erosion problems on an Alfisos in Western Nigeria and their control. Monograph 1, Ibadan, Nigeria: International Institute of Tropical Agriculture.

Niccoli, R., Porto, P., Stillitano, T., Zimbone, S.M., 2008. Valutazione dell'indice di aggressività della pioggia e mappatura delle isoerodenti in Calabria. L'acqua. 2: 41-50.

Onchev, N.G., 1985. Universal Index for calculating rainfall erosivity. In Soil erosion and conservation, ed. S.A. El-Swaify, W.C. Moldenhauer, A. Lo. Ankeny, Soil Conservation Society of America.

Park, S.W., Mitchell, J.K., Bubenzer, G.D., 1982. Splash erosion modeling: Physical analyses. Transactions of the American Society of Agricultural Engineers, 25: 357-361.

POR Calabria 2000-2006, Asse 1, Misura 1.4, Azione 1.4.c, Lotto Progettuale N.2, 2010. Pericolosità legata ai fenomeni di intensa erosione idrica areale e lineare, a cura di O. Terranova.

Renard, K.G., Freimund, J.R., 1994. Using monthly precipitation data to estimate the R-factor in the revised USLE. Journal of Hydrology, 157: 287-306.

Richardson, C.W., Foster, G.R., Wright, D.A., 1983. Estimation of erosion index from daily rainfall amount. Transactions of the ASAE, 26 (1): 153-156.

Sharma, P.P., Gupta, S.C., Rawls, W.J., 1991. Soil detachment by single raindrops of varying kinetic energy. Soil Sci. Soc. Am. J., 55: 301-307.

Sorrentino, G., 2001. Indagine regionale sulla stima dell'aggressività della pioggia nello studio dell'erosione idrica. Tesi di laurea. Facoltà di Ingegneria, Corso di Laurea in Ingegneria Civile, Indirizzo Idraulico – Università degli Studi della Calabria, 215 p.

Terranova, O.G., 2004. Caratteri statistico-probabilistici degli eventi pluviometrici in Calabria. CNR-IRPI U.O.S. di Cosenza, Rapporto Interno.

Terranova, O.G., Antronico, L., Coscarelli, R., Iaquinta, P., 2009. Soil erosion risk scenarios in the Mediterranean environment using RUSLE and GIS: An application model for Calabria (southern Italy). Geomorphology, 112: 228-245.

Terranova, O.G., Iaquinta, P., 2011. Temporal

13-24_terranova:Layout 1 30-08-2013 12:00 Pagina 24

properties of rainfall events in Calabria (Southern Italy). Nat. Hazards Earth Syst. Sci., 11: 751–757.

Uijlenhoet, R., Stricker, J.N.M., 1999. A consistent rainfall parameterization based on the exponential raindrop size distribution. Journal of Hydrology, 218: 101-127.

Van Dijk, A.I.J.M., Bruijnzeel, L.A., Rosewell, C.J., 2002. Rainfall intensity-kinetic energy relationships: a critical literature appraisal. Journal of Hydrology, 261: 1-23.

Versace, P., Ferrari, E., Gabriele, S., Rossi, F., 1989. Valutazione delle piene in Calabria. CNR, Gruppo Nazionale per la Difesa delle Catastrofi Idrogeologiche. Geodata, Publ. 30.

Ward, J.H., 1963. Hierarchical Grouping to optimize an objective function. Journal of American Statistical Association, 58(301): 236-244.

Wischmeier, W.H., Smith, D.D., 1958. Rainfall energy and its relation to soil loss. Transaction of the American Geophysical Union, 39: 285-291.

Wischmeier, W.H., Smith, D.D., 1978. Predicting rainfall erosion losses: a guide to conservation planning. USDA Handbook 537, Washington, DC.

Zanchi, C., Torri, D., 1980. Evaluation of rainfall energy in central Italy. In Assessment of Erosion, eds: De Boodt, M., Gabriels, D., Wiley, Toronto, 133-142.

Zhang, X.Y., Drake, N.,Wainwright, J., 2002. Scaling land-surface parameters for global scale soil-erosion estimate. Water Resources Research, 38: 191-199.

Modelling phenotypical traits to adapt durum wheat to climate change in a Mediterranean environment

Pasquale Garofalo[1], Michele Rinaldi[1 2]*

Abstract: *In water-limited environments, water is the main limiting factor of crop production, especially in rainfed crops such as durum winter wheat (*Triticum durum *Desf.). Consequently, also in climatic change projections, it is essential both to recognise characteristics in breeding programs that can lead to drought tolerance and to reduce the time needed to observe variations of these traits on crop yield. Moreover, changing in management strategies could improve crop adaptation to climate change, not considered in this approach. Crop growth models can assist breeding research in identifying these traits. The CropSyst model was parameterized for durum wheat cultivated in Southern Italy: crop characteristics were analyzed, development (grain filling duration and phenologic response to water stress), canopy expansion (specific leaf area, leaf duration and ratio between leaf and stem) and water uptake (root length). Model sensitivity was evaluated varying one parameter at a time and changing the value by ± 5, ± 10 and ± 20% of calibrated values. Wheat was simulated with past real daily climatic data (55 years, from 1952 to 2006) and future daily climatic data predicted with an HADCM3 global climatic model (100 years, from 2000 to 2100) where an average air temperature increase of +2 °C is expected as well as a CO_2 concentration of 550 ppm (IPCC, A2 scenario). Leaf area duration and specific leaf area proved to be the parameters with the greatest impacts on wheat yield, with changing in wheat yield from -20 to16% and from -38 to 35% respectively as consequence to variation for these parameters oscillating between -20 and 20%. The ratio between the leaf and the stem biomass accumulation was inversely and linearly related to grain yield. Lengthening or shortening the grain filling duration did not seem to provide benefits in term of grain yield. The "non-response" in term of grain yield to water stress highlights that the wheat crop was optimized yet in Mediterranean environment in order to maintain production stability in drought conditions which could accelerate different crop phenological stages. The variation of maximum root depth (from 0.8 to 1.2 m) did not result in any significant variation in grain yield. The changes of crop morphology could also enhance climate change adaptation.*
Keywords: *in-silico genotype, CropSyst simulation model, crop yield, specific leaf area, leaf area duration.*

Riassunto: *In ambienti a sussidio idrico limitato, è l'acqua a rappresentare il fattore limitante le produzioni, specie per colture coltivate in asciutto, come il frumento duro (*Triticum durum *Desf.). Conseguentemente, anche in vista di cambiamenti climatici, è essenziale sia individuare nei programmi di miglioramento genetico quelle caratteristiche vegetali che possono portare a tollerare meglio lo stress idrico e sia ridurre il tempo necessario per valutare gli effetti delle variazioni di questi tratti sulla produzione. I modelli di crescita colturale possono aiutare i breeders nell'individuare questi tratti. Il modello CropSyst è stato parametrizzato per il frumento duro coltivato nel Sud Italia: le caratteristiche colturali analizzate sono state: sviluppo (durata del riempimento della granella e risposta fenologica allo stress idrico), espansione della canopy (area fogliare specifica, durata fogliare e rapporto foglie-culmo) e assorbimento idrico (lunghezza radicale). La sensibilità del modello ai cambiamenti di queste caratteristiche è stata valutata variando i parametri del ± 5, ± 10 e ± 20% dei valori calibrati. Il frumento è stato simulato per il passato con dati climatici giornalieri reali (55 anni, dal 1952 al 2006) e per il futuro con dati climatici giornalieri generati con il modello climatico globale HADCM3 (100 anni, dal 2000 al 2100), prevedendo un aumento medio delle temperature di +2 °C così come una concentrazione della CO_2 atmosferica di 550 ppm (IPCC, scenario A2). La durata fogliare e l'area fogliare specifica si sono dimostrati essere i parametri con il maggiore impatto sulla produzione finale con variazioni sulla produttività del frumento rispettivamente dal -20 al 16% e dal -38 al 35% per oscillazioni di tali parametri compresi tra -20 e 20%. Il rapporto foglie-culmo della biomassa accumulata è stato inversamente e linearmente correlato alla produzione, mentre nessun effetto ha dimostrato l'allungamento o l'accorciamento della durata della fase di riempimento del seme. La mancata riposta in termini produttivi a variazioni del parametro sulla risposta fenologica allo stress idrico, evidenzia come questa coltura sia stata già ben selezionata per l'ambiente Mediterraneo al fine di mantenere una certa stabilità di produzione in condizioni asciutte, accorciando la durata delle diverse fasi fenologiche. La variazione della massima profondità radicale (da 0.8 a 1.2 m) non ha significativamente influenzato la produzione finale. Le variazioni morfologiche della coltura possono essere utili anche nel processo di adattamento ai futuri cambiamenti climatici.*
Parole chiave: *genotipo, modello di simulazione CropSyst, produzione, area fogliare specifica, durata dell'area fogliare.*

Consiglio per la Ricerca e la Sperimentazione in Agricoltura
* Corresponding author: e-mail: garofalopasquale@virgilio.it
[1] Unità di Ricerca per i Sistemi Colturali degli Ambienti caldo-aridi, Bari
[2] Centro di Ricerca per la Cerealicoltura, Foggia
Received 06 December 2012, accepted 17 April 2013.

1. INTRODUCTION

In Mediterranean environments, water is the major limiting factor on field crop production, especially for crops that are not usually irrigated, such as durum winter wheat. In these envi-

ronments, the main goal for plant breeders is to focus on the complex interaction between crop growth and water availability, in order to maximize and stabilize the commercial yield. An improvement in crop performance under drought conditions has been achieved in recent years through the selection of traits that involved, for example, anthesis-silking interval in maize (Edmaedes *et al.*, 2004), transpiration efficiency in wheat (Condon *et al.*, 2004) or modification in growth habits for many species in response to different seasonal water supply.

As reported by several authors, the major genes that control plant growth and development are the same that are involved in stress response and thus for drought adaptation. Hsiao (1973) reports that cell expansion (and therefore plant growth) is the first process that suffers in a decrement in tissue water potential. Reymond *et al.* (2003) reports that leaf elongation has a strong genetic control, influenced by the water used by the crop throughout the season. From these examples it is clear how the identification of certain traits involved in rationalization and full exploitation of crop-available water is a crucial target in breeders' research on how to improve drought resistance and/or tolerance.

Some authors (Campos *et al.*, 2004; Cooper *et al.*, 2006) underlined how research studies to improve drought resistance should follow two steps; the first is to identify candidate traits, the second is to select or to engineer new adaptation genes. For the first step, an aid to identifying candidate traits in drought resistance and/or adaptation can be given by the crop simulation models. Jordan *et al.* (1983) carried out simulations to evaluate strategies for crop improvement in drought regions by changing simple crop traits, such as root depth, maturity time and osmotic adjustment.

The response of crops to water stress conditions and changing root volume was evaluated by Jones and Zur (1984). Sinclair and Muchow (2001) analyzed a number of plant traits in maize, such as leaf size, rate of leaf appearance, stomata closure and grain growth duration in order to improve crop yield in a water-limited environment.

Water availability during different wheat crop growth stages affects biomass accumulation, phenological path and yield components. Rajala *et al.* (2009), report as drought prior the pollination and terminal drought decrease net photosynthesis and stomatal conductance and, consequently, final dry biomass. Drought before pollination influences yield components, resulting in a lower number of fertile florets per number of spikes and number of grain per spike; water availability after pollination increases single grain weight, furnishing grain yield greater than well watered wheat plants. On the contrary, terminal drought reduces significantly the single grain weight compared to well watered treatment, maintaining the same number of fertile florets, but reducing the number of grains per spike: this causes a low grain yield.

Cereals use different strategies to adapt to different conditions of limited water supply (Tambussi *et al.*, 2007); this adaptation can follow two different strategies; avoiding the risk of drought disease, for example by shortening the growing cycle or improving the root system (avoidance), or tolerating the water deficit, ensuring adequate productivity also under water stress (tolerance).

Temperature is a crucial factor for wheat productivity, which determines both phenological development (Bauer *et al.*, 1984) and growth rates (Grace, 1988). Besides, temperature affects leaf appearance (Baker *et al.*, 1980), respiration (Goudriaan *et al.*, 1985), rate of grain-filling (Wardlaw, 1994), evapotranspiration and water stress (Ritchie, 1972). It is possible to link temperature to wheat response, as water stress, phenology (vegetative and reproductive stages) and physiology (photosynthesis, respiration and grain-filling). All these effects are self-correlated and it is difficult to separate their overall effect on grain yield and, consequently, identify a clear relationship between wheat productivity and temperature.

In Mediterranean environments, the wheat development and reproductive stages occur with air temperatures usually higher than the optimal. High temperatures during the grain filling stage can reduce single grain weight as reported by several authors (Savin *et al.*, 1996; Passarella *et al.*, 2002; Plaut *et al.*, 2004). This trend was confirmed also for other cereals, such as sorghum, as reported by Rinaldi and De Luca (2012), with a decrease in term of grain yield up to 20% compared to current sorghum grain yield, as result of long term simulations, the latter set to future maximum temperature increment up to 5 °C.

On the other hand, Rinaldi *et al.* (2009) reported as the response of three crop simulation models for durum wheat productivity in Mediterranean environment to temperature increment was contrasting.

Anyway, because of their dynamic response, crop simulation models also offer the opportunity to explore the effects of changing the rates of various physiological processes, driven by the simple traits previously identified for crop simulations. For example, Hoogenboom *et al.*, (1994) used the BEANGRO model to investigate the effects of changing specific leaf area (*SLA*), root portioning, rooting depth and root length, root weight on seed yield ratio and water use efficiency (*WUE*) of the common bean. PNUTGRO was used by Boote and Jones (1988) to evaluate 16 parameters on groundnut yield under rain-fed conditions over 21 years. They found that yields increased over 15% by lengthening the duration of the vegetative and reproductive phases and canopy photosynthesis. An important issue that could be addressed by simulation models is predicting the response for the novel genotype both in different environments and for the same environment in different climatic conditions. Indeed, the evaluation of a new genotype in different conditions and over several years requires a great deal of time and human resources. It is expensive, and not entirely practical, to assess different plant germoplasms using conventional multi-site and multi-season trials. This aspect is of crucial importance in creating new genotypes whose value should be evaluated on expected future climatic scenarios, obtainable by means of global climatic models. In fact, as reported by the Intergovernmental Panel on Climate Change (Bates *et al.*, 2008), anthropogenic greenhouse gas emission, if not reduced, could lead to an increase of global surface temperature from 1.5 to 4.5 °C.

Rosenzweig and Tubiello (1996) used CERES-wheat to evaluate the effect of changes in minimum and maximum temperature on wheat yields: temperature increase involves in a contrasting path for dry biomass, with positive or negative oscillations compared to baseline simulated biomass; however, they reported from slight to high decrement in term of yield, if daily mean temperature raises from +1 to +4 °C. Semenov (2009) reported a study on wheat, using 100 years of synthetic climatic data generated by the LARS-WG stochastic weather generation and calibrated in two locations in the UK and Spain. He concluded that changes in parameters controlling the effects of water stress on leaf senescence and biomass accumulation had the largest impact on grain yield under drought (up to 70% in yield compared with control), whereas phyllochron and grain weight did not improve yields.

The aim of this study is to analyze the effects of variations in different traits of durum wheat on grain yield as affected by future climate change, also if in this approach adaptation strategies, crop management are not considered.

2. MATERIALS AND METHODS

2.1 The simulation model

CropSyst is a multi-year, multi-crop, daily time-step cropping system simulation model, used to simulate soil water budget, crop phenology, canopy and root growth, biomass production, crop yield, residue production and decomposition, soil erosion by water and salinity (Stockle *et al.*, 2003).

The simulation of crop development is based on thermal time which is necessary to reach a given growth stage, taking into account average air temperature above a base temperature and below a cut-off temperature.

Potential biomass is calculated from the crop potential transpiration-dependent biomass production, multiplying the biomass-transpiration coefficient with the potential transpiration, the latter divided by the daytime mean atmospheric vapour deficit. This relationship, however, shows an important weakness; at low VPD it predicts infinite growth.

To overcome this problem, a second estimate of unstressed biomass production is calculated multiplying the radiation-use efficiency by the daily amount of crop-intercepted photosynthetically active radiation. During each time step, the potential rate is taken as the minimum between the two potential biomasses. The actual biomass is calculated from the potential biomass for which water or nitrogen limitation determines a reduction.

The increase of leaf area during the vegetative period, expressed as leaf area per unit soil area (leaf area index, *LAI*) is calculated from the model by the ratio between the specific leaf area (*SLA*) and the cumulated aboveground biomass, the latter multiplied by the partitioning coefficient for the biomass of the leaves.

Root growth in CropSyst is described in terms of root depth and root density. Root depth is synchronized with leaf area growth and influenced by water or nitrogen concentration.

Grain yield simulation depends on cumulated

Layer	Depth (m)	Sand (%)	Clay (%)	Silt (%)	Permanent wilt point (m^3/m^3)	Field capacity (m^3/m^3)	Bulk density (t/m^3)	Vol. WC at -1500 J/kg (m^3/m^3)	Vol. WC at -33 J/kg (m^3/m^3)	pH
1	0.20	12.9*	43.7*	43.4*	0.22*	0.44*	1.20*	0.25**	0.41**	8.5*
2	0.40	12.9*	43.7*	43.4*	0.22*	0.44*	1.20*	0.25**	0.41**	8.5*
3	0.60	12.9*	43.7*	43.4*	0.22*	0.44*	1.20*	0.25**	0.41**	8.5*
4	0.70	9.6*	54.6*	35.8*	0.30*	0.44*	1.45*	0.30**	0.44**	8.5*
5	1.13	21.5*	34.6*	43.9*	0.19***	0.35***	1.29***	0.19***	0.35***	8.5*
6	1.35	34.4*	27.7*	37.9*	0.16***	0.30***	1.35***	0.16***	0.30***	8.5*

* Measured

** Computed by CropSyst model from user specified value

*** Estimated from texture

Tab. 1 - Values of parameters, describing the soil characteristics, used to perform the simulation in the study area (Foggia).
Tab. 1 - Valori dei parametri delle caratteristiche del suolo, usati per la simulazione nell'area di studio (Foggia).

plant biomass and the relative harvest index, modified according to the water and nitrogen stress intensity that occur during flowering and grain filling.

The first step adopted by CropSyst to estimate dry biomass is to calculate the potential biomass, deriving from optimal conditions in terms of water supply. Actual biomass is estimated by replacing the potential transpiration (*Tp*) with actual transpiration (*Tact*) as a consequence of water limitation. The ratio between *Tact* and *Tp*, both derived by model outputs, was used to calculate the water stress index (*WSI*), in order to show whether the variation in crop parameters can influence grain yield in relation to different *WSI* levels. If *Tact* fits with *Tp*, the *WSI* is equal to 1 (no stress), whereas the value 0 indicates the maximum stress.

The CropSyst version used for this research was 4.05.05. Durum wheat crop parameters for the Simeto cultivar were obtained from previous calibration activity in the same location (Donatelli *et al.*, 1997; Garofalo *et al.*, 2009).

The yearly output considered in this study were the peak of *LAI*, grain yield, aboveground dry biomass, potential transpiration and actual transpiration. In addition, *WSI* and flowering-maturity duration were also used to evaluate model sensitivity to crop parameter changes.

For each simulation output (100 years), the mean value, standard deviation and coefficient of variation (*CV*) as ratio between standard deviation and mean were calculated.

2.2 Location and climate

The pedo-climatic conditions chosen for this study are representative of the Mediterranean environment, as well as the durum wheat cultivar (Simeto) which is widely used by local farmers.

The site used was near Foggia (Apulia region, Italy; 41° 27' lat. N, 15° 04' long. E, 90 m asl); the soil is a vertisol of alluvial origin, Typic Calcixerert (Soil Taxonomy 10th, USDA, 2006). In Tab.1 the soil crop input for the CropSyst simulation are shown. The climate is "accentuated thermo-Mediterranean" (FAO-UNESCO, 1963) classification, with minimum temperatures below 0 °C in the winter and maximum temperatures above 40 °C in the summer. Annual rainfall (mean 550 mm, considering a 50-year long period) is mostly concentrated during the winter months and class "A pan" evaporation exceeds 10 mm d^{-1} in summer (average of maximum daily values recorded in July and August).

A "*past*" simulation, representing the reference period or the baseline, was carried out with measured daily climatic data (55 years, from 1952 to 2006). A "*future*" long term simulation (100 years) was performed using daily climatic data predicted by the Joint Research Centre (Ispra, Italy) with an HADCM3 global climatic model and IPCC A2 scenario. These data were statistically downscaled to a 50 km grid for a better adaptation to real conditions, from 2000 to 2100 (Pizzigalli *et al.*, 2012). These climatic data were used in previous works at different time frames (30 years) (Rinaldi and De Luca, 2012; Ventrella *et al.*, 2012), but in this specific sensitivity analysis the main focus is about average climatic behaviour of XXI century.

2.3 Crop model traits

Traits concerning wheat drought avoidance and tolerance were examined, as described below,

varying one parameter at a time and changing the value for each trait by ± 5, ± 10 and ± 20% of calibrated values.

2.3.1 Specific Leaf Area (SLA)
SLA represents the mean leaf area per unit of dry leaf weight; it measures leaf density or relative thickness (Hunt, 1982). As it is influenced by environment and growth stages, it is a useful variable for characterising the development of photosynthetic apparatus of crop plants. An increase in the leaf area development of a cereal crop is associated with an increment in water use efficiency (Lopez-Castaneda and Richards, 1994). Indeed, an increase in leaf area affects soil surface shading and reduces soil water evaporation, increases weed competition for solar radiation capture (Coleman *et al.*, 2001) and permits a more stable transpiration in case of low pressure deficit (Fischer, 1979). Lopez-Castaneda *et al.* (1995) showed that an increase in *SLA* on wheat was due to leaf area increase more than a reduction of leaf weight; this was accompanied by greater photosynthesis activity, as reported by Richards (2000). Xinyou *et al.* (1999) identified at least three chromosomal regions associated with genotypic variations for *SLA* in barley. Moreover, Rebetzke (2004) indicates that there is the possibility of an increased *SLA* in new wheat genotypes, with a possible variation of about 20%.
The calibrated value of *SLA* was 17 m^2 kg^{-1}.

2.3.2 Leaf Duration (LD)
Leaf duration represents the time that elapses between the appearance and senescence of a new green leaf. This parameter, coupled with *SLA*, greatly influences the amount of photosynthetically active leaf dry matter, crucial for solar radiation interception and plant biomass accumulation.
An increase in leaf duration is one of the key strategies used to improve grain yield under water-limited conditions (Triboi and Triboi-Blondel, 2002). Simon (1999) crossed 4 wheat cultivars, observing variations of 33% in leaf duration after breeding between crossed varieties as a consequence of heritability. The same author pointed out that breeding work in improving leaf duration is slow and that consequently, any further research should be carried out in this way.
The effect of leaf duration on yield in wheat was evaluated changing the calibrated value of 720 growing degree days (*GDD*).

2.3.3 Ratio between leaf and stem (RLS)
This parameter adjusts the proportion of cumulative biomass that is partitioned to green leaf area production as the crop accumulates biomass during the active growth stage. It is used to determine the amount of green area index produced in a day. CropSyst, according to the dry biomass calculated in the previous day, estimates the daily green area, using *SLA* and *RLS* coefficients. This parameter is reported as the basis for grain yield production in wheat (Jaradat, 2009). Results for grain yield as a consequence of variations in stem and leaf partition are not easy to predict; a greater allocation of dry matter to the stem could increase the translocation to the grain during the grain filling period. On the other hand, a greater leaf surface would allow a better pattern for light interception and transpiration.
In CropSyst, *RLS* is a coefficient used in the calculation of new green leaf area produced in a day: it is inversely related to green leaf area.
RLS was changed in this simulation by ± 20%, a range that is between the genetic variation in leaf surface observed by Shearman *et al.* (2005) and the genetic variation for stem cumulated dry matter as reported by Jaradat (2009).

2.3.4 Grain filling duration (GFD)
Conflicting results in terms of the beneficial effects on grain yield emerged with regard to the length of the grain filling phase. Evans and Fisher (1999) suggested that an increased grain-filling period is a possible trait to increase wheat yield. By contrast, Ehdaie (1995) showed that there was a negative association between yield and the length of period from anthesis to maturity in different cultivars of wheat. Further, Semenow and Shewry (2011) reported that heat stress around flowering produced significant yield losses in wheat growing in North Europe.
In CropSyst, grain yield is calculated as the biomass at harvest multiplied by the harvest index adjusted for sensitivity to water stress that occurs during grain filling. An increase in the grain filling period potentially enhances the amount of biomass accumulated by the crop by transpiration or intercepted radiation. Generally, grain filling occurs during low water soil storage and/or low water supply and therefore lengthening in this phenological stage may determine a reduction in terms of harvest index.
The grain filling duration was changed by ± 20% using a calibrated value of 560 *GDD*, whereas genetic variations for *GFD* were reported to be ±

40% by various authors (Akkaya *et al.*, 2006; Robert *et al.*, 2001).

2.3.5 Phenological response to water stress (PRWS)

Temperature is the primary environmental factor controlling development of wheat, whereas other factors, such as water, play a secondary but still important role (Bauer *et al.*, 1984; Baker *et al.*, 1986; McMaster, 1997; McMaster *et al.*, 1999). McMaster and Wilhelm (2003) report that several wheat cultivar within a water stress treatment, reached all growth stages earlier under water stressed conditions except for emergence and jointing. Moreover, in almost every case, cultivars achieved each growth stage at different times within a water treatment, with differences among cultivars of 43.8% when referred to a mean value of *GDD* required to attain maturity.

In CropSyst, water stress tends to increase the crop canopy temperature, which may accelerate the accumulation of degree days needed to reach different phenological stages. In particular, this coefficient (set as 1 for the calibrated crop) is a part of the *Tmax* calculation actively perceived by the crop; the greater this value, the quicker the crop reaches different phenological stages.

2.3.6 Maximum root depth (MRD)

Maximum root depth is a crop model parameter that influences water soil extraction from the deepest layers; the model simulates the attainment of this value at the beginning of senescence in unstressed plants and it is used to estimate the effective root depth for each day, taking into account the actual canopy expansion.

As reported by Tripathi and Mishra (1986), wheat root depth can extend more than 1.50 m also in rain-fed conditions. In this sensitivity analysis, *MDR* calibrated value of 1 was changed between 0.8 and 1.2 m.

3. RESULTS

During the wheat growing period it is possible to observe as *future* winter minimum (*Tmin*) and maximum temperature (*Tmax)* are always greater than in the *past*, with a mean temperature (*Tmean*) 1.03 °C higher. In March and April the *past* scenario has a *Tmean* slightly greater than the *future* (0.64, on average), whereas *Tmean* was similar in May. On the contrary, in *future* June, the increase is 1.8 °C for *Tmin* and 2.7 °C for *Tmax*.

Globally, it is possible to assess that during the crop growth season, +1°C is the average increase in term of temperature, compared to the *past*, with the greater raise during the grain filling stage, and cumulated rain predicted by the climatic model is lower than the *past* of only 13 mm.

The first simulation was carried out using the calibrated crop parameters in order to compare *"past"* vs *"future"* climatic scenarios. Daily average temperatures (*Tmean*) in the previous 50 years (*past*) and in the next 100 years (*future*) in the A2 scenario are shown in Fig. 1. From wheat sowing to flowering, the *past* climate was characterized by a *Tmean* slightly lower if compared with *future*; this explains the gap of 11 days between *past* and *future* flowering dates. In the second part of growing cycle, *Tmean* in *past* and *future* scenarios were very similar and the time elapsed from sowing to grain maturity was 147 days in the *past* and 152 in the *future* scenario.

CropSyst simulated in the *future* an average of 2700 kg ha^{-1} (± 383 kg ha^{-1}) of wheat grain yield, slightly greater if compared to 2567 kg ha^{-1}(± 322 kg ha^{-1}) derived from the simulation made for the previous 50 years (*past*). Same trend is reported by Ventrella *et al.* (2012), which indicated wheat yield increment of 11% compared to the baseline, after long term simulation with CERES-wheat model set to future increment in term of T_{max} (projected for 30 years) equal to 2.3 °C. This

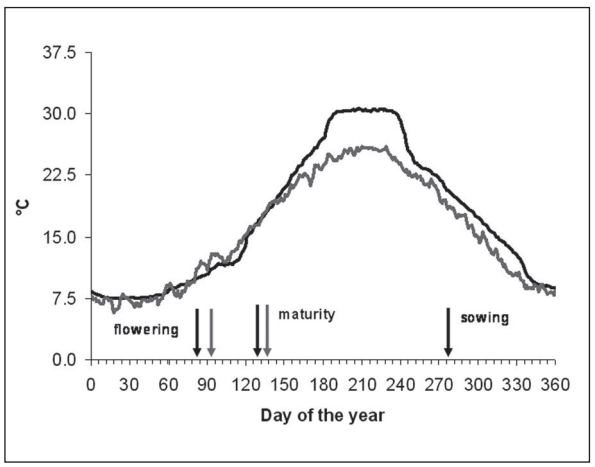

Fig. 1 - Daily mean temperature for the future (black line) and past (gray line). In graph are reported the flowering and grain maturity time, for the future (black arrow) and for the past (gray arrow). Sowing date is the same for all scenarios.
Fig. 1 - Temperatura media giornaliera per il futuro (linea nera) e per il passato (linea grigia). In grafico sono riportate le date di fioritura e maturità, per il futuro (freccia nera) e per il passato (freccia grigia). La data di semina è la stessa per tutti gli scenari.

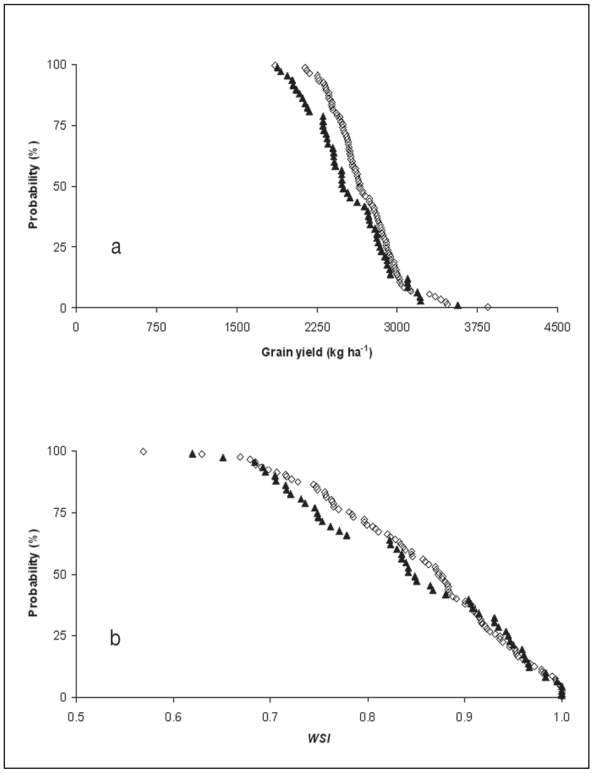

Fig. 2 - Cumulative distribution functions of probability to exceed values of grain yield (a) and Water Stress Index (*WSI*) (b), for the *past* (full triangle) and for the *future* (empty rhombus).
Fig. 2 - Funzioni di distribuzione cumulata della probabilità di eccedere valori di produzione di granella (a) e Water Stress Index (WSI) (b), per il past *(triangolo pieno) e per il* future *(rombo vuoto).*

difference could be explained by the time elapsed between grain filling and grain maturity for both scenarios. In fact, CropSyst estimated 30 vs 33 days for wheat to gain the grain maturity, in the *past* and in the *future*, respectively. As reported in Fig. 2a, the fiftieth percentile oscillates between 2480 for the *past* and 2650 kg ha^{-1} for the *future* while the minimum wheat yield in this environment was similar for both climatic scenarios and equal to about 1800 kg ha^{-1}. This trend is confirmed by the cumulative probability to exceed *WSI* values (Fig. 2b), which shows that for both time series, the actual crop transpiration simulated by the model is always greater than the 60% of potential crop transpiration. Fig. 2b also indicates that for both simulated periods the previously "calibrated" wheat is well suited to this environment, since already at the fiftieth percentile, actual transpiration exceeds 80% of potential transpiration in the *past* and *future* scenarios.

3.1 Specific Leaf Area

Variations in *SLA* determined a high impact on grain yield. In fact, tuning *SLA* from -20% to +20% of input, a large range of variation in grain yield (from -37.8% to 34.7%) was observed, with yield of 2074 and 3027 kg ha^{-1}, respectively (Tab. 2). The coefficient of variation was, respectively, 15.1 and 12.9% for -20% and 20% in *SLA* changes. Moreover, a small variation of this parameter caused significant variations in wheat productivity; a -5% change in *SLA* caused a reduction in yield of about 8.7% if compared with the average yield for the calibrated crop (2701 kg ha^{-1}), whereas an increase in productivity of about 10% was observed if *SLA* was increased of 5%.

Tab. 2 shows that the response of this parameter was influenced by water stress (*Tp* and *Tact*). When the *WSI* is high (*Tact* is different from *Tp*) the yield obtained from the simulation with high *SLA* values was greater if compared with that obtained with calibrated or low *SLA* values (Fig. 3).

3.2 Leaf Duration

The lengthening of the "active" leaves duration during crop cycle produces a delay of senescence and, consequently, has a positive effect in increasing grain yield. In fact, the model simulated a rise of about 20% (3130 kg ha^{-1}) in response to an increase in *LD* of 20%. This linearity is also maintained in the other steps of *LD* variation, whereas an increase of 10% and

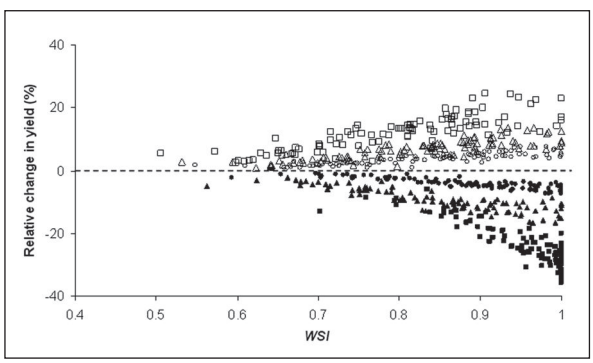

Fig. 3 - Relative change in grain yield in response to a -20% (full square), -10% (full triangle), -5% (full circle), +5% (empty circle), +10% (empty triangle) and +20% (empty square) variation of Specific Leaf Area (*SLA*, base value = 17 kg m^{-2}) versus *WSI* (0 = maximum stress; 1 = no stress).
Fig. 3 - Variazione relativa della produzione di granella in risposta a modificazioni del -20% (quadrato pieno), -10% (triangolo pieno), -5% (cerchio pieno), +5% (cerchio vuoto), +10% (triangolo vuoto) e +20% (quadrato vuoto) dell'Area Fogliare Specifica (SLA, valore di riferimento = 17 kg m^{-2}) rispetto al WSI (0 = massimo stress; 1 = assenza di stress).

Traits	Units and calibrated values	Perturbated values %	Peak of LAI $m^2 m^{-2}$	Grain yield kg ha^{-1}	Above ground dry biomass kg ha^{-1}	Potential transpiration mm	Actual transpiration mm	WSI	Flowering-Maturity days
SLA	$m^2 kg^{-1}$	*-20 (13.6)*	1.6 (13.6)	2074 (15.1)	7000 (15.2)	128 (16.7)	120 (14.8)	0.95 (6.6)	54 (7.9)
	17	*-10 (15.3)*	2.0 (10.9)	2443 (12.6)	8264 (12.6)	188 (13.2)	159 (13.7)	0.85 (11.8)	54 (7.9)
		-5 (16.2)	2.3 (9.8)	2591 (12.1)	8783 (11.9)	176 (13.8)	153 (13.5)	0.88 (10.6)	54 (7.9)
		+5 (17.9)	2.8 (8.1)	2804 (12.0)	9541 (11,5)	202 (12.6)	168 (13.7)	0.84 (12.4)	54 (7.8)
		+10 (18.7)	3.0 (7.5)	2884 (12.3)	9829 (11.6)	213 (12.2)	174 (13.9)	0.82 (13.0)	54 (7.8)
		+20 (20.4)	3.4 (6.5)	3027 (12.9)	10354(11.9)	234 (11.5)	185 (14.4)	0.80 (14.0)	54 (7.8)
LD	*°C d*	*-20 (576)*	2.3 (9.7)	2177 (12.4)	7380 (12.5)	175 (13.9)	153 (13.5)	0.88 (10.6)	54 (7.9)
	720	*-10 (648)*	2.4 (9.2)	2451 (11.8)	8316 (11.6)	183 (13.4)	157 (13.5)	0.86 (11.2)	54 (7.8)
		-5 (684)	2.5 (9.1)	2578 (11.8)	8753 (11.6)	186 (13.3)	159 (13.5)	0.86 (11.5)	54 (7.8)
		+5(756)	2.6 (8.9)	2816 (12.2)	9564 (11.7)	191 (13.4)	161 (13.6)	0.85 (11.7)	54 7.9)
		+10 (792)	2.6 (8.8)	2927 (12.5)	9940 (11.9)	192 (13.0)	162 (13.6)	0.85 (11.8)	54 (7.9)
		+20 (864)	2.6 (8.6)	3130 (13.2)	10633 (12.5)	195 (12.8)	164 (13.6)	0.85 (11.9)	54 (7.8)
RLS	$m^2 kg^{-1}$	*-20(2.5)*	2.9 (9.7)	2872 (12.8)	9777 (12.2)	207 (13.1)	170 (14.0)	0.83 (12.8)	54 (7.8)
	3.10	*-10 (2.8)*	2.7 (9.3)	2786 (12.3)	9471 (11.9)	197 (13.1)	165 (13.8)	0.84 (12.2)	54 (7.8)
		-5 (2.9)	2.6 (9.1)	2741 (12.1)	9314 (11.7)	193 (13.2)	163 (13.7)	0.85 (11.8)	54 (7.9)
		+5 (3.3)	2.4 (8.8)	2657 (11.8)	9016 (11.5)	184 (13.2)	158.(13.4)	0.86 (11.2)	54 (7.8)
		+10 (3.4)	2.4 (8.6)	2616 (11.6)	8872 (11.4)	181 (13.2)	156 (13.3)	0.87 (10.9)	54 (7.8)
		+20 (3.7)	2.2 (8.4)	2532 (11.4)	8579 (11.2)	173 (13.2)	152 (13.1)	0.88 (10.3)	54 (7.9)
GFD	*°C d*	*-20 (448)*	2.5 (9.0)	2707 (11.0)	9177 (10.9)	170 (13.8)	151 (13.5)	0.89 (10.1)	48 (8.4)
	560	*-10 (504)*	2.5 (9.0)	2704 (11.8)	9173 (11.6)	179 (13.3)	156 (13.4)	0.88 (10.9)	51 (8.1)
		-5 (532)	2.5 (9.0)	2702 (11.9)	9171 (11.6)	184 (13.3)	158 (13.5)	0.87 (11.2)	53 (8.0)
		+5 (588)	2.5 (9.0)	2699 (11.9)	9168 (11.6)	194 (13.1)	163 (13.6)	0.85 (12.2)	55 (7.8)
		+10 (616)	2.5 (9.0)	2697 (11.9)	9167 (11.6)	198 (12.9)	165 (13.6)	0.84 (12.3)	57 (7.6)
		+20 (672)	2.5 (11.9)	2694 (11.9)	9164 (11.6)	208 (12.8)	168 (13.8)	0.82 (12.8)	59 (7.4)
PRWS	*-*	*-20 (0.8)*	2.5 (9.0)	2701 (11.9)	9170 (11.6)	189 (13.2)	160 (13.5)	0.86 (11.6)	54 (7.8)
	1	*-10 (0.9)*	2.5 (9.0)	2701 (11.9)	9170 (11.6)	189 (13.2)	160 (13.5)	0.86 (11.6)	54 (7.8)
		-5 (0.95)	2.5 (9.0)	2701 (11.9)	9170 (11.6)	189 (13.2)	160 (13.5)	0.86 (11.6)	54 (7.8)
		+5 (1.05)	2.5 (9.0)	2700 (11.9)	9170 (11.6)	189 (13.2)	161 (13.6)	0.86 (11.6)	54 (7.9)
		+10 (1.1)	2.5 (9.0)	2700 (11.9)	9169 (11.6)	189 (13.2)	160 (13.5)	0.86 (11.5)	54 (7.9)
		+20 (1.2)	2.5 (9.0)	2700 (11.9)	9169 (11.6)	189 (13.2)	160 (13.5)	0.86 (11.5)	54 (7.8)
MRD	*m*	*-20 (0.8)*	2.5 (9.1)	2669 (12.3)	9076 (11.8)	188 (13.2)	157 (13.9)	0.84 (12.3)	54 (7.8)
	1.0	*-10 (0.9)*	2.5 (9.0)	2690 (12.0)	9137 (11.7)	188 (13.2)	159 (13.7)	0.85 (11.8)	54 (7.8)
		-5 (0.95)	2.5 (9.0)	2696 (12.0)	9155 (11.6)	189 (13.2)	160 (13.6)	0.85 (11.6)	54 (7.8)
		+5 (1.05)	2.5 (8.9)	2704 (11.9)	9180 (11.6)	189 (13.2)	161 (13.5)	0.86 (11.5)	54 (7.8)
		+10 (1.1)	2.5 (8.9)	2706 (11.9)	9188 (11.5)	189 (13.2)	161 (13.5)	0.86 (11.4)	54 (7.8)
		+20 (1.2)	2.5 (8.9)	2710 (11.8)	9198 (11.5)	189 (13.1)	161 (13.4)	0.86 (11.4)	54 (7.8)
Simulation results with calibrated values			**2.5 (9.0)**	**2701 (11.9)**	**9170 (11.6)**	**189 (13.2)**	**160 (13.5)**	**0.88 (11.5)**	**54 (7.8)**

SLA = Specific Leaf Area; *LD* = Leaf Area Duration; *RLS* = Ratio between Leaf and Stem; *GFD* = Grain Filling Duration; *PRWS* = Phenological response to water stress; *MRD* = Maximum Root Depth; *LAI* = Green Leaf Area Index; *WSI* = Water Stress Index.

Tab. 2 - Mean values and variation coefficients (bracket), for some outputs simulated by CropSyst in 100 years for the future, in response to change in cultivar parameters. For perturbated values in brackets are reported specific values of each traits used in the simulation.

Tab. 2 - Medie e coefficienti di variazione (in parentesi), di alcuni output derivanti dalla simulazione di CropSyst per 100 anni futuri, in risposta della variazione dei parametri colturali. Per i parametri variati (terza colonna) in parentesi sono riportati i valori specifici di ciascun tratto usato nella simulazione.

5% resulted in an average value for grain yield of 2927 and 2816 kg ha^{-1}, respectively (Tab. 2). A decrease of yield of 19.4, 9.3 and 4.5 % if compared with the calibrated crop (2701 kg ha^{-1}) was simulated by the model, consequence to a reduction in *LD* of 20, 10 and 5%, respectively.

The variability in grain yield over the years (*CV*) was between 13.2 observed in *LD* +20% and 11.8% recorded in *LD* -10 and -5%; this variation in *LD* did not influence crop *Tp* and *Tact* in any significant way, keeping the *Tp* (175 mm for -20%; 195 mm for 20%) and *Tact* (153 mm for -20%; 164 mm for +20%) close to the values obtained with the calibrated crop parameter (189 mm for *Tp* and 160 mm for *Tact*).

The model used *LD* to calculate the dry biomass gained for every day, but not to estimate the different phases length: consequently, the time elapsed between grain filling and grain maturity resulted similar in the *LD* variation and equal to 54 days.

Fig. 4 shows that increasing water stress (low *WSI*), the crop with high *LD* values produced more yield; for instance, when the *WSI* is approximately 0.6, the crop with *LD* -20% suffered a yield decrease of 10% if compared with the calibrated crop, whereas crops with *LD* +20% showed a relative change in yield of about 7%.

3.3 Ratio between leaf and stem

CropSyst simulations reported that at -20% of calibrated value, grain yield increased by 6.3%, whereas an increase at +20% determined a

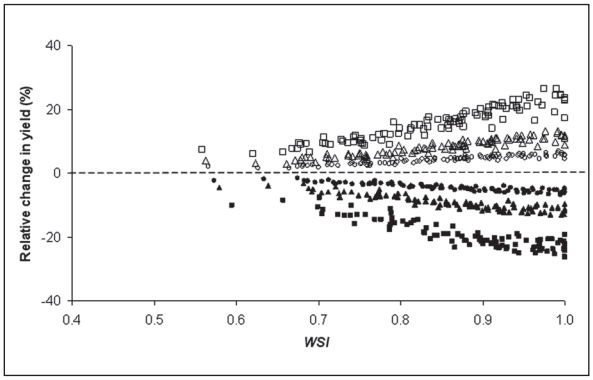

Fig. 4 - Relative change in grain yield in response to a -20% (full square), -10% (full triangle), -5% (full circle), +5% (empty circle), +10% (empty triangle) and +20% (empty square) variation in Leaf area Duration (*LD*, base value = 720 growing degree days) versus *WSI* (0 = maximum stress; 1 = no stress).

Fig. 4 - Variazione relativa della produzione di granella in risposta a modificazioni del -20% (quadrato pieno), -10% (triangolo pieno), -5% (cerchio pieno), +5% (cerchio vuoto), +10% (triangolo vuoto) e +20% (quadrato vuoto) della Durata dell'Area Fogliare (LD, valore di riferimento = 720 gradi giorno) rispetto al WSI (0 = massimo stress; 1 = assenza di stress).

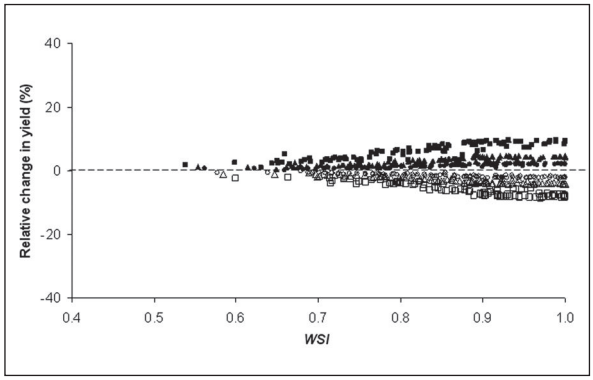

Fig. 5 - Relative change in grain yield in response to a -20% (full square), -10% (full triangle), -5% (full circle), +5% (empty circle), +10% (empty triangle) and +20% (empty square) variation in Ratio between Leaf and Stem (*RLS*, base value = 3.10 m^2 kg^{-1} versus *WSI* (0 = maximum stress; 1 = no stress).

Fig. 5 - Variazione relativa della produzione di granella in risposta a modificazioni del -20% (quadrato pieno), -10% (triangolo pieno), -5% (cerchio pieno), +5% (cerchio vuoto), +10% (triangolo vuoto) e +20% (quadrato vuoto) del Rapporto Area Fogliare/ Peso del Culmo (RLS, valore di riferimento = 3.10 m^2 kg^{-1}) rispetto al WSI (0 = massimo stress; 1 = assenza di stress).

reduction in grain yield of 6.3%. Halving the changed value for *RLS* also halved the relative change in yield (Tab. 2). Thus, the existence of a linear proportionality of *RLS* with grain yield suggests breeding programs improving the wheat plant "stem vs leaves" proportion.

The water stress level influenced productivity at the variation of this parameter very poorly, as reported in Fig. 5; in fact, at high values of water stress (*WSI* between 0.5 and 0.6), the maximum gap in yield between the modified crop (-20 and +20% of *RLS*) and the calibrated crop was only ±2.5%.

3.4 Grain filling duration

This parameter did not influence wheat yield productivity. In fact, considering the two extreme values for attainment of physiological maturity (2204 vs 2428 *GDD*), the yield oscillated between 2707 kg ha^{-1} (*GFD* -20%) and 2694 kg ha^{-1} (*GFD* +20%) (Tab. 2), with *CV* ranging between 10.9 and 11.6 for -20 and 20% in *GFD*, respectively. Variation in time necessary to reach the grain physiological maturity from the start of grain filling, resulted different among wheat trait alterations; 11 days was the maximum gap, observed between -20 and 20% in *GFD*. A reduction in *GFD* had as a consequence the soil moisture preservation, thanks to the less transpired crop water; on average, water saving was about 10 mm, an amount not particularly large, but enough to prevent water stress in the final phase of crop cycle.

The variation in terms of productivity, as a consequence of changes in *WSI*, was the same for all the six levels of modified crop parameter. In fact, the grain yield response, considering the grain filling-maturity stage time, was slightly affected by water stress, but considerably influenced by air temperature. Even though the lengthening of period from grain filling to maturity would let to increase the time to allocate the dry matter to the grain, it is more probable that the crop would suffer for high temperatures. Therefore, the response in term of yield and yield variation compared to the calibrated value at different level of *WSI*, was similar for all perturbed traits.

3.5 Phenological response to water stress

The modification of *PRSW* in the calibrated crop (with 1 as calibrated value) did not produce variation in grain yield (Tab. 2). In fact, grain yield values with the modified *PRSW* were constantly around 2701 kg ha^{-1}, with a *CV* value of 11.9 over the total years; the shortening of crop development due to variations in *PRWS* was only 2 days for flowering, peak *LAI* and

physiological maturity dates between the two extremes (+ and – 20% of *PRWS*). The time from grain filling to maturity remained 54 days, because all phenological stages were shifted among modified traits (Tab. 2). This trend was also confirmed by the yield response to *WSI*, which resulted almost identical in all water stress conditions.
From these observations, it is possible to conclude that wheat crop was yet optimized in breeding programs in Mediterranean environments and it is able to maintain constant production also in drought conditions.

3.6 Maximum root depth
This trait influenced grain yield, especially when it was reduced. If we consider the minimum root length value (0.8 m) set at -20% of the *MRD* calibrated value, the variation in grain yield was -5.0%. This gap was smaller with an increment in *MRD*, with a decrease in grain yield of 2.1% and 0.9% for -10 and -5% variations in *MRD*, respectively, with no water saving in terms of crop consumption (Tab. 2). Increasing the *MRD*, some limited advantages in terms of yield were observed; from 1.5 to 2.6% in grain yield improvement with an *MRD* rise from 5 to 20%.
Despite the fact that the benefits in terms of average yield are not so remarkable, an increase in *MRD* ensured the same level of relative change in yield in response to variations in *WSI* (Fig. 6). This is of particular importance, because in water-limited environments, water stress conditions will become more frequent: thus, a trait that requires improvement in cereal breeding programs is the ability of new varieties to explore a larger soil volume and to extract more water.

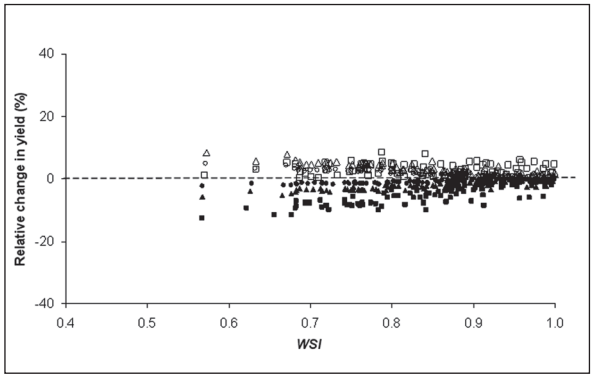

Fig. 6 - Relative change in grain yield in response to a -20% (full square), -10% (full triangle), -5% (full circle), +5% (empty circle), +10% (empty triangle) and +20% (empty square) variation in Maximum Root Depth (*MRD*, base values = 1.0 m) versus *WSI* (0 = maximum stress; 1 = no stress).
Fig. 6 - Variazione relativa della produzione di granella in risposta a modificazioni del -20% (quadrato pieno), -10% (triangolo pieno), -5% (cerchio pieno), +5% (cerchio vuoto), +10% (triangolo vuoto) e +20% (quadrato vuoto) della Massima Profondità Radicale (MRD, valore di riferimento = 1.0 m) rispetto al WSI (0 = massimo stress; 1 = assenza di stress).

4. DISCUSSION

The sensitivity analysis carried out with future climatic data allowed to assess the genetic wheat traits more sensitive in grain yield forecasting and water supply conditions.
SLA, *LD* and *RLS* were the traits whose alteration produced the greatest impact on grain yield. These traits modified leaf activity, increasing the surface (as in the case of *SLA*), renewing the leaves (*RLS*) or extending the biomass accumulation period through the lengthening of leaf vitality (*LD*).
The greatest contribution of *SLA* in raising wheat grain yield is the increase of water transpired by the crop; at a constant value of transpiration water efficiency (implemented as a crop parameter), the cumulated biomass is linearly related to water use. At *SLA* +20%, both *Tp* and *Tact* increased by 24% and 15%, respectively, a small change if compared with the *Tact* reported for the calibrated crop (160 mm, Tab. 2), but enough to raise grain yield by 12%. This improvement in productivity is greater than that reported by Semenov (2009) in England and Wales, where an increase or reduction in leaf surface area did not seem to introduce benefits for the wheat yield. Compared to the calibrated crop, wheat with a higher *SLA* can adapt better to the *WSI*; in the same stress conditions, plants with a greater *SLA* are able to extract more water if compared with the calibrated crop, with a rise in yield productivity at the same level as *WSI*.
Tp and *Tact* were similar in calibrated and modified crop when *RLS* value was reduced. However, the improvement in simulated grain yield was significant. The leaf surface area responds to changes in *RLS* and this outcomes a faster emission of new green leaves, consequence of new cumulated biomass. At high levels of water stress simulated by the model, calibrated and *RLS* modified crops showed the same yield response, because the green leaves reduced photosynthetic activity and, consequently, new biomass for crop growth and leaf emission; however, at optimal levels of water supply, more green leaves mean greater productivity.

The observations on wheat showed that cultivars with a "stay-green" trait let the plant to maintain more green leaves, especially in a post-anthesis phase and/or in drought conditions. Furthermore, they have a high grain yield and biomass (Christopher *et al.*, 2008; Foulkes *et al.*, 2007; Richards, 2006). Increasing *LD*, CropSyst simulations confirmed the results reported in literature, also in cases with lower values of *WSI* (greater water stress).

Traits that could vary the phenological length of crop cycle in response to water stress (*PRWS*) or part of it (*GFD*) did not produce significant variations in grain yield, also as a consequence of different *WSI*. Foulkes *et al.*, (2007) reported similar results for two populations of wheat under drought conditions, whose variations in yield were not correlated to variations in flowering or grain filling dates in response to water stress. Similar conclusions, in a study on the response of wheat productivity to variations in simple traits, were obtained by Semenov (2009) using pedo-climatic data from two locations in the UK and Spain. On the contrary, Ehdaie (1995) showed that there was a negative correlation between yield and the length of the period from anthesis to maturity among eight wheat cultivars under water-deficit conditions. Similarly, Sinclair and Muchow (2001), reported that shortening the crop growth duration of maize caused a significant decrement in grain yield. Our opinion is that Simeto wheat cultivar characteristics had been well fitted for Southern Italy environment, with an optimal phenology under existing conditions; current climatic conditions, probably, already correspond to an extreme condition for the crop, already adapted to this environment. Therefore, the climate change predicted for the *future*, with a global warming of about +2°C, would not result in variations on the final yield, also in response to variations in *WSI*.

Changing the maximum root depth, some advantages were achieved in the model simulation; increasing the *MRD*, wheat *Tp* and *Tact* did not change, since the largest amount of water extraction occurred in the first 0.8 m of soil depth (not shown) due to the root density distribution simulated by CropSyst. Besides, root water conductance is linked to fraction cover and so an increase in water availability does not correspond to a proportional increment in water transpired by the crop, if this is not allowed by a higher transpiring plant surface. The effects of *MRD* were slightly more effective in the *future* years when water stress will be more severe.

5. CONCLUSIONS

From this work, some consideration about the main traits that should be considered in durum wheat breeding programs emerged; the specific leaf area, the leaf area duration and the ratio between leaf and stem dry matter partition resulted the more sensitive traits on grain yield. However, it is necessary to underline that the phenotypical crop response is a consequence of an interaction between genetic traits and the environment where these traits are emphasized; the environment could shift genetic breeding work on some determined traits rather than others; alternatively, agronomical practices could improve the final yield. For this reason, it would be useful to introduce in the simulations also variations in the pedo-climatic conditions and agronomical practices, in order to examine the responses of variation of genetic traits to a larger range of combinations and so, to suggest the best breeding programs.

Finally, a more multi-disciplinary approach is also desirable (agronomists, breeders, plant physiologists) to better adapt crop genotypes to future climate changes.

ACKNOWLEDGMENTS

This work has been partly supported by Italian Ministry of Agriculture and Forestry Policies contract n. 209/7393/05 and n. 28373/7303/09 (AQUATER Project, Coordinator: dr. M. Rinaldi) and partly by Italian Ministries of Finance and Economy, of Education, University and Research, of Environment and Territory, of Agricultural, Food and Forestry Policies, contract n. 285 – 20/02/2006 (CLIMESCO Project, Coordinator: dr. D. Ventrella).

REFERENCES

Akkaya, A., Dokuyucu, T., Kara, R., Akçura, M. 2006. Harmonization ratio of post- to pre-anthesis durations by thermal times for durum wheat cultivars in a Mediterranean environment. Eur. J. Agron. 4:404-408.

Baker, C.K., Gallaher, J.N. and Monteith, J.L. 1980. Daylenght change and leaf appearance in winter wheat. Plant Cell Environ. 7: 463-466.

Baker, J.T., Pinter, P.J., Reginato, R. J. & Kanemasu, E.T. 1986. Effects of temperature

on leaf appearance in spring and winter cultivars. Agron. J. 78:605-613.
Bates, B.C., Kundzewicz, Z.W., Wu, S., Palutikof, J.P. 2008. In: IPCC Secretariat (Editor), IPCC Technical Paper VI. Geneva, pp. 210
Bauer, A., Frank, A. B. & Black, A.L. 1984. Estimation of spring wheat leaf growth rates and anthesis from air temperature. Agron. J. 76:829-835.
Boote, K.J., Jones, J.W. 1988. Applications of, and limitations to, crop growth simulations models to fit crops and cropping systems to semi-arid environments,. In F.R Bidinger and C. Johansen (eds.), Drought Research Priorities in the Dryland Tropics. ICRISAT Center, Pantacheru, A.P., India, pp. 63-75.
Campos, H., Cooper, A., Habben, J.E., Edmeades, G.O., Schussler, J.R. 2004. Improving drought tolerance in maize: a view from industry. Field Crops Res. 90:19-34.
Coleman, R. K., Gill, G.S., Rebetzke, G.J. 2001. Identification of quantitative trait loci (QTL) for traits conferring weed competitiveness in wheat (*Triticum aestivum* L.). Aust. J. Agric. Res. 52:1235-1246.
Condon, A.G., Richards, R.A., Rebetzke, G.J., Farquhar, G.D. 2004. Breeding for high water-use efficiency. J. Exp. Bot. 55: 2447-2460.
Cooper, M., Podlich, D.W., Löffler, C.M., Van Eeuwijk, F., Chapman, S.C. 2006. Genotype-by-environment interaction under water-limited conditions. In: Ribaut J-M (ed) Drought adaptation in cereals. Food Products Press, New-York, pp 51-96.
Cristopher, J.T., Manshadi, A.M., Hammer, G.L., Borell, A.K. 2008. Developmental and physiological traits associated with high yield and stay-green phenotype in wheat. Aust. J. Agric. Res. 59:354-364.
Donatelli, M., Stockle, C., Ceotto, E., Rinaldi, M., 1997. Evaluation of CropSyst for cropping systems at two locations of northern and southern Italy. Eur. J. Agron, 6: 35-45.
Edmeades, G.O., Mc Master, G.S., White, J.W., Campos, H. 2004. Genomic and the physiologist: bridging the gap between genes and crop response. Field Crops Res. 90:5-18.
Ehdaie, B. 1995.Variation in water use efficiency and its components in wheat. II. Pot and field experiments. Crop Sci. 35, 1617-1626.
Evans, L.T., Fischer, R.A. 1999. Yield potential: Its definition, measurement and significance. Crop Sci. 39(6), 1544-1551.
FAO-UNESCO 1963. Bioclimatic map of the Mediterranean Zone, explanatory notes. Paris, France.
Fischer, R.A. 1979. Growth and yield limitation to dryland wheat yield in Australia: a physiological framework. J. Aust. Inst. Agri. Sci. 45, 83-94
Foulkes, M.J., Sylvester-Bradley, R., Weightaman, R., Snape, J.W. 2007. Identifying physiological traits associated with improved drought resistance in winter wheat. Field Crops Res. 103, 11-24.
Garofalo, P., Di Paolo, E., Rinaldi, M. 2009. Durum wheat (*Triticum durum* Desf.) in rotation with faba bean (*Vicia faba* var. *minor* L.): long-term simulation case study. Crop Pasture Sci. 60, 240-250.
Goudriaan, J., Van Laar, H.H., Van Keulen, H., Louwerse, W., 1985. Photosynthesis, CO_2 and plant production. In: Day, W. and Atkin, R.K. eds. Wheat growth and modelling. Plenum, New York, 107-122. NATO Advanced Science Institute Series. Serie A. Life Sciences no. 86.
Grace, J. 1988. Temperature as a determinant of plant productivity. In: S.P. Long and F.I. Woodward (Editors), Plants and Temperature. Company of Biologists, Cambridge, pp. 91 -107.
Hoogenboom, G., Whithe, J.W., Jones, J. W., Boote, K.J. 1994. BEANGRO: a process-oriented dry bean model with a versatile user interface. Agron. J. 86, 182-190.
Hsiao, T.C. 1973. Plant responses to water stress. Annual Review of Plant Physiology 24, 519-570.
Hunt, R. 1982. Plant growth curves. Edward Arnold, London, 248 pp.
Jaradat, A.A. 2009. Modeling Biomass Allocation and Grain Yield in Bread and Durum Wheat under Abiotic Stress. Aust. J. Crop Sci. 3(5), 37-248.
Jones, J.W., Zur, B. 1984. Simulation of possible adaptive mechanisms in crops subjected to water stress. Irrig. Sci. 5, 251-264.
Jordan, W.R., Dugas, W.A. and Shouse, P.J. 1983. Strategies for crop improvement for drought-prone regions. Agric. Water Manage. 7, 281-299.
López-Castañeda, C., Richards, R.A. 1994. Variation in temperate cereals in rainfed environments. III. Water-use efficiency. Field Crops Res. 39, 85-98.
López-Castañeda, C., Richards, R.A., Farquhar, G.D. 1995. Variation in early vigour between wheat and barley. Crop Sci. 35:472-479.

McMaster, G. S. 1997. Phenology, development, and growth of the wheat (*Triticum aestivum* L.) shoot apex: a review. Adv. Agron. 59:63-118.

McMaster, G.S., Lecain, D. R., Morgan, J. A., Aiguo, L. & Hendrix, D. L. 1999. Elevated CO_2 increases CER, leaf and tiller development, and shoot and root growth. J. Agron. Crop Sci. 183:119-128.

Mcmaster, G.S., Wilhelm, W.W. 2003. Phenological responses of wheat and barley to water and temperature: improving simulation models. J. Agric. Sci. 141:129-147.

Passarella, V.S., Savin R., Slafer, G.A. 2002. Grain weight and malting quality in barley as affected by brief periods of high temperature under field conditions. Aust. J. Agr. Res. 53:1219-1227.

Pizzigalli, C., Palatella, L., Zampieri, M., Lionello, P., Maglietta, M.M., Paradisi, P. 2012. Dynamical and statistical downscaling of precipitation and temperature in a Mediterranean area. Ital. J. Agron. 7: 3-12.

Plaut, Z., Butow, B.J., Blumenthal, C.S., Wrigley, C.W. 2004. Transport of dry matter into developing wheat kernels and its contribution to grain yield under post-anthesis water deficit and elevated temperature. Field Crops Res. 86:185-198.

Rajala, A., Hakala, K., Makela, P., Muurien, S., Peltonen-Sainio, P. 2009. Spring wheat responce to timing of water deficit through sink and grain filling capacity. Field Crop Res. 114:263-271.

Rebetzke, G.J., Botwright, T.L., Moore, C.S., Richards, R.A., Condon, A.G. 2004. Genotypic variation in specific leaf area for genetic improvement of early vigour in wheat. Field Crops Res. 88:179-189.

Reymond, M., Muller, B., Leonardi, A., Charcosset, A., Tardieu, F. 2003. Combining quantitative trait loci analysis and an ecophysiological model to analyze the genetic variability of the responses of leaf growth to temperature and water deficit. Plant Physiol. 131:664-675.

Richards, R.A. 2000. Selectable traits to increase crop photo-synthesis and yield of grain crops. J. Exp. Bot. 51:447-458.

Richards, R.A. 2006. Physiological traits used in the breeding of new cultivars for Water-scarce environments. Agric. Water Manag. 80:197-211.

Rinaldi, M., De Luca, D., 2012. Application of EPIC model to assess climate change impact on sorghum in Southern Italy. Ital. J. of Agron. 7, 1:74-85.

Rinaldi, M., D'andrea, L. Ruggieri, S., Garofalo, P., Moriondo, M., Ventrella, D., 2009. Influenza dei cambiamenti climatici sulla coltivazione del frumento duro. Ital. J. Agrometeorology, 2:32-33.

Ritchie, J.T. 1972. Model for predicting evaporation from a row crop with incomplete cover. Wat. Resources Res. 8(5):1204-1213.

Robert, N., Hennequet, C., Bérard, P. 2001. Dry matter and nitrogen accumulation in wheat kernel: genetic variation in rate and duration of grain filling. J. Genet. Breed. 55:297-305.

Rosenzweig, C., Tubiello, N. 1996. Effects of changes in minimum and maximum temperature on wheat yields in the central US. A simulation study. Agr. Forest Meteorol. 80:215-230

Savin, R., Stone, P.J., Nicolas, M.E. 1996. Response of grain growth and malting quality of barley to short periods of high temperature in field studies. Aust. J. Agric. Res. 47: 465-477.

Semenov, M.A. 2009. Impacts of climate change on wheat in England and Wales. J. R. Soc. Interface 6:343-350.

Semenov, M.A., Shewry, P.R. 2011 Modelling predicts that heat stress, not drought, will increase vulnerability of wheat in Europe. Science Report 1, 66: 1-5.

Shearman, V.J., Sylvester-Bradley, R., Scott, R.K., Foulkes, M.J. 2005. Physiological processes associated with wheat yield progress in the UK. Crop Sci. 45:175-185.

Simón, M.R. 1999. Inheritance of the flag leaf angle, flag leaf area and flag leaf area duration in four wheat crosses. Theor. Appl. Genet. 97:310-314.

Sinclair, T.R., Muchow, R.C. 2001. System analysis of plant traits to increase grain yield on limited water supplies. Agron. J. 93:263-270.

Stöckle, C., Donatelli, M., Nelson, R. 2003. CropSyst: a cropping system simulation model. Eur. J. Agron., 18:289-307.

Tambussi, E.A., Bort, J., Araus, J.L. 2007. Water use efficiency in C3 cereals under Mediterranean conditions: a review of physiological aspects. Ann. Appl. Biol. 150: 307-321.

Triboi, E., Triboi-Blondel, A.M. 2002. Productivity and grain or seed composition: a new approach to old problem: invited paper. Eur. J. Agron. 16:163-186.

Tripathi, R.P., Mishra, R.K. 1986. Wheat root growth and seasonal water use as affected by irrigation under shallow water table conditions. Plant Soil 92:181-188.

USDA 2006. Keys to Soil Taxonomy. 10th edn, pp.333. Available at: ftp://ftp-fc.sc.egov.usda.gov/NSSC/Soil_Taxonomy/keys/keys.pdf

Ventrella, D., Charfeddine, M., Moriondo, M., Rinaldi, M., Bindi, M., 2012. Agronomic Adaptation Strategies under Climate Change for Durum Wheat and Tomato in Southern Italy: Irrigation and Nitrogen Fertilization. Regional Environmental Change, 12, 3: 407-419.

Ventrella, D., Rinaldi, M., 1999. Comparison between two simulation models to evaluate cropping systems in Southern Italy. Yield response and soil water dynamics. Agric. Med. 129: 99-110.

Wardlaw, I.F. 1994. The effect of high temperature on kernel development in wheat: variability related to pre-heading and post-anthesis conditions. Aust.J. Plant Physiol., 21:731-739

Xinyou, J., Kroff, M.J., Stam, P. 1999. The role of ecophysiological models in QTL analysis: the example of specific leaf area in barley. Hereditary 82:415-421.

Crop rotation, fertilizer types and application timing affecting nitrogen leaching in nitrate vulnerable zones in Po Valley

Alessia Perego[1], Andrea Giussani[2], Mattia Fumagalli[1], Mattia Sanna[1], Marcello Chiodini[1], Marco Carozzi[1], Lodovico Alfieri[1], Stefano Brenna[2], Marco Acutis[1]*

Abstract: *A critical analysis was performed to evaluate the potential risk of nitrate leaching towards groundwater in three Nitrate Vulnerable Zones (NVZs) of the Lombardia plain by applying the ARMOSA crop simulation model over a 20 years period (1988-2007). Each studied area was characterized by (i) two representative soil types, (ii) a meteorological data set, (iii) four crop rotations according to the regional land use, (iv) organic N load, calculated on the basis of livestock density. We simulated 3 scenarios defined by different fertilization time and amount of mineral and organic fertilizers. The A scenario involved no limitation in organic N application, while under the B and C scenarios the N organic amount was 170 and 250 kg N $ha^{-1}y^{-1}$, respectively. The C scenario was compliant with the requirement of the 2012 Italian derogation, allowing only the use of organic manure with an efficiency greater than 65%. The model results highlighted that nitrate leaching was significantly reduced passing from the A scenario to the B and C ones ($p<0.01$); on average nitrogen losses decreased by up to 53% from A to B and up to 75% from A to C.*
Keywords: *nitrogen fertilization, crop simulation model, nitrate leaching, crop rotation.*

Riassunto: *È stata condotta un'analisi modellistica al fine di valutare il potenziale rischio di lisciviazione dei nitrati verso le acque sotterranee in tre zone vulnerabili ai nitrati (ZVN) della pianura lombarda, applicando il modello di simulazione colturale ARMOSA utilizzando un data set meteorologico di 20 anni (1988-2007). Per ogni area in esame sono stati identificati due suoli rappresentativi, le rotazioni colturali principalmente adottate e il quantitativo medio annuale di carico di azoto organico, calcolato in base alla densità di bestiame. Abbiamo definito 3 scenari di simulazione (A,B,C) che si differenziano in termini di dose di fertilizzante organico (illimitato, 170, 250 kg N $ha^{-1}anno^{-1}$, rispettivamente per A, B e C), minerale e per l'epoca di concimazione. Lo scenario C è conforme alla deroga alla direttiva nitrati avuta per le regioni padane nel 2012, che prescrive modalità di distribuzione dell'N organico tali da garantire un'efficienza teorica di almeno il 65%. I risultati evidenziano una diminuzione della lisciviazione passando dallo A al B e C ($p<0.01$); mediamente l'azoto lisciviato diminuisce fino al 53% e al 75% passando rispettivamente da A a B e da A a C.*
Parole chiave: *fertilizzazione azotata, modelli di simulazione colturale, lisciviazione dell'azoto, sistemi colturali.*

INTRODUCTION

Agricultural activities are the primary source of no-point pollution due to nitrogen (NO_3-N) losses towards groundwater (Kersebaum *et al.*, 2006). The vulnerability of crop land to nitrate leaching is evaluable by taking into account pedoclimatic condition such as soil permeability, skeleton content, mean annual rainfall (Thorup-Kristensen, 2006) and the local amount of nitrogen from animal waste which can be potentially applied.

The designation of Nitrates Vulnerable Zones (NVZ) in Italy falls under the competence of Region Government. Designation, which took place in the late nineties, has been enlarged between 2006 and 2008; it is based on the criteria set out in article 3 and Annex 1 of nitrates directive, on the basis of the results of monitoring programmes assessing nitrate concentration in surface and groundwater and trophic status of surface waters. In Lombardia NVZs represent approximately 67% of the Utilized Agricultural Area (UAA) in Northern Italy. In detail the percentage of NVZs over the UAA exceeds 80% in Lombardia, whereas NVZs represent 56% of the regional plain areas (Regione Lombardia, 2006a). In plain area of Lombardia (from 44°50'N to 45°50'N and from 8°40'E to 11°80'E), UUA is about 790,000 ha and the main cropping systems are maize-based (Zea mays L., Fumagalli, 2011). Such crops have a relative high N requirement and a potential N uptake which allows for elevated N input up to 300 kg ha^{-1}. Farming systems in the plain of the region are strictly linked to livestock type and account for the 36% and 64% of the national cattle

* Corresponding author: e-mail: alessia.perego@unimi.it
[1] Dipartimento di Scienze Agrarie e Ambientali, Università degli Studi di Milano
[2] Ente Regionale per i Servizi alla Agricoltura e Foreste
Received 20 April 2013, revised 04 May 2013.

and pigs respectively (Carozzi *et al.*, 2013a). The average nitrogen load from livestock is about 172 kg N ha^{-1}. In the western area, where cereal farms are predominant, the mean annual nitrogen load from livestock is low (from 30 to 90 kg N $ha^{-1}y^{-1}$) whereas in the central and eastern parts the presence of livestock farms (mainly dairy, cattle and swine) determines high organic nitrogen loads (from 190 to 350 kg N $ha^{-1}y^{-1}$, Regione Lombardia, 2006b). Such high livestock density involves high availability of N manure but also serious problems related to manure stock and disposal. In Lombardia the percentage of soils in NVZs per texture classes are (I) 4% for soil with sand > 60%, (II) 93% for soils with sand < 60% and clay < 35%, (III) 3% for soils characterized by a clay content > 35% (Calzolari *et al.*, 2001).

Over the last decade, results in measurements carried on Lombardia watertable showed a slightly reduction in nitrate concentration (mg NO_3 L^{-1}). Regional Environmental Agency (ARPA) monitored nitrate in groundwater in 335 wells. Well depth ranges from 2 to 40 m, while the depth to the bottom of the screen level from 12 to 25 m; all wells are within the unconfined aquifer. Average of measured concentrations of the whole regional area was 18.3 over the period from 2002 to 2005, and 17.4 mg NO_3 L^{-1} from 2006 to 2008. Over such two periods NO_3 concentration (mg NO_3 L^{-1}) was 21.4 in 2002-2005 and 20.9 in 2006-2008 in NVZs, whereas was 14.6 and 13.3 mg NO_3 L^{-1} in the zones not designated as vulnerable to nitrate.

In such contest alternative cropping systems and agricultural management could represent an opportunity to reduce nitrate leaching, avoiding any economic decrease in crop yield. The aim of this work was to evaluate nitrate leaching under three alternative scenarios of cropping systems by applying ARMOSA simulation model (Acutis *et al.*, 2007) in three areas of Lombardia plain. One of the studied scenarios was defined according to the outline of the obtained request for derogation from Italian Government (2011/721/UE). In particular, we tested the leaching risk in relation with the amount of mineral and organic N fertilizers. In fact, several experimental findings (Borin *et al.*, 1997; Morari and Giupponi, 1997; Acutis *et al.*, 2000) confirmed high losses via leaching when elevated mineral N amount was applied. The introduction of a double cropping system is promoted because the autumn-winter crops are able to uptake the residual soil mineral N (Thorup-Kristensen, 2001; Kramberger *et al.*, 2008; Trindade *et al.*, 2008), to reduce potential nitrate leaching. In fact, one of the main factors determining the amount of leached N into ground water is the presence of a plant cover (Di and Cameron, 2002) which depletes the soil of mineral N by taking it up and consequently decreasing its leaching (Kramberger *et al.*, 2009). Moreover, the double cropping system provides additional feedstock for livestock utilization (Fumagalli, 2012).

2. MATERIALS AND METHODS

2.1 The studied area

We first identified three areas of the Lombardia plain that are characterized by different pedo-climatic conditions (Fig. 1); the three areas are currently classified as NVZs by the Italian legislation, in compliance with the European Union Nitrate Directive 91/676/EEC. The climate and soil related variables of the three areas are reported in Tab.1.

Since the modelling analysis was performed at local scale, then municipality borders were taken into account in defining the three studied areas to assess the local risk of N leaching. In terms of modelling application, each individuated area represented a simulation unit.

The ARMOSA model run over a period of 20 year using a set of daily meteorological data (1988 - 2007) observed by three weather stations set in each area. Such meteorological stations belong to the Regional Network Service. Meteorological variables, daily observed over the period of 1988-2007, were maximum and minimum value of temperature (°C), and rainfall (mm). Solar radiation was estimated by using the Hargreaves equation (Hargreaves and Samani, 1985), which was previously calibrated using observed data from reference weather stations. For each area two soils were individuated from the Regional Pedolological Map (Regione Lombardia, 2009), being the most representative in terms of UAA (%).

2.2 Scenarios definition

The modeling analysis performed by ARMOSA model consisted primarily of the scenario definition. In order to test different agriculture management three scenarios were defined: (I) the A scenario, with no limitation in organic N application (A), (II) the B scenario, in which the threshold of N fertilization from manure is set on 170 kg N $ha^{-1}y^{-1}$, (III) the C scenario, defined according to the outline of the obtained derogation of, in which the N input is enhanced from 170 to 250 kg N $ha^{-1}y^{-1}$, and mineral N fertilizers amount decreases

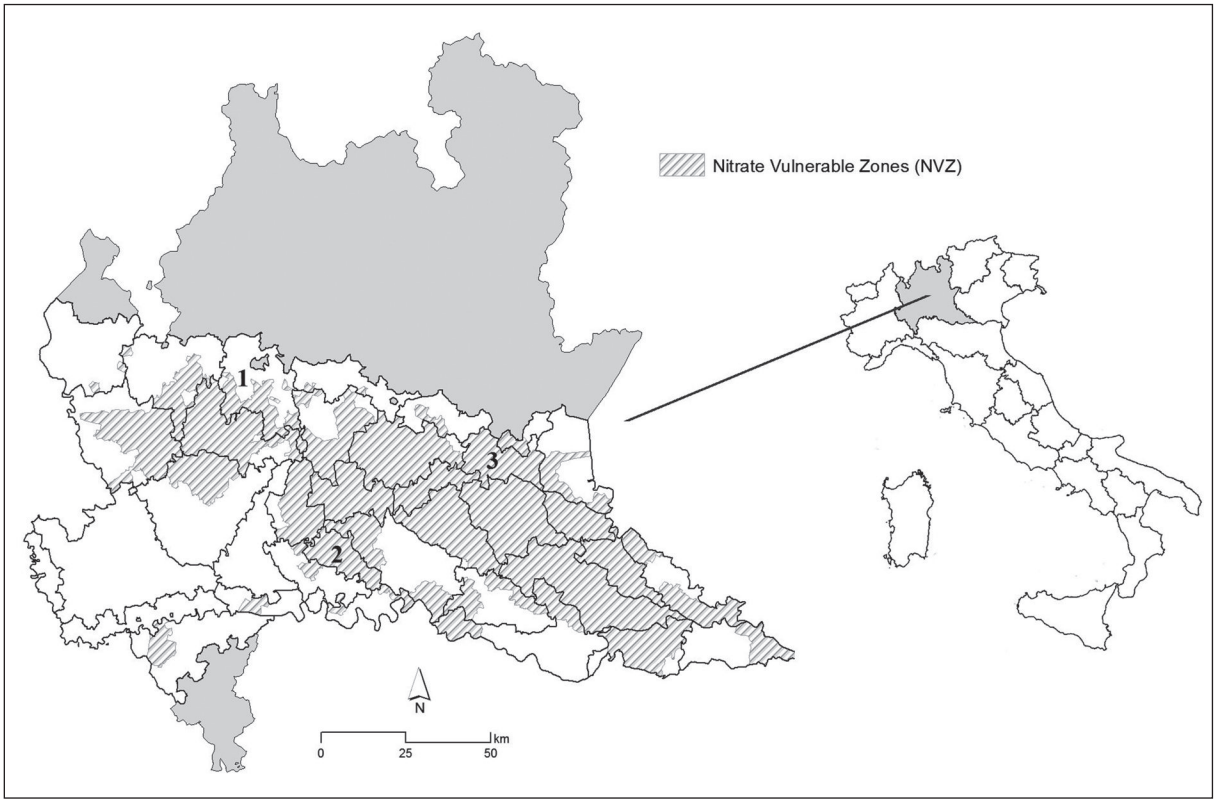

Fig. 1 - The designated Nitrate Vulnerable Zones (NVZs) in the Lombardia plain. The three studied areas are marked by "1", "2", "3". The grey area is the mountain region of Lombardia.
Fig. 1 - Le Zone Vulnerabili ai Nitrati in pianura lombarda. Le tre aree in esame sono contrassegnate da "1", "2", "3". L'area in grigio indica la zona montagnosa della Lombardia.

according to crop N requirement. B differs from A in terms of N organic fertilization. Main differences from A to C consist of (I) higher N organic, (II) avoiding manure application on bare soil, (III) crop rotations including catch crops. Particularly, C was defined: (I) by introducing new crops in the rotation with the aim of further reducing N losses maintaining economic profitability, (II) reducing the N applied from chemical fertilizers.

Crop rotations were individuated according to the Regional land use (Regional data base SIARL, 2003-2007). We took into account in the analysis crop rotations adopted at least in the 5% of the UAA; four crop rotations were then identified

Area	mean annual rainfall (mm)	mean annual rainy days	ET_{ref} (mm)	max T(°C)	min T(°C)		Sand (%)	Silt (%)	Clay (%)	Organic carbon (%)
1	766-1553	64-111	896-947	17-20	8-10	soil 1	24	58	18	0.5
						soil 2	70	22	8	1.2
2	523-959	59-90	975-1056	17-19	6-10	soil 1	55	40	5	0.6
						soil 2	32	48	20	1.0
3	708-1240	62-103	1030-1085	18-20	8-10	soil 1	39	40	21	0.6
						soil 2	35	43	22	0.7

Tab. 1 - Main climate (1988-2007 period) and soil related variables of the three studied areas. The soil variables are expressed as percentage on weight basis considering a profile depth of 1 m.
Tab. 1 - Principali caratteristiche climatiche (del periodo 1988-2007) e pedologiche delle tre aree in esame. I dati relativi al suolo sono espressi come percentuale sul peso.

being characterized by a large area of cultivation in the three studied areas. Within any area, the relative area devoted to maize crop included both grain and silage maize (M rotation). The Me rotation consisted in permanent meadows. In A and B scenarios the MW rotation included grain maize and winter wheat (*Triticum aestivum* L.), while in C scenario it was modified by introducing a summer herbage of foxtail millet (*Setaria italica* L.) after winter wheat harvest to ensure crop N up take in summer. Only in the case of C scenario, the MR rotation, as double crop rotation of silage maize of FAO class 500 and Italian ryegrass (*Lolium multiflorum* Lam.), was introduced to simulate the effectiveness of a cover crop to reduce nitrate leaching over the autumn-winter period.

In order to simulate the identified rotations, we used previously calibrated values of crop parameters of maize, wheat and Italian ryegrass (Perego, 2010). In particular, for maize was used a parameterization for a FAO 600 hybrid which generally reaches physiological maturity over a period of 150 days. Meadows were parameterized starting from values reported by van Heemst (1988); then parameters were adapted according to existing studied carried out in Po plain (Sacco *et al.*, 2003; Grignani *et al.* 2003). Foxtail millet parameters were calibrated in agreement with observed data of northern Italy (Onofri *et al.*, 1990). Sowing, harvest and cutting dates were chosen according to ordinary management of farmers. Typically maize and meadows were sown at the beginning of spring, while foxtail millet was planted in summer and winter wheat and Italian ryegrass in autumn. Four cuttings of meadows were simulated. The nitrogen parameters of the ARMOSA model (Acutis *et al.*, 2007, Perego *et al.*, 2010) was calibrated on more than 2000 measures of soil nitrate contents observed in Lombardia plain according to Perego *et al.* (2012).

The amount of organic N fertilizer was derived from the regional database and was calculated on the basis of the livestock breeding of the three studied areas (Regione Lombardia, 2008). In the A and B scenario the organic N fertilization was split in autumn (50%) and spring (50%) for maize and meadows. In the case of maize crops, once calculated the organic N input, the amount of mineral N fertilization was then calculated, in order to guarantee at least 350 kg N $ha^{-1}y^{-1}$, as farmers usually do (Grignani and Zavattaro, 2000; Mantovi *et al.*, 2006; Perego *et al.*, 2012). The mineral fertilization was simulated at V6-V8 stage of maize development. Winter wheat was fertilized with 200 kg N $ha^{-1}y^{-1}$ as mineral N at 2 distributions. In B and C scenarios thresholds of organic N fertilization were set on 170 and 250 kg N $ha^{-1}y^{-1}$, respectively. Particularly, in C scenario manure N was applied only in spring or summer, avoiding any spreading in autumn if no crop is sown during such period. Tab. 2 summarizes the N amount applied to crops under the three scenarios in the three studied areas.

In the area 1, irrigation was not simulated in agreement with the ordinary agricultural practices of the area. In the area 2, we simulated four border irrigation treatments of 80 mm each from June to August to maize crop, whereas foxtail millet was irrigated three times. In area 3, 5 irrigations were simulated with 50 mm for maize and 3 for foxtail millet, being an area in which sprinkler irrigation is adopted.

2.3 The ARMOSA model overview

In order to assess the effectiveness of the management in agreement with the derogation on water quality, nitrogen losses to water from the main agricultural systems under the specific conditions of Lombardia plain were estimated through a dynamic soil-crop model. ARMOSA (Acutis *et al.*, 2007, Perego *et al.*, 2010) is a simulation model specifically developed on the basis of field trial data observed over years in the ARMOSA project monitoring sites. ARMOSA implements several alternatives for each process, using approaches already well known and largely validated in the scientific literature and used for practical application. In detail, reference evapotranspiration can be computed using Hargreaves, Priestley-Taylor or Penman-Monteith approach. Crop growth model development was based on SUCROS–WOFOST (used, among others application, at European scale for the Bulletin of yield prediction for wheat, maize and other important crops, Supit *et al.*, 1994). Water dynamics can be simulated using the cascading approach, or the Richards' equation, solved as in the SWAP (Van Dam *et al.*, 1997; Van Dam and Feddes, 2000) model. Such Richards' equation solution has showed to be the best performing one with very detailed soil moisture data set (Bonfante *et al.*, 2010). Nitrogen dynamics is simulated according to the SOILN approach (Johnsson *et al.*, 1987, Eckersten *et al.*, 1996), but with some improvements. In ARMOSA each type of organic matter has own mineralization rates, respiration losses and C/N ratio, allowing for separate calculations for the different types of organic

Rotation	Crop	Area	Scenario					
			A		B		C	
			Org	Min	Org	Min	Org	Min
M	Maize	1	246	104	170	180	250	100
		2	320	100	170	180	250	100
		3	330	100	170	180	250	100
Me	Meadows	1	0	150	0	150	250	100
		2	132	0	170	0	250	100
		3	132	0	170	0	250	100
MW	Maize	1	176	174	170	180	176	149
	W. Wheat		0	200	120	60	0	165
	F.millet*		n.s.	n.s.	n.s.	n.s.	0	100
		2	320	0	170	180	250	100
			0	200	170	30	0	100
			n.s.	n.s.	n.s.	n.s.	250	0
		3	330	0	170	180	250	100
			0	200	170	30	0	100
			n.s.	n.s.	n.s.	n.s.	250	0
MR	Maize		n.s.	n.s.	n.s.	n.s.	250	130
	It. ryegrass		n.s.	n.s.	n.s.	n.s.	0	0

*Italian ryegrass and foxtail millet, manured in summer after wheat harvest at the end of June, were not simulated (n.s.) under the A and B scenarios

Tab. 2 - Mean annual N fertilizer amount (N kg $ha^{-1}y^{-1}$) applied to crops under A, B and C scenarios. Org. and Min. stand respectively for organic and mineral N fertilizers.
Tab. 2 - Quantitativi medi annuali (kg N $ha^{-1}y^{-1}$) di fertilizzanti azotati da effluenti animali (Org.) e minerali (Min.) applicati alle colture delle quattro rotazioni simulate nei tre scenari.

fertilizers or crop residuals incorporated into the soil. Distinct pools of NH_4-N and NO_3-N simulated; NH_4-N pool can be up taken by plants, oxidised to NO_3-N, fixed by the clay component of the soil, and immobilised in the organic matter; losses due to ammonia volatilization are also simulated. NO_3-N pool is subject to plant uptake, leaching and denitrification. It is possible to define sowing and harvest DOY (day of the year), crop rotation, automatic irrigation, set of fertilization management, LAI forcing. Results concerning the model calibration and validation, which were carried out using a large set of data observed from representative arable land in Lombardia plain, are detailed described by Perego (2010), who reported mean values of the Nash–Sutcliffe efficiency index of 0.94, 0.69, 0.52, 0.88 for crop biomass, crop N uptake, soil water content, N leaching, respectively.

2.4 Statistical analysis

A statistical analysis was carried out in order to test the significance of scenario and crop rotation in affecting N losses via leaching. The statistically significance was calculated by using SPSS 20.0 statistics package. We performed a rank transformation of the simulated data set due to not homogeneity of the variances, according to Conover and Iman (1981) and Acutis *et al.* (2012); a two-way ANOVA was then executed (α=0.05) for N leaching and crop yield, as dependent variables, alternatively. A multiple pair-wise comparison was performed using the Dunn-Sidak's test (Sokal and Rohlf, 1981), obtaining a full control of type I error.
In order to find and rank for importance the correlations between N leaching and independent variables involved in the studied continuum crop-soil, a step-wise linear regression was carried out for each crop rotation. This type of regression analyses tries to obtain the optimal subset of the independent variables, getting to a regression model including only significant variables. Within any rotation, the standard coefficient *beta* was calculated for each independent variable.

3. RESULTS

3.1 N leaching under the different scenarios and crop rotations

The mean annual N leaching were calculated under each scenario and crop rotation. Testing the effect of interaction between scenario and

rotation on N leaching, a Dunn-Sidak's test was executed (Tab. 3). In such way it was possible to identify which was the most sustainable rotation in terms of N leaching. The Me rotation resulted to be the best rotation in every scenario, while M rotation (monoculture of maize) determined the highest leaching losses. The MW and MR rotations had the intermediate position in every scenario. Fig. 2 shows the mean annual N leaching simulated under the different combinations of scenario x rotations. The outstanding result was the strongly decrease by up to 50% of N leaching passing from A to C scenario. Moreover, under the C scenario the MR crop rotation involved a decrease by 50% of the leaching associated to the M rotation.

Although the N leaching varied substantially under the different combinations of scenario and rotation, significant difference in crop yield resulted just in the case of the M rotation. In fact, the interaction between the two independent factors resulted to be highly significant ($p<0.01$) because maize grain yield in the area 1 was higher under the C scenario (13000 kg ha^{-1}) compared to the mean value in A and B scenarios (9100 kg ha^{-1} on average). On the contrary, maize grain yield was significantly lower ($p<0.01$) under C scenario in comparison with the production under A and B.

The wheat crop yield did not change substantially under the three scenarios as much as the Italian ryegrass, maize 500 FAO and foxtail millet biomass ($p>0.05$). Meadows yield increased significantly from A and B to C scenario only in the area 3 ($p<0.01$), passing from 7800 kg of dry matter ha^{-1} to 10500 kg ha^{-1}. Such production was the highest because the mean annual production was 6100 and 9200 kg ha^{-1} respectively area 1 and 2. Fig. 3 shows the mean crop yield under the three scenarios.

Stepwise regressions for N leaching (dependent variable) were executed within any crop rotation. The independent variables which were taken into account in this analysis were: (I) organic N and (II) mineral N fertilization, (III) soil mineralization rate, (IV) annual rainfall + irrigation, (V) percolation water, (VI) soil water content at the saturation point , (VII) soil organic carbon, (VIII) crop yield and N uptake (IX), and (X) crop evapotranspiration (ETc). Within each rotation the linear regression had good value of R^2 (0.78 to 0.95) and statistically significant (Tab. 4). The beta standard coefficients gave a measure of the weight of each factor: on average, the mineral N fertilization appeared to be mostly relevant within any rotation. The percolation and the organic N fertilization resulted relevant variables in affecting N leaching, together with the mineralization rate under the M and MW crop rotations.

		Rotation			
Scenario	Area	M	Me	MW	MR
A	1	65c	3a	16b	n.s.
	2	59c	1a	19b	n.s.
	3	75c	1a	41b	n.s.
B	1	64c	3a	48b	n.s.
	2	31b	1a	23b	n.s.
	3	36b	4a	21a	n.s.
C	1	26b	3a	21b	14ab
	2	26b	5a	18b	11ab
	3	28b	1a	22b	15ab

Tab. 3 - Mean annual N leaching (kg N $ha^{-1}y^{-1}$) for each simulated Scenario X Rotation. Numbers followed by different letter within a row are significantly different ($p<0.05$) according to Dunn-Sidak's test, where a was the best value being associated to lowest value of leaching. M=maize; Me=meadows; MW=maize, wheat (and f.millet under the C scenario); MR=maize and It.ryegrass.

Tab. 3 - Quantitativi medi annuali di azoto lisciviato (kg N $ha^{-1}y^{-1}$) per ogni combinazione di scenario X sistema colturale. I valori riportati in tabella seguiti da lettere differenti, entro la singola riga, differiscono tra loro ($p<0.5$) secondo il test di Dunn-Sidak, dove la lettera a è assegnata alla combinazione in cui la lisciviazione è più ridotta. M=mais; Me=prati permanenti; MW=mais, frumento (e panico nello scenario C); MR=mais e loiessa.

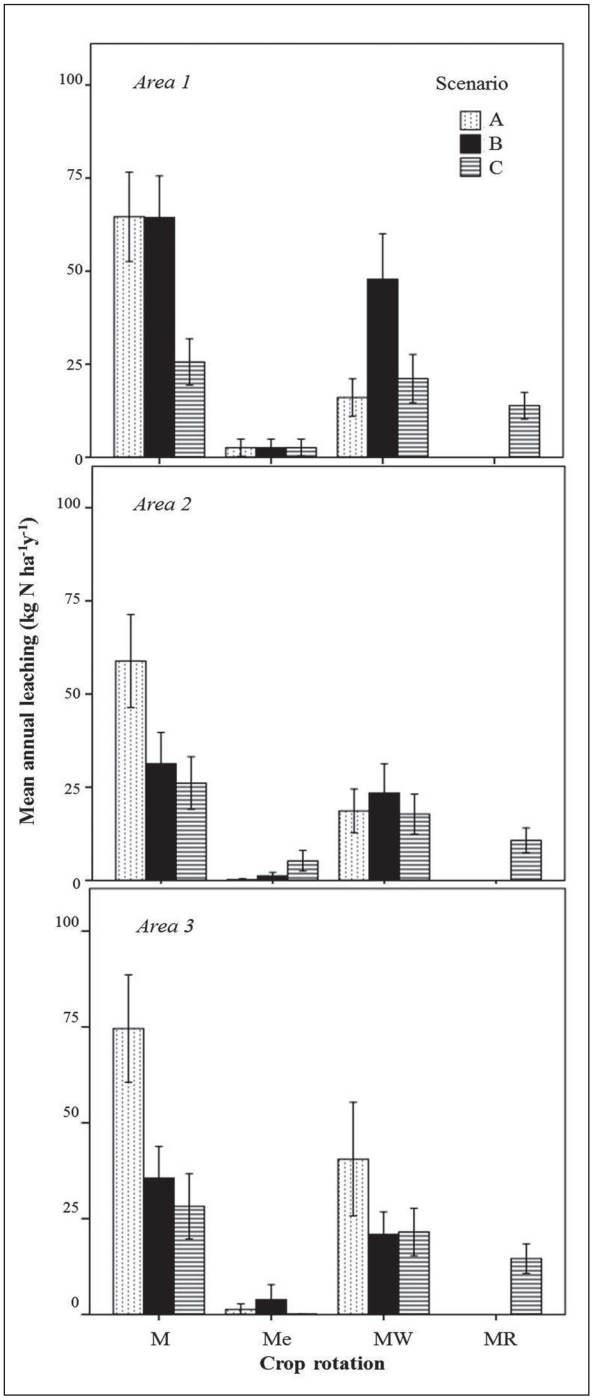

Fig. 2 - Mean annual N leaching (kg ha^{-1} y^{-1}) in the three studied areas under the A, B, C scenarios and the simulated crop rotations. The error bars are the 95% C.I. M=maize; Me=meadows; MW=maize, wheat (and f.millet under the C scenario); MR=maize and It.ryegrass.
Fig. 2 - Quantitativi medi annuali di azoto lisciviato (kg N $ha^{-1}y^{-1}$) nelle tre aree in esame e nei tre scenari A, B e C per ogni rotazione colturale simulata. Le barre di errore rappresentano gli intervalli fiduciali della media al 95%. M=mais; Me=prati permanenti; MW=mais, frumento (e panico nello scenario C); MR=mais e loiessa.

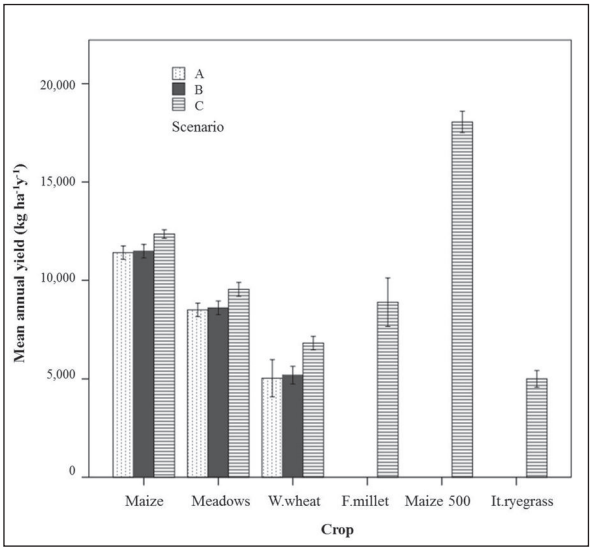

Fig. 3 - Mean annual yield (kg $ha^{-1}y^{-1}$) of each crop under the three scenarios. The yield is expressed as dry matter of above ground biomass, except for maize and wheat for which the grain vield is reported, and is the average of the crop production simulated in the three studied areas. Error bars: 95% C.I.
Fig. 3 - Grafico riportante la media delle produzioni (kg $ha^{-1}y^{-1}$) calcolate come media delle rese simulate nelle tre aree in esame. La resa è espressa come sostanza secca della biomassa vegetale epigea, fatta eccezione per mais e frumento dei quali si riporta la produzione di granella. Le barre di errore rappresentano gli intervalli fiduciali della media al 95%.

3.2 N leaching in the three studied area

The total amount of N leaching in each studied area was calculated under the three scenarios as weighted mean on the basis of the relative area (UUA%) devoted to each crop rotation as indicated by the Regional database. In the three areas a comparison between the effect of the A with the B and C scenarios showed a net decrease of N leaching amount (Tab. 5). In fact, the mean annual N leaching were 32, 24 and 11 kg N $ha^{-1}y^{-1}$ under A, B and C, respectively. ANOVA test confirmed the statistically significance of the scenario factor in determining N leaching ($p<0.01$). The Dunn-Sidak post-hoc test confirmed that each scenario effect changed substantially to the others ($p<0.05$). On average, N leaching decreased by 62% passing from A to C, and by 48% from A to B with the exception of the area1 where higher leaching resulted. That was probably due to the mineral fertilization simulated for the wheat crop together with the seasonal high rainfall of that area.
Evaluating the N leaching within any area, the C scenario resulted to be the best combination of cropping systems and agricultural management.

	Rotation			
	M	Me	MW	MR
R^2	0.91	0.78	0.77	0.95
sig.	< 0.01	< 0.01	< 0.01	< 0.01
Beta Standardized Coefficients				
organic N fertilization	0.96			1.48
mineral N fertilization	1.33	1.07		-1.17
mineralization rate	0.71		0.68	
rainfall + irrigation				
percolation		1.47	1.97	
crop ET				
soil organic carbon %				
soil water content at saturation %				
crop yield		-0.66		
crop N uptake			-0.33	-0.62

Tab. 4 - Beta standardized coefficients of the multiple step-wise linear regression calculated for N leaching under the simulated crop rotations. The beta coefficient was reported only for the three most relevant variables in determining N leaching losses. M=maize; Me=meadows; MW=maize, wheat (and f.millet under the C scenario); MR=maize and It.ryegrass.
Tab. 4 - Coefficienti standardizzati beta della regressione lineare step-wise calcolata per l'azoto lisciviato simulato nelle quattro rotazioni. Per ogni rotazione sono riportati i coefficienti beta relativi alle tre variabili maggiormente significativi nel determinare la lisciviazione. M=mais; Me=prati permanenti; MW=mais, frumento (e panico nello scenario C); MR=mais e loiessa.

	Scenario				
Area	A	B	B to A	C	C to A
1	19	32	-68%	10	47%
2	37	21	43%	14	62%
3	40	19	53%	10	75%

Tab. 5 - Mean annual N leaching (kg N $ha^{-1}y^{-1}$) calculated on the basis of the UUA (%) devoted to the simulated crop rotations within the three studied areas. The decrease (%) in N leaching from A to B and to C scenario is reported.
Tab. 5 - Lisciviazione media annuale dell'azoto (kg N $ha^{-1}y^{-1}$) calcolata in base alla SAU (%) destinata alle rotazioni colturali simulate entro le tre aree in esame. La tabella riporta inoltre la diminuzione percentuale delle perdite di azoto per lisciviazione calcolate passando dallo scenario A agli scenari B e C.

4. DISCUSSION

The ARMOSA model application allowed to analyze all the interactive factors determining N leaching from arable land, evaluating different cropping systems and management.
With regard to crop production, the model simulated in agreement with existing studies carried out under similar conditions in Po plain. Considering grain maize production, Grignani *et al.* (2007) reported experimental results of trials in Piemonte (2003-2005) where grain yield was 12,000 kg ha^{-1} with an average crop N uptake of 200 to 300 kg N ha^{-1}. Such results are consistent with our simulated mean grain maize yield of 11,700 kg ha^{-1} and a mean crop N uptake of 279 kg N ha^{-1}. With regard to winter wheat grain production and crop N uptake, simulated values (5,400 kg ha^{-1}, 160 kg ha^{-1}) are in fully agreement with regional average data (5,900 kg ha^{-1}, ISTAT, 2010) and experimental studies of Grignani *et al.* 2003, reporting a grain yield of 6000 kg ha^{-1} and an average N uptake of 175 kg N ha^{-1}. The model underestimated silage maize and Italian ryegrass dry matter production if compared to field experiments (Onofri *et al.*, 1993; Grignani *et al.*, 2003) although regional data confirmed an average dry matter production of Italian ryegrass of 4,200 kg ha^{-1} (ISTAT, 2010). Moreover, the simulated average of N up take of the double cropping systems was 279 kg N ha^{-1}, which not

	N Balance								
	Input			Output					
Scenario	Fer.	Cr. Res.	Atm. Dep.	Cr.Up.	Lea.	Min.	Vol.	Den.	Imm.
A	281	29	22	164	31	106	9	2.1	21
				49%	9%	32%	3%	0.6%	6%
B	277	28	22	176	26	94	10	1.2	20
				54%	8%	29%	3%	0.4%	6%
C	239	41	22	156	15	87	8	1.1	35
				52%	5%	29%	3%	0.4%	12%

Tab. 6 - Mean annual nitrogen balance simulated under the three scenarios. The items of the balance are reported as kg N ha-1y-1 and as percentage of the mean annual N input. Fer.=fertilization, Cr. Res.=crop residues, Atm.Dep.=atmosferical deposition, Cr.Up.=crop uptake, Lea=leaching, Min.=mineralization, Vol.=volatilization, Den.=denitrification, Imm.=immobilization.

Tab. 6 - Bilancio medio annuale dell'azoto simulato nei tre scenari simulati. Le voci di bilancio sono espresse in termine assoluto (kg N $ha^{-1}y^{-1}$) e come percentuale rispetto al quantitativo di azoto applicato alle colture. Fer.=fertilizzazione, Cr. Res.=residui colturali, Atm.Dep.=deposizione atmosferica, Cr.Up.=assorbimento della coltura, Lea=lisciviazione, Min.=mineralizzazione, Vol.=volatilizzazione, Den.=denitrificazione, Imm.=immobilizzatione.

differs from the range of 248-293 reported by Grignani *et al.*, 2003.

The simulated meadows production (8,900 kg ha^{-1}) was slightly higher than regional data (ISTAT, 2010), whereas simulated foxtail millet production (8,800 kg ha^{-1}) and N uptake (101 kg N ha^{-1}) were consistent with results reported by Onofri *et al.* (1990) from field trials in Po plain were ranges of production and N uptake were from 4,000 to 7,000 kg ha^{-1} and 96 to 176 kg N ha^{-1}, respectively.

The ARMOSA model calculated all the items of the soil surface N balance and they are reported in Tab. 6. The N losses via leaching were in agreement with results reported in Po valley by Morari and Giupponi (1997) and Mantovi *et al.* (2006). The mean annual volatilization of 11 kg N $ha^{-1}y^{-1}$ was consistent with results reported by Carozzi *et al.* (2012 and 2013b) under slurry spreading in Po Valley. The simulated denitrification losses were 1.5 kg N $ha^{-1}y^{-1}$, which are slightly lower than results reported by Ventura *et al.* (2008).

The overall N efficiency increased from 49 to 52% passing from the A to the C scenario. Although the efficiency under the B scenario (54%) was higher than the C one, the B outline would be difficult to be adopted by farmers because of high livestock density. Particularly, under the C scenario the N leaching represented the 5% of N input, volatilization losses 3% and denitrification 1%. Therefore, 12% of N surplus was incorporated into soil organic matter through immobilization process. The C management could contribute more than the B one in enhancing soil organic matter representing a proper management to prevent the soil degradation (Bernardoni *et al.*, 2012).

With regard to N leaching, the Me rotation resulted to be the best rotations in every scenario, while M rotation (monoculture of maize) was associated to the highest leaching losses. The MW and MR crop rotations, which include maize as prevalent crop, were a good compromise between productivity and environmental sustainability.

The outstanding result of scenarios comparison was the significantly decrease of N leaching when the C scenario was adopted maintaining crops yield at standard level and contributing to reduce N leaching losses to groundwater.

5. CONCLUSIONS

The ARMOSA simulation results highlighted that the C scenario can be considered as an interesting solution in order to face the current concern of N leaching in Lombardia plain. In fact, grain maize crops, as well as silage maize in a double-cropping systems with Italian ryegrass had an high N uptake and it involved a certain decrease of the N losses. Moreover, the length of biological cycle of FAO 600 maize hybrids generally reached 150 days, so that crop N uptake corresponded to the period in which soil mineralization rate is particularly high, determining a large mineral N availability useful for crop growth. The increase of organic N supply with the consequent low mineral fertilization, allowed for obtaining high Nitrogen use efficiency (N uptake/N input). Under C scenario, the replacement of mineral-N

fertilizer with manure-N involved a significant decrease of mineralization rate in the three areas included in this study.
The ARMOSA results show that winter wheat followed by summer herbage allowed for high N uptakes as much as the adoption of the double cropping system of forage maize and Italian ryegrass. Moreover, management adopted under the C scenario can help to enhance the efficiency of farmyard manure use and to increase the soil content of organic matter thanks to an higher amount of organic fertilizer and crop residues incorporated into the soil.

ACKNOWLEDGEMENTS
This study was carried out in the project ARMOSA, where soil water and nitrate dynamics are measured and analyzed under different cropping systems at monitoring sites in arable farms. The project is currently on-going and coordinated by the Department of Agricultural and Environmental Science of the University of Milan, the Regional Agency for Agricultural and Forestry Development of Lombardy Region, and the Institute for Mediterranean Agricultural and Forestry Systems - National Research Council of Ercolano, Naples.

REFERENCES
Acutis, M., Scaglia, B., Confalonieri, R., 2012. Perfunctory analysis of variance in agronomy, and its consequences in experimental results interpretation. European Journal of Agronomy, 43: 129-135.

Acutis, M., Brenna, S., Pastori, M., Basile, A., De Mascellis, R., Bonfante, A., Manna, P., Perego, A., Fumagalli, M., Gusberti, D., Velardo, M.C., Trevisiol, P., Sciaccaluga, M., Albani, G., Malucelli, F., Vingiani, S., Orefice, N., 2007. "Modellizzazione della dinamica dell'acqua e dell'azoto nei suoli agricoli lombardi -Progetto ARMOSA" - ("Modelling water and nitrogen dynamics in Lombardia") Regione Lombardia quaderno della ricerca n. 65.

Acutis, M., Ducco, G., Grignani, C., 2000. Stochastic use of the LEACHN model to forecast nitrate leaching in different maize cropping systems. European Journal Agronomy, 13: 191-206.

Bernardoni, E., Carozzi, M., Acutis, M., 2012. Technical approach for the measurement of surface runoff. Italian Journal of Agrometeorology, 1: 41-50.

Bonfante, A., Basile, A., Acutis, M., De Mascellis, R., Manna, P., Perego, A., Terribile, F., 2010. SWAP, CropSyst and MACRO comparison in two contrasting soils cropped with maize in Northern Italy. Agricultural Water Management, 97: 1051–1062.

Borin, M., Giupponi, C., Morari, F., 1997. Effects of four cultivation systems for maize on nitrogen leaching. 1. Field experiment. European Journal Agronomy, 6: 101-112.

Carozzi, M., Loubet, B., Acutis, M., Rana, G., Ferrara, R.M., 2013a. Inverse dispersion modelling highlights the efficiency of slurry injection to reduce ammonia losses by agriculture in the Po Valley (Italy). Agricultural and Forest Meteorology, 171: 306-318.

Carozzi, M., Ferrara, R.M., Rana, G., Acutis, M., 2013. Evaluation of mitigation strategies to reduce ammonia losses from slurry fertilisation on arable lands. Science of the Total Environment, 449: 126–133.

Carozzi, M., Ferrara, R.M., Fumagalli, M., Sanna, M., Chiodini, M., Perego, A., Chierichetti, A., Brenna, S., Rana, G., Acutis, M., 2012. Field-scale ammonia emissions from surface spreading of dairy slurry in Po Valley. Italian Journal of Agrometeorology, 4: 25-34.

Conover, W.J., Iman, R.L., 1981. Rank transformations as a bridge between parametric and nonparametric statistics. American Statistical Association, 35: 124–129.

Eckersten, H., Janssson, P.E., Johnsson, H., 1996. SOILN model, user's manual, 3th Ed. Comm. 96:1, Swedish Univ. Agriculture Science, Dpt. of Soil Sciences, Uppsala.

Facchi, A., Gandolfi, C., Ortuani,B., Maggi, D., 2005. Simulation supported scenario analysis for water resources planning: a case study in northern Italy. Water Science Technology, 51: 11-18.

Fumagalli, M., Acutis, M., Mazzetto, F., Vidotto, F., Sali, G., Bechini, L., 2011. An analysis of agricultural sustainability of cropping systems in arable and dairy farms in an intensively cultivated plain. European Journal of Agronomy, 34. 71-82.

Fumagalli, M., Acutis, M., Mazzetto, F., Vidotto, F., Sali, G., Bechini, L., 2012. A methodology for designing and evaluating alternative cropping systems: application in dairy and arable farms. Ecological Indicators, 23: 189-201.

Grignani, C., Bassanino, M., Sacco, D., Zavattaro, L., 2003. A nutrient balance for creating a fertilization plan. Rivista di Agronomia, 37: 155-172.

Grignani, C., Zavattaro, L., 2000. A survey on actual agricultural practices and their effects on the mineral nitrogen concentration of the soil solution. European Journal of Agronomy, 12: 251-268.

Grignani, C., Zavattaro, L., Sacco, D., Monaco, S., 2007. Production, nitrogen and carbon balance of maize-based forage systems. European Journal of Agronomy, 26: 442-453.

Hargreaves, G.H., Samani, Z.A., 1985. Reference crop evapotranspiration from temperature. Applied Engineering in Agriculture, 1: 96-99.

ISTAT (Istituto Nazionale di Statistica), 2010. Verified on December 24th, 2010. Available on http://agri.istat.it/jsp/Introduzione.jsp?id=15A|18A|25A.

Johnson, P.A., Shepherd, M.A., Smith, P.N., 1997. The effects of crop husbandry and nitrogen fertilizer on nitrate leaching from a shallow limestone soil growing a five course combinable crop rotation. Soil Use Management, 13, 17-23.

Kersebaum, K.C., Matzdorf, B., Kiesel, J., Piorr, A., Steidl, J., 2006. Model-based evaluation of agri-environmental measures in the Federal State of Brandenburg (Germany) concerning N pollution of groundwater and surface water. Journal of Plant Nutrition and Soil Science, 169: 352-359.

Kramberger, B., Gselmana, A., Janzekovic, M., Kaligaric, M., Bracko, B., 2009. Effects of cover crops on soil mineral nitrogen and on the yield and nitrogen content of maize. European Journal of Agronomy 31, 103–109.

Kramberger, B., Lukac, B., Gruskovnjak, D., Gselman, A., 2008. Effects of Italian ryegrass and date of plow-in on soil mineral nitrogen and sugarbeet yield and quality. Agronomy Journal, 100: 1332-1338.

Mantovi, P., Fumagalli, L., Beretta, G.P., Guermandi, M., 2006. Nitrate leaching through the unsaturated zone following pig slurry applications. Journal of Hydrology, 316: 195-212.

Morari, F., Giupponi, C., 1997. Effects of four cultivation systems for maize on nitrogen leaching. 2. Model simulation. European Journal of Agronomy, 6: 113-123.

Onofrii, M., Tomasoni, C., Borrelli, L., 1993. Confronto tra ordinamenti cerealicolo-foraggeri, sottoposti a due livelli di input agrotecnico, nella pianura irrigua lombarda. I Produzioni quanti-qualitative. Rivista di Agronomia, 27, 3: 160-172.

Onofrii, M., Tomasoni, C., Borrelli, L., Berardo, N., 1990. Valutazione quanti-qualitativa di graminacee foraggere estive: panico e miglio perlato. Informatore Agrario, 48: 31-35.

Perego, A., 2010. Modelling nitrogen dynamics in crop and soil: from site-specific to regional application in northern Italy. Ph.D. Thesis, University of Milano, 176 pp.

Perego, A., Basile, A., Bonfante, A., De Mascellis, R., Terribile, F., Brenna, S., Acutis, M., 2012. Nitrate leaching under maize cropping systems in Po Valley (Italy). Agriculture, Ecosystem & Environment, 147: 57-65.

Regione Lombardia, 2006a. Regional Acts implementing the Action Programmes. Deliberazione della Giunta regionale n. 8/3439 del 7 novembre 2006. Adeguamento del Programma d'azione della Regione Lombardia di cui alla d.g.r. n. 17149/96 per la tutela e risanamento delle acque dall'inquinamento causato da nitrati di origine agricola per le aziende localizzate in zona vulnerabile, ai sensi del d.lgs. n. 152 del 3 aprile 2006, art. 92 e del D.M. n. 209 del 7 aprile 2006.

Regione Lombardia, 2006b. Programma di tutela e uso delle acque. Allegato 7 alla Relazione generale. Stima dei carichi effettivi di azoto e fosforo da agricoltura nelle acque di superficie, Milano, Italy, 53 pp.

Regione Lombardia, 2008. SIARL Sistema Informativo Agricolo Regione Lombardia.

Regione Lombardia, 2009. Servizio download dati geografici vettoriali. Verified October 20, 2009. Available at: http://www.cartografia.regione.lombardia.it/usedde/clientDDE.jsp;

Sacco, D., Bassanino, M., Grignani, C., 2003. Developing a regional agronomic information system for estimating nutrient balances at a larger scale. European Journal of Agronomy, 20: 199-210.

Sokal, R.R., Rohlf, F.J., 1981. Biometry, 2nd ed..W. H. Freeman and Company, New York.

SPSS, 2012. SPSS for Windows, Version 20.0.1 Chicago, IL.

Supit, I., Hooijer, A.A., van Diepen, C.A., 1994. System description of the WOFOST 6.0 crop simulation model implemented in CGMS. Volume 1: Theory and Algorithms. EUR 15956, Office for Official Publications of the European Communities, Luxembourg, 146 pp.

Thorup-Kristensen, K., 2001. Are differences in root growth of nitrogen catch crops important for their ability to reduce soil nitrate-N

content, and how can this be measured? Plant Soil 230, 185–195.
Thorup-Kristensen, K., Salmerón Cortasa, M., Loge, R., 2009. Winter wheat roots grow twice as deep as spring wheat roots, is this important for N uptake and N leaching losses? Plant Soil, 322: 101–114.
Trindade, H., Coutinho, J., Jarvis, S., Moreira, N., 2008. Effects of different rates and timing of application of nitrogen as slurry and mineral fertilizer on yield of herbage and nitrate-leaching of a maize/Italian ryegrass cropping system in north-west Portugal. Grass Forage Science, 64: 2-11.
Ungaro, F., Calzolari, C., Busoni, E., 2001. Development of pedotransfer functions using a group method of data handling for the soil of the Pianura Padano–Veneta region of North Italy: water retention properties. Geoderma, 124: 293-317.
Van Dam, J.C., Feddes, R.A., 2000. Numerical simulation of infiltration, evaporation and shallow groundwater levels with the Richards equation: simulation of field scale water flow and bromide transport in a cracked clay soil. Journal of Hydrology, 233, 72–85.
Van Dam, J.C., Huygen, J., Wesseling, J.G., Feddes, R.A., Kabat, P., van Walsum, P., Groenendijk, P., van Diepen, C.A., 1997. Simulation of water flow, solute transport and plant growth in the Soil-Atmosphere-Plant environment, Theory of SWAP version 2.0, Report 71, Technical Document 45. DLO Winand Staring Centre, Wageningen.
Van Heemst, H.D.J., 1988. Plant data values required for simple crop growth simulation models: Review and bibliography. Simulation Report CABO-TT nr. 17. Centre for Agrobiological Research (CABO) and Dep. Theoretical Production Ecol., Agricultural University Wageningen, Wageningen, The Netherlands.
Ventura, M., Scandellari, F., Ventura, F., Guzzon, B., Rossi Pisa, P., Tagliavini, M,. 2008. Nitrogen balance and losses through drainage waters in an agricultural watershed of the Po Valley (Italy). European Journal of Agronomy, 29: 108-115.

The ARCIS project

Valentina Pavan[1], Gabriele Antolini[1], Giacomo Agrillo[2], Luca Auteri[1] , Roberto Barbiero[3], Veronica Bonati[2], Fabio Brunier[4], Carlo Cacciamani[1], Orietta Cazzuli[5], Andrea Cicogna[6], Chiara De Luigi[9], Luca Maraldo[7], Gianni Marigo[8], Roberta Millini[8], Elvio Panettieri[3], Sara Ratto[4], Christian Ronchi[9], Serenella Saibanti[3], Angela Sulis[5], Fausto Tomei[1], Rodica Tomozeiu[1], Igor Torlai[4], Giulia Villani[1]*

Abstract: *Monitoring and description of the observed climate are extremely important not only on the scientific point of view, but also for their contribution to decision making at political level. In fact, they represent both a crucial contribution to the assessment of the climatological characteristics of a region, and a starting point for all activities related with planning of infrastructures, land use and agricultural and energy production. In Italy, climate monitoring activities are currently covered at local level by Regional Meteorological Services, and at national level by National Institutions like Aereonautica Militare and CRA-CMA. The project ARCIS (ARchivio Climatologico per l'Italia Settentrionale), started in 2008 and now approaching its first renewal, represents an effort done by some Italian Regional Meteorological Services in order to coordinate their activities in the field of climatology. The main target of this project consists of building a unified, high-density and long term climatological data base, which can be used in order to issue climatological products at super-regional scale, using shared methodologies for the treatment of climatological data. In the present note is a description of the project, of its aims, of some preliminary results and of its future perspectives.*
Keywords: *climatology, Northern Italy, spatial interpolation, precipitation, quality control of meteorological data.*

Riassunto: *Il monitoraggio e la descrizione del clima osservato sono attività di grande rilevanza non solo ai fini della ricerca scientifica ma anche ai fini della gestione territoriale. Esse infatti sono sia un contributo essenziale allo studio delle caratteristiche climatologiche di una regione che la base di partenza necessaria per tutte le attività connesse alla pianificazione, all'uso del territorio e alla produzione agricola e di energia. In Italia, le attività di monitoraggio climatico a livello locale fanno parte dei compiti istituzionali dei Servizi Meteorologici Regionali, ma nello stesso tempo altre Istituzioni Nazionali, come l'Aereonautica Militare e il CRA-CMA, svolgono simili attività a livello nazionale. Il progetto ARCIS (ARchivio Climatologico per l'Italia Settentrionale), iniziato nel 2008 ed ora prossimo al suo primo rinnovo, rappresenta il tentativo di alcuni Servizi Meteorologici Regionali italiani di coordinare le loro attività nel campo della climatologia. La principale finalità del progetto è la creazione di un data base climatologico centralizzato, ad alta densità di stazioni e continuativo per lunghi periodi di tempo, che permetta di pubblicare prodotti climatologici a scala sovra-regionale, utilizzando standard condivisi di trattamento dei dati storici a valenza climatica. Nella presente nota è descritto il Progetto, i suoi obiettivi, i risultati sin qui ottenuti e le prospettive future.*
Parole chiave: *climatologia, Nord Italia, interpolazione spaziale, precipitazioni, controllo qualità di dati meteorologici.*

INTRODUCTION

Monitoring and description of the observed climate are extremely important not only on the scientific point of view, but also for their contribution to decision making at political level. In fact, they represent both a crucial contribution to the assessment of the geographical and the climatological characteristics of a region, and a starting point for all activities related with planning of infrastructures, land use and agricultural and energy production.

In Italy, hydrological and climatological monitoring were institutionally covered by the Servizio Idrografico e Mareografico Nazionale (SIMN). After this Service was closed, starting from about 2001 its duties were assigned to local Regional Meteorological Services (RMSs). Several of these Services have taken up all monitoring activities and associated duties, continuing to issue the main official products offered by the SIMN for the territory included in their administrative borders. All the same, the fragmentation of these activities into several contributions, depending on administrative jurisdiction, has gradually produced several differences between the climate services offered by the different regions, together with some institutional inefficiencies. These translated into a general difficulty for the users in accessing the climatological products and data, mainly due to the fact that in some regions the official Institute covering these activities has changed in time and

* Corresponding author: e-mail: vpavan@arpa.emr.it
[1] ARPA Emilia-Romagna, Servizio IdroMeteoClima
[2] ARPA Liguria
[3] Provincia Autonoma di Trento
[4] Regione Autonoma Valle d'Aosta
[5] ARPA Lombardia
[6] OSMER Friuli-Venezia Giulia
[7] Provincia Autonoma di Bolzano
[8] ARPA Veneto
[9] ARPA Piemonte
Received 14 February 2013, accepted 18 February 2013.

that the Institutional Reference at national level may be different for each RMS, ranging from the Environmental Agency, to Civil Protection Agency or even to Institutes connected with the University. Several efforts have been tried in order to offer climatological products at national or at least super-regional level. Some of these efforts are linked to research activities mostly connected with international or European projects (Brunetti *et al.*, 2006; Frei and Schär, 1998), others are the result of the work of National Institutions coordinating the activity of some of the RMSs (see for example the experience of the 'Sistema nazionale per la raccolta, l'elaborazione e la diffusione di dati Climatologici di Interesse Ambientale', SCIA, described in http://www.scia.sinanet.apat.it/). In general, most of these climatological products are characterised by problems in the time and space coverage of the climatological observing network, due to the difficulty in the collection of data (Frei and Schär, 1998), or by low density of stations linked to the choice of using only data of Institutes monitoring climate at national level, like Aereonautica Militare (Toreti and Desiato, 2007; Toreti *et al.*, 2006; Brunetti *et al.*, 2006).

The growing difficulties recognised by the RMSs in covering their duties related with climate monitoring, in making their products known outside their administrative jurisdictions and in collaborating to research and to institutional activities both at national and at international level have resulted into the acknowledgement of the need to coordinate their activities related with the production of climate products. The ARCIS project (ARchivio Climatologico per l'Italia Settentrionale) is the first effort done by some RMSs aimed at coordinating their climatological activities independently from their own institutional references at super-regional level. It consists of a five year agreement, signed in 2008 by several Italian regions, now approaching at its first renewal, aimed at building a common, high density climatological data base of daily data as a starting point in order to issue climatological super-regional products and services. Although the original agreement mentioned only the necessity of building a shared climatological data base of daily data and of establishing a scientific working group which would identify and implement the project activities, the project has managed not only to reach its original goal, but also to design and to start the activities related with the use of data and with the production of common climatological products (like an up to date atlas of precipitation over Northern Italy). The following document describes the objectives of the project and its first preliminary results.

THE ARCIS PRODUCTS

During the first five years of work, the ARCIS working group has managed to produce:

- a shared climatological data base of observational station data, accessible only to the project participants;
- a public web site, (*http://www.arcis.it/*) where the project and its results are described and where the public products are made available;
- commonly approved methodologies used to check the data quality, the homogeneity of climatological time series and their synchronicity;
- commonly approved methodologies finalised to produce a daily analysis for each surface climatological parameter;
- a group of preliminary results including a climatology of precipitation and temperature for the territory covered by the Administrations participating to the project.

In the following, it is given a brief overview of each product, a more detailed description of data, methods and final results being demanded to future publications.

THE DATA BASE

The data base includes daily precipitation and minimum and maximum temperature data covering the period from 1961 to 2010. It was decided not to include in this data base all data recorded for these three parameters over the period and territory of interest. On the contrary, each RMS has performed a preliminary selection of data so as to include in the data base only the data recorded at stations presenting characteristics of good data quality and high temporal coverage. In case a station presenting a long climatological time series did not cover the whole period addressed by the project, it was decided to cover the remaining time window with the data of another station, located as close as possible to the original one and presenting similar characteristics of high quality and statistical homogeneity. This choice allowed to manage the problem connected with the automation of the climate monitoring network, often connected with a change in location of the original climatological stations, and with the necessary changes in the location of the stations, connected with a change in their surrounding environment.

Currently, the ARCIS data base includes about 700 climatological time series of daily precipitation and

about 200 time series of daily minimum and maximum temperature. Fig. 1 shows the maps of the ARCIS precipitation (a) and temperature (b) monitoring network, different symbols referring to stations maintained by different RMSs. Although the precipitation density is already high in large areas of the domain and presents a high level of continuity in time, it is meant to be improved in the near future by increasing the station density where necessary. On the contrary, the density of the temperature monitoring network is thought to be still insufficient both for its spatial distribution and its temporal coverage in order to produce robust evaluations of the regional climate variability.

THE QUALITY CONTROL METHODS

Before use, all data are checked for quality and all climatological time series are checked for homogeneity and synchronicity, by means of methods approved by all partners.

The selected quality control strategy is mostly based on the work described in Pavan *et al.* (1999). Data are first checked for their plausibility, that is whether their values fall within the range covered by the instrument used to measure them. Then, their internal consistency is checked (requiring for example that minimum temperature is less than or equal to the maximum temperature in the same day and same location). Finally, the data undergo climatological, spatial and temporal checks in order to assure consistency between data recorded at different locations at the same time or at subsequent time.

Then all time series are checked for their statistical homogeneity using three tests: the Standard Normal Homogeneity Test (SNHT; Alexandersson and Moberg, 1997), the Craddock (Craddock, 1979) and the Vincent test (Vincent, 1998).

Finally, all time series recognised to be homogeneous are checked for their synchronicity, by testing that the observational time at which data are recorded at one station are in agreement with those at which data are recorded at all other stations. When a systematic disagreement is found between the observational times at two stations for one or more period, the time at which data are attributed are corrected. This procedure assumes that the observational time is known to be correct at least at one station. Applying it before producing daily analysis map allows to avoid most inconsistencies between data and to improve the quality of the daily final products.

More details on the methods of quality control, homogeneity testing and synchronicity testing and correction over mentioned can be found in Antolini *et al.* (2013).

THE ANALYSES

All data satisfying the requirements of quality described before can be used by the ARCIS partners in order to produce daily analysis over the

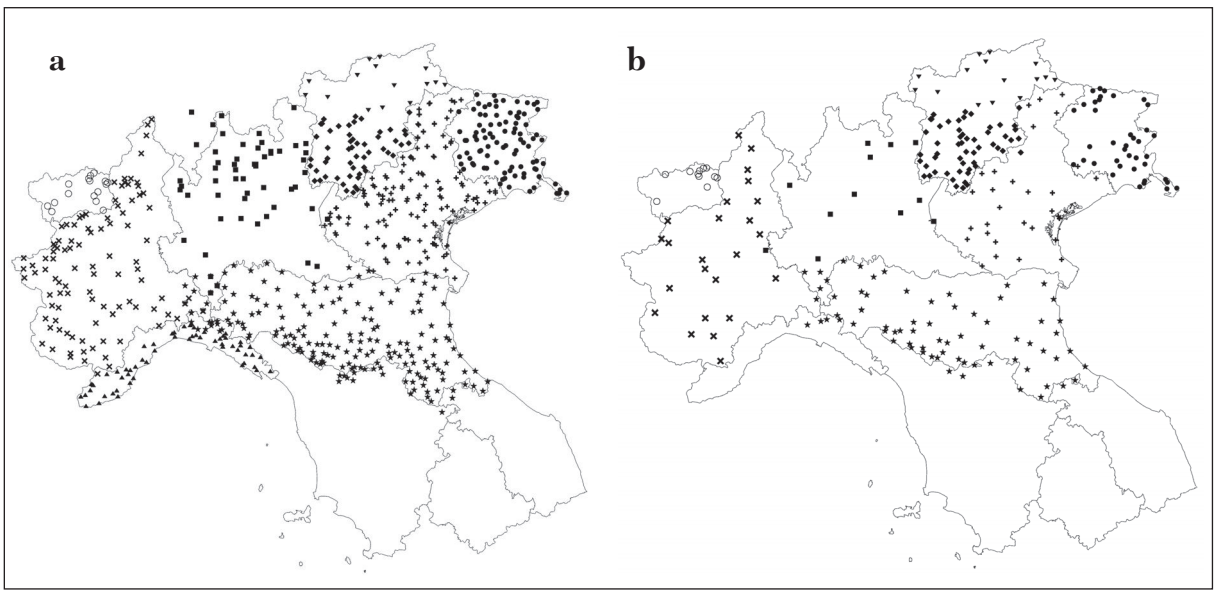

Fig. 1 - Maps of the precipitation (a) and temperature (b) ARCIS monitoring network. Different symbols refer to stations maintained by different RMSs.

Fig. 1 - Mappe delle reti di monitoraggio ARCIS per la precipitazione (a) e la temperatura (b). I diversi simboli indicano stazioni mantenute da diversi SMR.

whole territory covered by the ARCIS conventions. At present two methods have been used in order to produce preliminary climate products.

On the one side, an objective analysis is being produced on a 10 km regular grid by interpolating the station data using specific methods based on Kriging (Krige, 1951), customised depending on the surface parameter considered (Antolini *et al.* 2013).

On the other side, the same data have been used in order to produce an optimal interpolation analysis (Uboldi *et al.*, 2008; Kalnay, 2003) on a regular grid of about 13 km resolution (Ronchi *et al.*, 2008).

By applying to each field these analysis methods, it was possible to produce daily maps for each parameter and, starting from those, compute climatological mean values, trends and their significance both at annual and at seasonal scale.

Panels a and b in Fig. 2 show the maps of the total annual precipitation climatology for the period 1961-2000, obtained with the two analysis methodologies, namely (a) shows the results obtained by applying the method of Antolini *et al.* (2013), while (b) results obtained by applying the method of Ronchi *et al.* (2008).

The results obtained using the two analysis methods are similar and compatible with other results achieved within similar climatological exercises available in the literature, although in some cases the higher station density available within the ARCIS data base allows to detail the local climate variability both in time and in space.

FUTURE PERSPECTIVES

The ARCIS Project is now at its first renewal. The results achieved during these first five years are promising, especially in view of the fact that they have been produced as part of the operational activities of each RMS, without any extra-funding.

In the near future it is meant to publish the final results of the climatological analyses earlier mentioned in this note for the period 1961-2010 for precipitation: the high density, approximately spatially uniform and continuous time coverage of data collected within the ARCIS project for this parameter represent great improvements with respect to all climate products publicly available at present for Northern Italy. Next, it is meant to focus on the improvement of the temperature monitoring network both in terms of time and space, so as to allow to produce robust climate products also for this parameter.

Finally it is meant to extend this project to other regions who have already expressed interest for participating to this initiative. This particular step could be crucial in the perspective to make the ARCIS experience a paradigm for the advantageous development of a distributed national provider of climate services.

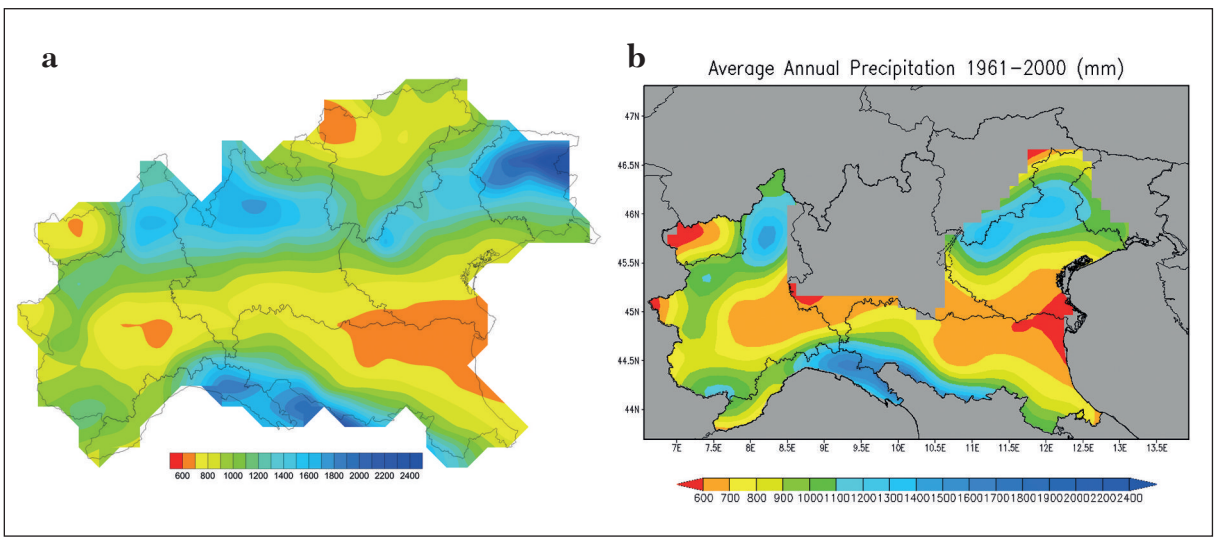

Fig. 2 - Maps of the total annual precipitation climatology 1961-2000, a) obtained using the method by Antolini et al (2013); b) obtained using the method by Ronchi et al (2008). In panel b, grey shading indicates area with insufficient station coverage in the ARCIS data-base at the time of the analysis computation.

Fig. 2 - Mappe di climatologia della precipitazione cumulata annua per il periodo 1961-2000, a) ottenuta usando il metodo di Antolini et al (2013); b) ottenuta usando il metodo di Ronchi et al (2008). Nel pannello b, l'ombreggiatura grigia indica aree con una copertura di stazioni insufficiente nel data-base ARCIS al tempo in cui l'analisi è stata calcolata.

REFERENCES

Alexandersson, H., Moberg, A., 1997: Homogenization of Swedish temperature data. Part I: a homogeneity test for linear trends. *International Journal of Climatology* **17**: 25-34.

Antolini, G., Pavan, V., Tomei, F., Auteri, L., Tomozeiu, R., Marletto, V., 2013: A high-resolution daily gridded climatic data-set for Emilia-Romagna (Italy) 1961-2010. Submitted to *International Journal of Climatology*.

Brunetti, M., Maugeri, F., Monti, T., Nanni, T., 2006: Temperature and precipitation variability in Italy in the last two centuries from homogenized instrumental time series, *International Journal of Climatology* **26**: 345-381.

Craddock, J.M., 1979: Methods for comparing annual rainfall records for climatic purposes. *Weather* **34**: 332-346.

Frei, C., Schär, C., 1998: A precipitation climatology of the Alps from high-resolution rain-gauge observations. International Journal of Climatology 18: 873-900.

Kalnay, E., 2003: Atmospheric modelling, data assimilation and predictability. Cambridge Univ. Press, 341 pp.

Krige, DG., 1951. A statistical approach to some basic mine valuation problems on the Witwatersrand. *Journal of the Chemical, Metallurgical and Mining Society of South Africa* **52**: 119-139.

Ronchi, C., De Luigi, C., Ciccarelli, N., Loglisci, N., 2008: Development of a daily gridded climatological air temperature dataset based on a optimal interpolation of ERA-40 reanalysis downscaling and a local high resolution thermometers network. Proceedings of the "European Conference on Applied Climatology (ECAC)", Amsterdam.

Toreti, A., Desiato, F., 2007. Temperature trend over Italy from 1961 to 2004. *Theoretical and Applied Climatology* **91**: 51-58.

Toreti, A., Fioravanti, G., Perconti, W,. Desiato, F., 2009: Annual and seasonal precipitation over Italy from 1961 to 2006. *International Journal of Climatology* **29**: 1976-1987.

Uboldi, F., Lussana, C. and Salvati, M., 2008: Three-dimensional spatial interpolation of surface meteorological observations from high-resolution local networks. Meteorological Applications, 15: 331-345, doi: 10.1002/met.76.

Vincent, LA., 1998: A technique for the identification of inhomogeneities in Canadian temperature series. *Journal of Climatology* **11**: 1094-1104.

Il sambuco come indicatore vegetale di cambiamenti climatici: analisi di serie storiche e verifica del modello fenologico IPHEN

Roberta Alilla[1], Chiara Epifani[1], Giovanni Dal Monte[1]*

Riassunto: *Il sambuco è una specie spontanea largamente diffusa sul territorio italiano ed europeo ed il monitoraggio dei suoi ritmi di fioritura ha fornito importanti indicazioni sul riscaldamento in atto alle medie latitudini. Al riguardo, le analisi eseguite sulle date di fioritura del sambuco raccolte nei Giardini Fenologici Italiani e collezionate nella Banca Dati Fenologica Nazionale, mostrano un quadro discordante. Infatti, nel Giardino Fenologico di S. Pietro Capofiume (BO), che possiede la serie storica più lunga, si osserva un anticipo della fioritura di circa 1 [d/y] dal 1990 al 2011, segnale non presente nei dati fenologici registrati nel GF di Fontanella-S. Apollinare (PG), la cui serie storica è peraltro più breve (1997-2011). Tuttavia, le date di fioritura osservate in S. Apollinare sono correlate in maniera significativa con le medie mensili (periodo Gennaio- Aprile) delle temperature minime e massime, con un anticipo di 7.5 [d] per ogni °C di aumento della temperatura minima e di 5.9 [d/°C] di quella massima. I dati fenologici raccolti in questi siti sono stati utilizzati per validare il modello fenologico IPHEN implementato dal CRA-CMA nel Sistema Informativo Agricolo Nazionale. La validazione ha evidenziato che il modello, con i parametri attuali, non rappresenta con sufficiente accuratezza le date di fioritura del sambuco nei due GF; in particolare, nel caso di S. Pietro Capofiume negli anni 2003-2006, a fronte di un anticipo nei dati di fioritura osservati, il modello ha stimato un ritardo di comparsa delle fasi. Il modello è stato, quindi, ricalibrato e validato su set di dati indipendenti e ha fornito prestazioni nettamente migliori in entrambi i GF.*
Parole chiave: *fenologia, modelli, ore normali di caldo, sambuco, giardini fenologici.*

Abstract: *The monitoring of black elder flowering rhythms has provided important information on climate warming occurred in the Northern mid-latitudes. In this regard, the analyses carried out on flowering dates of black elder gathered in the Italian Phenological Database, show a discordant situation. In fact, in the Phenological Garden of S. Pietro Capofiume (BO), which has the longest time series, we observe an advance of flowering of about 1 [d/y] from 1990 to 2011, while no signal there is in phenological data registered in the Phenological Garden of Fontanella-S. Apollinare (PG), whose time series is moreover shorter (1997-2011). However, flowering dates observed in S. Apollinare are significantly correlated with the monthly averages (January to April) of daily minimum and maximum temperatures, with an advance of 7.5 [d] for each °C of the minimum temperature increase and 5.8 [d/C] of the maximum. Phenological data collected at these sites were used to validate the IPHEN phenological model. Validation has shown that the model, with the current parameters, does not simulate with sufficient accuracy the elder blooming dates in these Gardens; in particular, in the case of S. Pietro Capofiume in the years 2003-06, compared with an advance in flowering observed data, the model estimated a delay of onset of phases. The model was then recalibrated and validated on independent data sets and thus it provided evidently better performance in both Gardens.*
Keywords: *phenology, models, Normal Heat Hours, elder, phenological gardens.*

INTRODUZIONE

Negli ultimi due decenni la fenologia vegetale ha assunto un ruolo di primaria importanza nell'ambito della verifica degli effetti dei cambiamenti climatici e delle strategie di adattamento ad essi (Walther *et al.*, 2002). Numerosi sono gli studi che confermano la relazione tra il riscaldamento globale e determinate fasi fenologiche, come l'anticipo dell'emissione delle foglie e la fioritura (Menzel and Fabian 1999; Beaubien and Freeland, 2000; Chmielewski and Rötzer, 2001; Menzel *et al.*, 2006). Tali studi richiedono una base dati solida, costituita da serie storiche di dati fenologici piuttosto lunghe e confrontabili tra loro. A questo proposito il CRA-CMA, nell'ambito del progetto di ricerca Agroscenari, ha realizzato una Banca Dati Fenologica Nazionale (BDFN) all'interno della Banca Dati Agrometeorologica Nazionale (BDAN) gestita dal Sistema Informativo Agricolo Nazionale (SIAN), allo scopo di raccogliere, controllare, standardizzare e mettere a disposizione i dati per i servizi agricoli e per la ricerca (Epifani *et al.*, 2013). Ad oggi, la BDFN raccoglie sia dati aggiornati raccolti da reti fenologiche

* Corresponding author: e-mail: roberta.alilla@entecra.it
[1] CRA - Consiglio per la ricerca e la sperimentazione in agricoltura (Unità di ricerca per la climatologia e la meteorologia applicate all'agricoltura, Roma)
Received 17 March 2013, accepted 17 April 2013.

attive, sia dati relativi ad alcune delle più importanti serie storiche italiane collezionati nei Giardini Fenologici appartenenti alla Rete dei Giardini Fenologici Italiani (Aronne *et al.*, 2012). Di queste, le più lunghe appartengono ai Giardini Fenologici di S. Pietro Capofiume (20 anni dal 1990 al 2011) e di Sant'Apollinare (15 anni dal 1997 al 2011).
Sempre all'interno del SIAN, è stato realizzato un ambiente di analisi e previsione fenologica multi-modello per la produzione di carte fenologiche a livello nazionale (Alilla *et al.*, 2013). Ai modelli fenologici preesistenti, implementati nel SIAN a partire dagli anni '90 (per mais precoce e tardivo, girasole, soia, barbabietola da zucchero, orzo, frumento duro e tenero) che funzionano accumulando gradi giorno (Growing Degree Days-GDD) (Miglietta, 1991; Porter *et al.*, 1987), il CRA-CMA ha recentemente aggiunto i modelli sviluppati nell'ambito del progetto IPHEN (Italian Phenological Network) dal DISAA dell'Università di Milano (Mariani *et al.*, 2013). Questi modelli sono calibrati e validati su serie storiche provenienti da differenti aree del territorio nazionale. Si caratterizzano per la parsimonia in termini di variabili di input e parametrizzazione minimale, in ragione della ridotta disponibilità di serie storiche fenologiche. Essi consentono la creazione di carte anche con dati di input incompleti per cui risultano piuttosto robusti e con una grande flessibilità, poiché si adattano ad un vasto insieme di specie e varietà. Forniscono, infine, come output la fase fenologica raggiunta dalla specie nella scala BBCH (Meier, 2001), che costituisce uno standard diffuso a livello nazionale e internazionale. Ad oggi sono stati implementati nell'ambiente SIAN i modelli IPHEN di alcune specie di interesse agricolo, allergologico, apistico ed ornamentale quali: vite (Chardonnay e Cabernet-Sauvignon), olivo, cipresso, robinia e sambuco.
Il sambuco (*Sambucus nigra* L.) è una specie spontanea appartenente alla famiglia delle Caprifoliacee. È un arbusto, piuttosto comune soprattutto nei luoghi incolti ed umidi. Fiorisce tra aprile e giugno i suoi fiori sono piccoli bianchi, riuniti in infiorescenze. Da sempre monitorato sia nei Giardini Fenologici Internazionali (IPG) che nei Giardini Fenologici Italiani (GFI), il suo studio ha fornito importanti informazioni come di indicatore vegetale dei cambiamenti climatici (Schaber and Badeck, 2005). Inoltre, risulta che il suo ritmo fenologico può essere correlato a quello di altre specie spontanee e coltivate, quali il mais ad esempio (Chiesura Lorenzoni, 2002).
In questo lavoro si presentano, innanzitutto, le analisi effettuate sulle date di fioritura del sambuco, utilizzando le serie di dati fenologici raccolti nei GFI di S. Pietro Capofiume dal 1990 al 2011 e di Sant'Apollinare dal 1997 al 2011, per verificare se il segnale del riscaldamento globale in atto è riscontrabile in Italia sulla base del monitoraggio fenologico. Gli stessi dati sono stati usati per la validazione del modello fenologico per il sambuco implementato nel SIAN a scala nazionale. Al riguardo una validazione preliminare era stata presentata nel 2012 (Alilla *et al.*, 2012), utilizzando set di dati fenologici meno ampi (1999-2011) e con la presenza di rilevamenti che l'analisi degli outlier aveva evidenziato come anomali.

MATERIALI E METODI

Dati

I dati fenologici provengono dai GF di S. Pietro Capofiume, Molinella (BO) (Servizio IdroMeteoClima dell'ARPA Emilia-Romagna) e di Fontanella-Sant'Apollinare, Marsciano (PG) (Università di Perugia, Centro di ricerca sul clima e i cambiamenti climatici), entrambi appartenenti alla Rete dei Giardini Fenologici Italiani. Gli esemplari di sambuco presenti in detti GF sono tutti cloni provenienti dalla propagazione delle piante di S. Pietro Capofiume, giardino che è stato avviato nel 1983 ed iscritto come primo, tra quelli italiani, nella rete IPG. Sono stati presi in considerazione i rilevamenti settimanali dal 1990 al 1991 e dal 1994 al 2011 per il GF di S. Pietro Capofiume e dal 1997 al 2011 per Sant'Apollinare; le serie sono lunghe rispettivamente 20 e 15 anni.
I dati di temperatura massima e minima giornaliera utilizzati nelle analisi feno-climatiche e come dati di ingresso del modello fenologico sono calcolati, a partire dai dati rilevati dalle stazioni, col metodo dell'Analisi Oggettiva (Libertà and Girolamo, 1991), su un grigliato di 10 km di lato. Le coordinate dei GF, dei nodi di griglia ad essi più vicini e le rispettive distanze, sono inserite in (Tab.1).
L'analisi si è concentrata sulle date di fioritura del sambuco, in particolare le date di rilevamento delle fasi BBCH:
- 61 (inizio fioritura: 10% dei fiori aperti)
- 65 (piena fioritura: almeno 50% dei fiori aperti, primi petali caduti)
- 67 (inizio sfioritura: fiori per lo più appassiti).

Modello fenologico

Nell'ambiente SIAN, le temperature orarie sono state calcolate a partire dalle temperature minime e massime giornaliere, tramite l'algoritmo di Parton e Logan (Parton and Logan, 1988). L'accumulo orario di calore assorbito dalle piante (NHH) viene simulato mediante una curva beta (Wang and Engel, 1998), con cui si associa il valore 0 per temperature esterne all'intervallo tra i cardinali termici minimo e

	Latitudine	Longitudine	Altitudine [m]	Distanza [Km]
S. Pietro Capofiume	44° 39' 17" N	11° 37' 25" E	10	
nodo 8160	44° 36' 0" N	11° 42' 0" E	8	8:5
S. Apollinare	42° 59' 50" N	12° 18' 55" E	270	
nodo 9756	43° 0' 0" N	12° 15' 36" E	306	4:5

Tab. 1 - Coordinate geografiche e altitudine dei Giardini Fenologici e dei nodi ad essi più vicini. Nell'ultima colonna la distanza in [Km] tra Giardino e nodo.
Tab. 1 - Geographical coordinates and elevation of the Phenological Gardens and the grid nodes closest to them. In the last column the distance [Km] between Garden and node.

massimo e valori compresi tra 0 ed 1 per temperature interne allo stesso intervallo. L'accumulo risulta pari ad 1 per temperature uguali al cardinale termico ottimale per lo sviluppo. Nel caso del sambuco, i cardinali termici (minimo, ottimo e massimo) impiegati come parametri della funzione beta sono rispettivamente 1, 20 e 32. Il modello fenologico per il sambuco, sviluppato dal DISAA (Unimi), è stato calibrato su set di dati forniti dall'Università di Bologna relativi ai periodi 1977-1988 e 1999-2005 (Mariani *et al.*, 2013). Il modello restituisce come output il valore della fase BBCH raggiunta in relazione all'accumulo giornaliero di NHH (NHHsum), calcolate a partire dal 1 Gennaio, secondo la funzione lineare seguente:

$$BBCH = 0.0164 \cdot NHHsum + 44.223$$

Analisi

Sono stati calcolati gli andamenti delle date di fioritura del sambuco negli anni per entrambi i GF e la correlazione tra l'inizio della fioritura e l'andamento dei valori medi delle temperature massime e minime nei primi quattro mesi dell'anno (il periodo gennaio-aprile che precede la fioritura di questa specie). Si presenta poi il confronto tra le date di fioritura osservate e simulate tramite il modello fenologico del sambuco implementato nel SIAN. Per valutare il grado di accuratezza con cui il modello ha simulato le date di fioritura osservate in campo, sono stati calcolati i seguenti indici (Loague and Green, 1991):

- il Mean Absolute Error (MAE: minimo e ottimo= 0)

$$MAE = \frac{1}{n}\sum_{i=1}^{n}\left|S_i - O_i\right|$$

- il Model Efficiency (EF: massimo e ottimo= 1)

$$EF = 1 - \frac{\sum_{i=1}^{n}\left(S_i - O_i\right)^2}{\sum_{i=1}^{n}\left(O_i - \overline{O}\right)^2}$$

- il Coefficient of Residual Mass (CRM: ottimo= 0)

$$CRM = \frac{\sum_{i=1}^{n} S_i - \sum_{i=1}^{n} O_i}{\sum_{i=1}^{n} O_i}$$

dove *O* indica le date osservate, *S* le simulate ed *n* il numero di confronti effettuati. Gli stessi indici hanno permesso di individuare una nuova combinazione di parametri del modello, che simula con risultati migliori le date di fioritura in anni particolarmente caldi.

RISULTATI E DISCUSSIONE

Gli andamenti delle date di fioritura del sambuco osservate nei due GF sono riportati nel grafico di (Fig.1). Dall'alto verso il basso sono rappresentati gli andamenti delle date di rilevamento in DOY (day of the year=giorno dell'anno) delle fasi BBCH 61, 65 e 67. Di seguito sono indicate le funzioni regressive, gli R^2 ed il livello di significatività associato (Tab. 2). Dalla tabella si deduce che nel giardino di S. Pietro Capofiume le date di fioritura presentano un anticipo significativo, pari a 1.14 [giorni/anno] ($p<0.01$) per l'inizio della fioritura, 0.79 [giorni/anno] ($p<0.05$) per la piena fioritura e 0.68 [giorni/anno] ($p<0.05$) per la fine della fioritura. In media si osserva, quindi, un anticipo della fioritura di circa un 1 giorno ogni anno, che corrisponde a circa 20 giorni nei 20 anni di analisi. Ciò conferma quanto già evidenziato, per la piena fioritura del sambuco nel GF di S. Pietro Capofiume in (Villani *et al.*, 2012). Altrettanto non si può dire per il GF di S. Apollinare, in cui la base dati è ridotta (15 anni) e gli andamenti non rivelano un segnale significativo.

Il grafico di (Fig. 2) rappresenta le correlazioni tra le date di inizio fioritura (BBCH 61) e i valori delle medie mensili del periodo (gennaio-aprile) di temperatura minima (in alto) e massima (in basso) giornaliera calcolate nei nodi di griglia più vicini ai due GF. In S. Apollinare, le correlazioni sono significative per entrambe le temperature con R^2 pari a 0.64 e 0.27 entrambi con livelli di

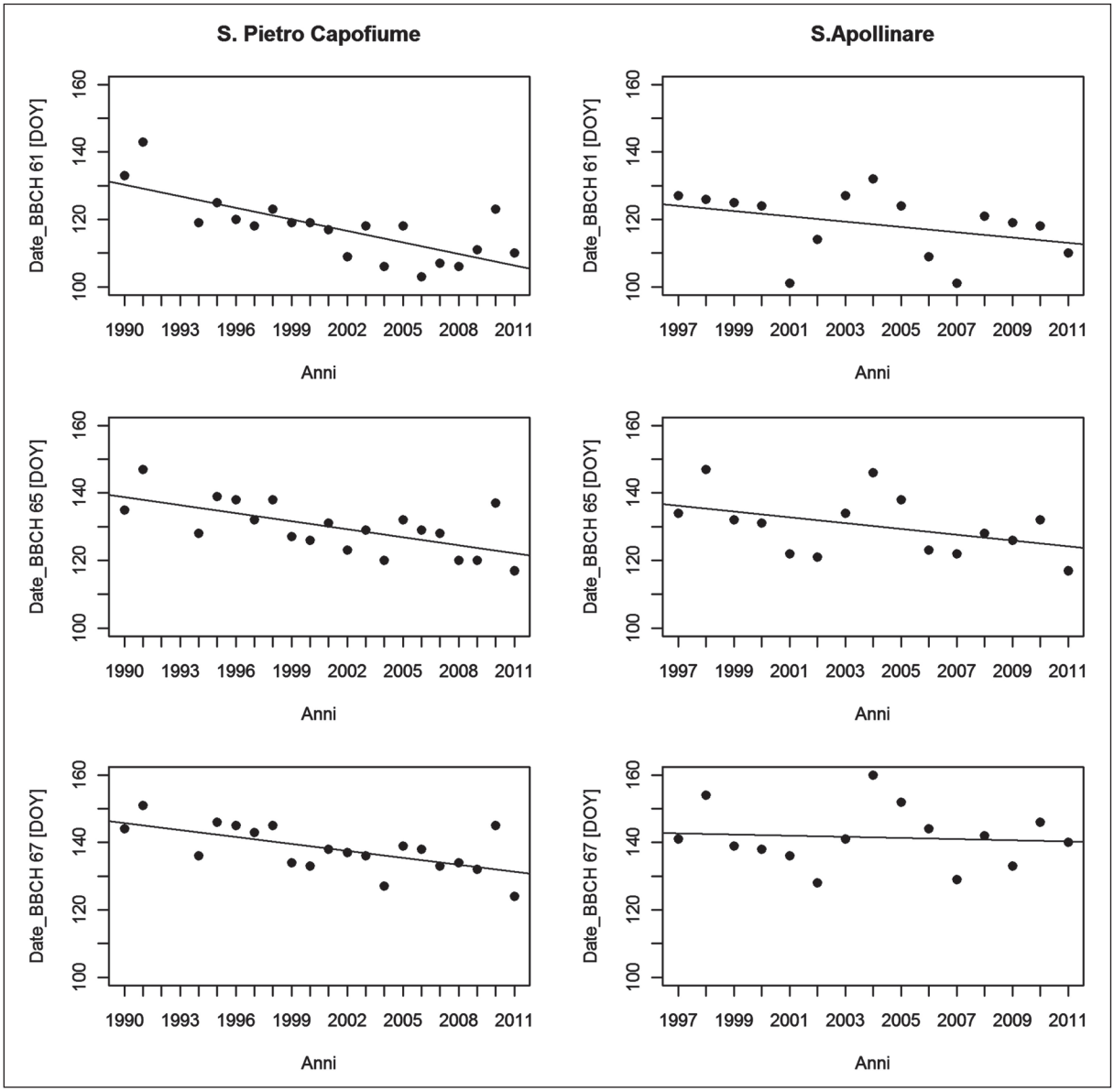

Fig. 1 - Andamento delle date di fioritura del sambuco osservate nei due GF. DOY= giorno dell'anno.
Fig. 1 - Trend of black elder flowering dates observed in two Phenological Gardens. DOY= day of the year.

	fase BBCH	equazione	R^2	
S. Pietro Capofiume	61	y= -1.14 x+ 2400.75	0.54	**
	65	y= -0.79 x+ 1718.58	0.41	*
	67	y= -0.68 x+ 1509.49	0.39	*
S. Apollinare	61	y= -0.79 x+ 1707.42	0.14	ns
	65	y= -0.87 x+ 1869.39	0.19	ns
	67	y= -0.17 x+ 477.92	0.01	ns

Tab. 2 - Regressioni tra anni (x) e date di fioritura (y) per ciascuna fase. Andamenti con *p < 0.05, **p < 0.01; ns=non significativo.
*Tab. 2 - Regressions between years(x) and flowering dates (y) for each stage. Trends with *p < 0.05, **p < 0.01; ns=not significant.*

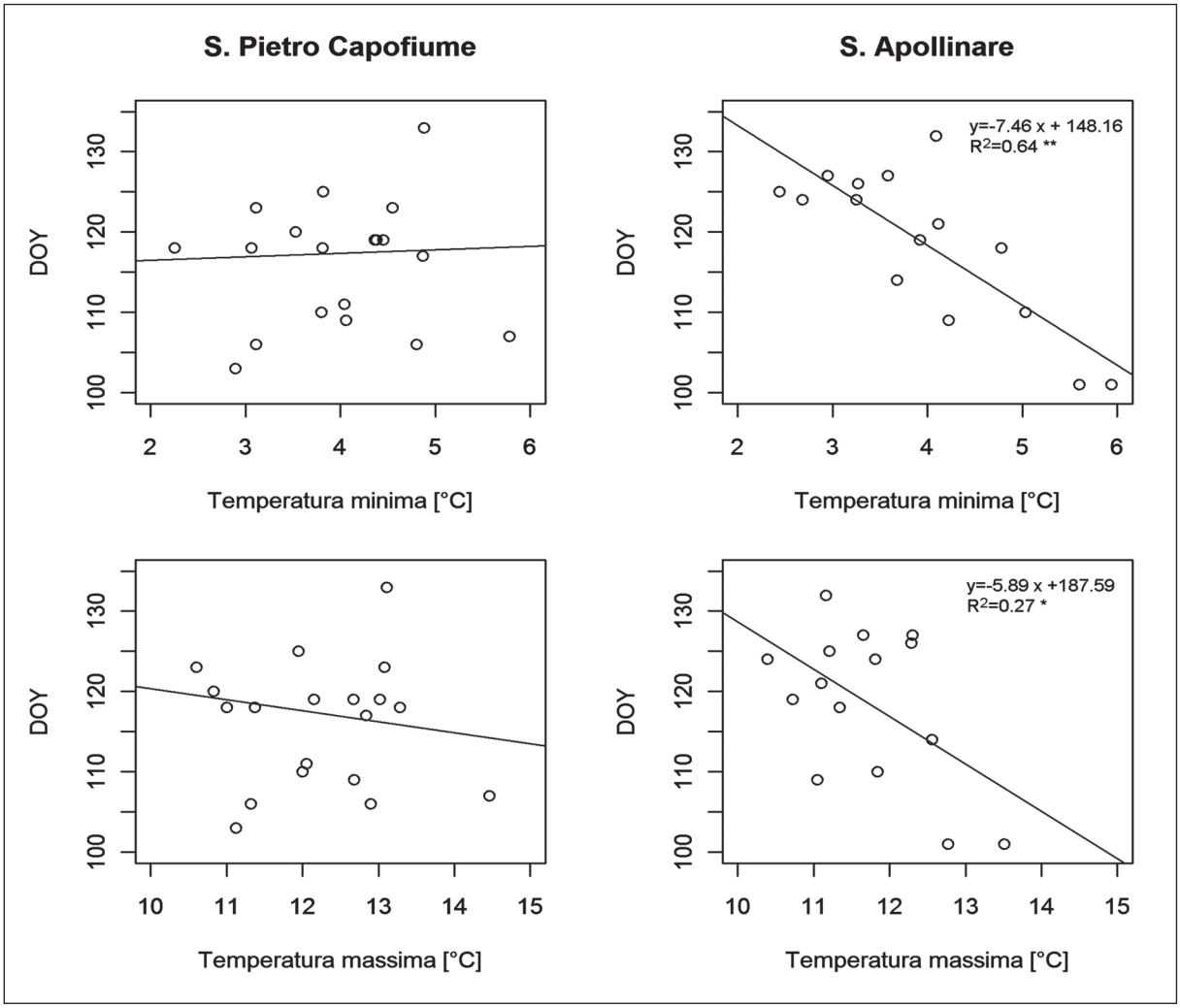

Fig. 2 - Correlazioni tra le date di inizio fioritura (BBCH61) (y) e i valori delle medie mensili del periodo (gennaio-aprile) delle temperature giornaliere minime (in alto) e massime (in basso). *p<0.05 ;**p<0.01.
*Fig. 2 - Correlations between the dates of the onset flowering (BBCH61) (y) and the values of the monthly average (January to April) of the daily minimum temperatures (top) and maximum (bottom). *p<0.05 ;**p<0.01.*

significatività (p<0.05). Tale stretta correlazione tra fioritura e temperature, per il sambuco era stata sottolineata da Orlandi *et al.* (2007). Per S. Pietro Capofiume, al contrario, queste correlazioni non sono significative. Il grafico di (Fig. 3) mostra, per gli anni 1997-2011, il confronto tra le date di fioritura osservate in campo e quelle simulate mediante il modello fenologico IPHEN implementato a scala nazionale nel SIAN. Come era stato già messo in evidenza con set di dati meno ampi da Alilla *et al*. (2012), dal confronto si denota un miglior accordo per quanto riguarda la simulazione della fenologia di S. Apollinare rispetto ai risultati di S. Pietro Capofiume, soprattutto per gli anni dal 2003 al 2006 in cui il modello sembra non rispettare l'andamento fenologico registrato in quelle stagioni e simula con netto ritardo le date di accadimento delle fasi. In Tab. 3 sono riportati i valori degli indici di valutazione del modello, calcolati per ciascuna fase fenologica. IL CRM sempre negativo indica che il modello sovrastima le date di fioritura rispetto all'osservato; l'efficienza del modello EF è sempre negativa nel sito di S. Pietro Capofiume e per la fase BBCH 67 di S. Apollinare: i valori di questo indice evidenziano quindi una ridotta prestazione da parte del modello, in particolare per S. Pietro Capofiume. Nel grafico di (Fig. 4) sono rappresentati i valori annuali di MAE [giorni] per ciascuna fase, calcolati in entrambi i GF, ed il valore medio (linea continua) indicato nella tabella riassuntiva (Tab. 3). Dal grafico si osserva un buon andamento dei valori di MAE sino al 2001, dopo di ché il MAE cresce, stabilendosi mediamente al di sopra di 10 e raggiungendo valori prossimi a 30 negli anni 2003-2006, precedentemente messi in risalto. Gli anni in que-

	MAE [d]			EF			CRM			MAE [d]	EF	CRM
	61	65	67	61	65	67	61	65	67	μ	μ	μ
S. Pietro Capofiume	10.9	11.9	9.7	-0.25	-0.22	-0.23	-0.09	-0.08	-0.06	10.8	-0.23	-0.08
S. Apollinare	6.4	9.3	6.7	0.38	0.04	-0.13	-0.04	-0.06	-0.03	7.5	0.10	-0.04

Tab. 3 - Valori degli indici di accuratezza del modello fenologico. μ= valore medio, d=giorni.
Tab. 3 - Accuracy Indices values of phenological model. μ= mean value, d=days.

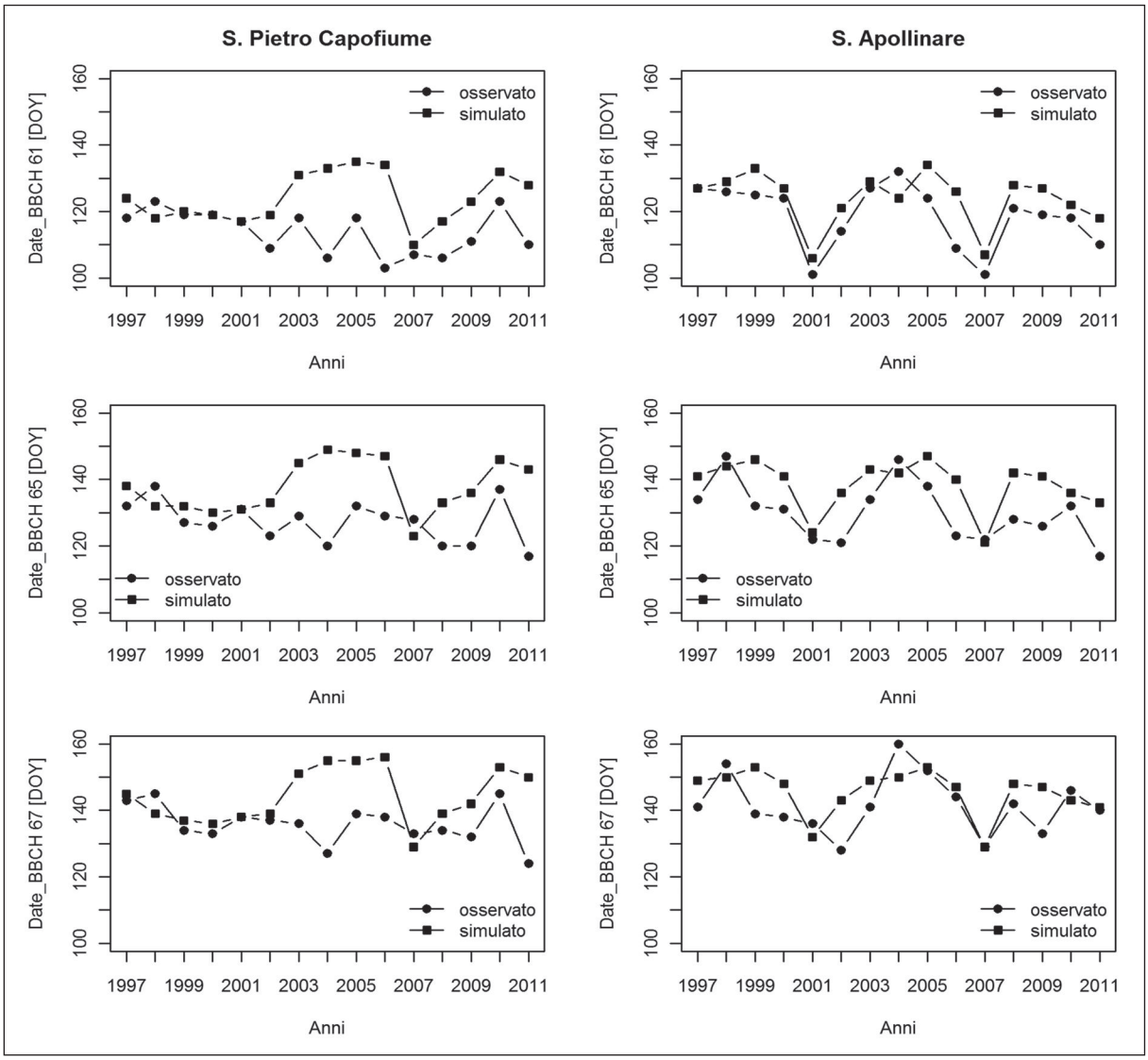

Fig. 3 - Confronto tra le date di fioritura osservate nei GF e quelle simulate mediante il modello fenologico per ciascuna fase. DOY= giorno dell'anno.
Fig. 3 - Comparison of flowering dates observed in the Gardens and those simulated by the model for each phenological stage. DOY= day of the year.

stione sono stati caratterizzati da temperature particolarmente elevate, e quindi da un anticipo delle fasi di fioritura; il modello, invece, in queste condizioni ha sorprendentemente stimato un ritardo nella comparsa delle fasi. Si è ipotizzato quindi che il modello non fosse riuscito ad accelerare l'accumulo di NHH a causa di cardinali termici, in particolare il massimo, troppo bassi. Sulla base di queste evidenze, si è pensato di verificare se le prestazioni del modello potessero migliorare effettuando una nuova calibrazione della curva beta, te-

stando combinazioni di cardinali termici più elevati e rispettivamente (cmin= 1, 2, 3 [°C]; copt= 20, 21, 22 [°C]; cmax= 32, 33, 34, 35 [°C]). La (Tab. 4) riporta i valori degli indici associati alla calibrazione; per brevità sono state elencate solo le combinazioni per cui i valori degli indici sono risultati migliori della combinazione originale (cmin=1, copt=20, cmax=32 [°C]; prima riga della tabella). Nonostante che per tutte le combinazioni l'efficienza (EF) del modello rimanga negativa ed esso sovrastimi comunque le date di fioritura rispetto all'osservato, la combinazione risultata ottimale è quella 1, 20, 34. Questa nuova combinazione è stata impiegata per validare nuovamente il modello nel GF di S. Pietro Capofiume per gli anni dal 1997- 2002 e 2007-2011 e nel giardino di S. Apollinare per il periodo 1997-2011; rispettivamente per 11 e 15 anni. I valori degli indici associati ai test di validazione sono riportati in Tab. 5. Si deduce che la combinazione di cardinali (1, 20, 34) risulta più efficace nella simulazione della fioritura del sambuco nei GF considerati. I valori del MAE medio, infatti, si riducono notevolmente: da 10.8 a 6.3[d] in S. Pietro Capofiume e da 7.5 a 5.8 [d] in S. Apollinare. Il modello simula con più accuratezza l'inizio della fioritura registrata nei due GF (con MAE rispettivamente

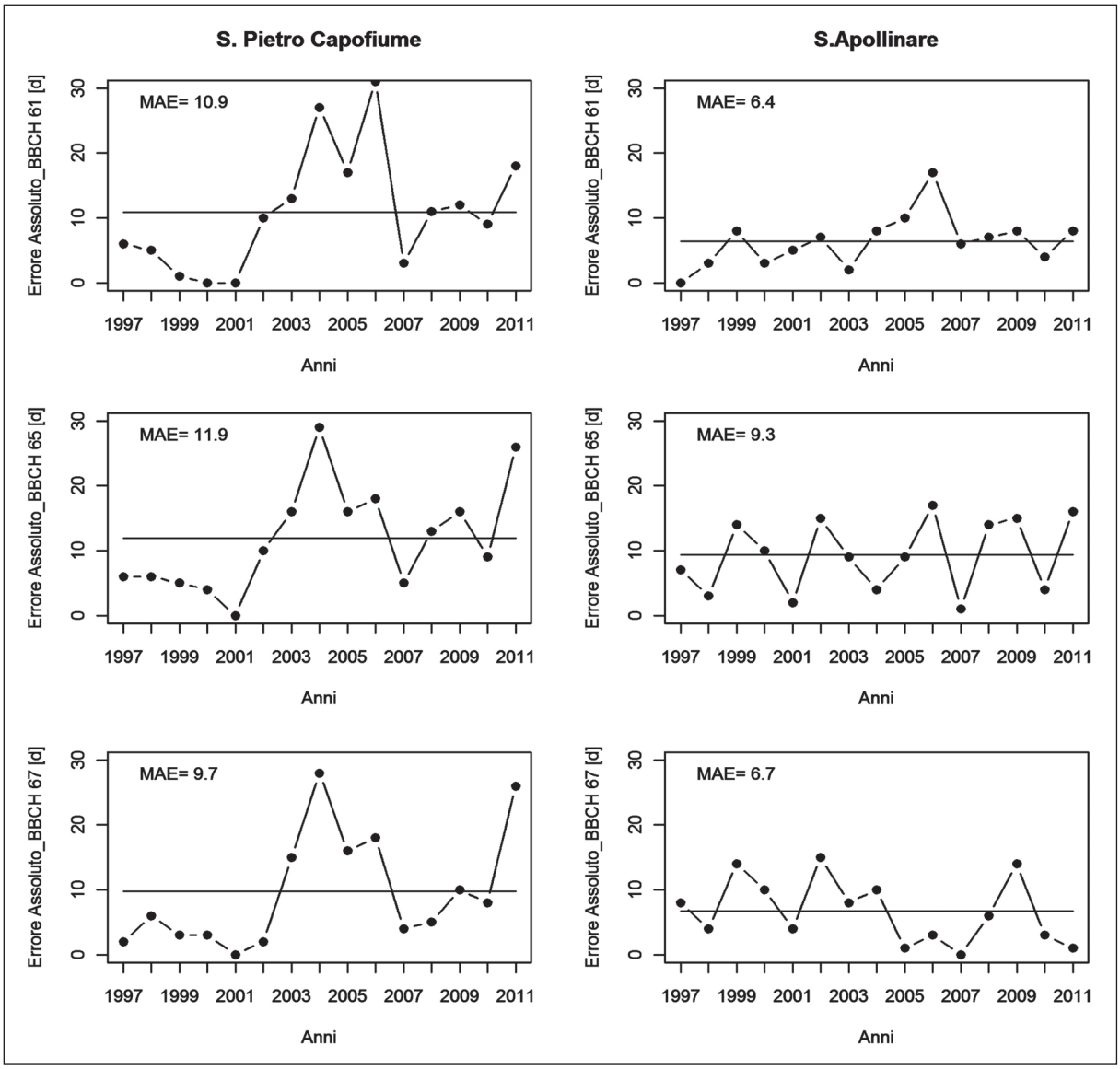

Fig. 4 - Errore assoluto [d] calcolato per ogni anno tra date simulate ed osservate di ciascuna fase. MAE = errore medio assoluto (linea continua) come indicato in (Tab. 3).
Fig. 4 - Absolute error [d] yearly calculated between simulated and observed dates for each stage. MAE = mean absolute error (solid line) as shown in (Tab. 3).

			MAE [d]			MAE [d]	EF	CRM
cmin [°C]	copt [°C]	cmax [°C]	61	65	67	μ	μ	μ
1	20	32	22.0	19:08	19.2	20.3	-0.08	-0.16
1	20	33	19.0	16:02	16.0	17.1	-0.10	-0.14
1	20	34	15.8	13:00	12.8	13.9	-0.13	-0.11
2	20	34	20.0	17:05	17.0	18.2	-0.10	-0.15

Tab. 4 - Valori degli indici di accuratezza calcolati per la calibrazione della curva beta. Cmin, copt, cmax= cardinale termico minimo, ottimale e massimo [°C]; μ= valore medio, d=giorni.
Tab.4 - Index of accuracy values calculated for the beta curve calibration. Cmin, copt, cmax= minimum, optimal and maximum cardinal temperature [°C]; μ= mean value, d=days.

	MAE [d]			MAE [d]	EF	CRM	
	61	65	67	μ	μ	μ	n
S. Pietro Capofiume	5.8	6.6	6.4	6.3	-0.62	0	11
S. Apollinare	4.2	6.3	7.0	5.8	0.15	0.01	15

Tab. 5 - Valori degli indici di accuratezza calcolati per la seconda validazione con la combinazione di cardinali termici della curva beta (1, 20, 34 [°C]); μ= valore medio, d=giorni, n= anni.
Tab. 5 - Index of accuracy values calculated for the second validation based on the cardinal temperature combination (1, 20, 34 [°C]). μ= mean value, d=days, n= years.

pari a 5.8 e 4.2 [d]), rispetto alle fasi successive. Indagini ulteriori saranno svolte per verificare le prestazioni del modello fenologico utilizzando come dati di ingresso le temperature misurate in stazioni meteorologiche prossime ai Giardini Fenologici.

CONCLUSIONI

Il sambuco è un valido indicatore della variabilità ambientale. In Germania, è stato documentato un significativo anticipo della fioritura del sambuco di circa 9 [giorni] nel periodo 1951-1999 ed in particolare di 14 [giorni] nel solo periodo 1984-1999 (Schaber and Badeck, 2005). In Italia, il segnale ricavabile dai dati esaminati non è così definito. Nel Giardino Fenologico più antico, S. Pietro Capofiume (BO), in cui si raccolgono dati fenologici dal 1990, l'anticipo è significativo sia per il sambuco, pari a 1.14 [giorni/anno] ($p<0.01$) per l'inizio della fioritura, 0.79 [giorni/anno] ($p<0.05$) per la piena fioritura e 0.68 [giorni/anno] ($p<0.05$) per la fine (Fig.1, Tab. 2), sia per altre specie (Villani *et al*., 2012). In S. Apollinare (PG), sebbene sia significativo l'anticipo delle fasi in relazione all'aumento delle temperature medie dei mesi che precedono la fioritura (Fig. 2) non si registra ad oggi una chiara tendenza fenologica negli anni, almeno sulla base della serie di dati raccolti dal 1997 al 2011 (Fig.1, Tab.2). Per quanto riguarda il modello fenologico IPHEN per il sambuco implementato nel SIAN, si deve concludere che non offra in quei siti l'accuratezza auspicabile (Fig. 3), considerando che i rilievi fenologici sono effettuati settimanalmente: la fioritura è simulata con una media di circa 11 giorni di scarto in S. Pietro Capofiume e con 7.5 giorni in S. Apollinare (Tab. 3). Il modello, almeno in questi siti, sovrastima i dati in campo (CRM<0) e non risulta sufficientemente accurato (MAE>7) ed efficiente (EF<0). Tale modello però è stato calibrato per simulare a scala nazionale la fenologia di questa specie, quindi per rappresentare condizioni ambientali molto diversificate dal punto di vista della latitudine e dell'altitudine. Il confronto dei risultati della simulazione con i dati rilevati a S. Pietro Capofiume ha evidenziato che negli anni (2003-2006) a fronte di un anticipo riscontrato nei dati rilevati, il modello ha stimato un ritardo nella comparsa delle fasi, con conseguente innalzamento dei valori di MAE (Fig. 4). Una nuova calibrazione (Tab. 4) effettuata su questi dati fenologici ha portato ad individuare una combinazione di cardinali termici che essenzialmente aumenta il cmax di 2 [°C] (da 32 a 34 [°C]), quindi consente di accumulare NHH a temperature maggiori di quanto non accada con la terna di cardinali (1, 20, 32). Questo spostamento verso temperature più elevate ha dato buoni risultati nella successiva validazione svolta su set di dati indipendenti. In particolare, in S. Pietro Capofiume negli 11 anni dal (1997-2002 e 2007-2011) il modello, così calibrato, ha restituito valori di MAE considerevolmente inferiori, passando da 10.8 a 5.8 [d]. Se un miglioramento del grado di accuratezza poteva essere ipotizzabile in S. Pietro Capofiume a causa dell'eliminazione di anni particolarmente critici, non era così scontato che la nuova combinazione di parametri fosse in grado di rappresentare con più efficacia anche le date di fioritura registrate in S. Apollinare (MAE medio da 7.5 [d] nella prima validazione, 5.8[d] nella seconda) (Tab. 5). I risultati confermano, ancora una volta, la necessità di disporre di serie storiche lunghe

di dati fenologici, (così come avviene per i dati meteorologici, per i quali il WMO raccomanda il calcolo delle normali climatiche su serie trentennali), affinché siano utili sia per analisi feno-climatiche sia per la calibrazione e la validazione di modelli. Inoltre si conferma che le annate che si discostano in maniera significativa dalla norma risultano estremamente utili per stressare i modelli e correggerne i limiti.

Pubblicazione della collana del Progetto Agroscenari, D.M. 8608/7303/2008 del 7.8.2008

BIBLIOGRAFIA

Alilla, R., Epifani, C., Dal Monte, G., 2012. Modelli e carte fenologiche nazionali: validazione del modello fenologico del sambuco. In Atti del XV Convegno Nazionale di Agrometeorologia, Palermo, 5-7 Giugno 2012. Italian Journal of Agrometeorology, Patron Ed. Bologna: 77-78.

Alilla, R., Epifani, C., Dal Monte, G., 2013. Italian phenological models and maps: the operational scheme. In Atti del Convegno "Agroscenari: agricoltori, politiche agricole e sistema della ricerca di fronte ai cambiamenti climatici", Ancona 1-2 Marzo 2012. Italian Journal of Agrometeorology, Patron Ed. Bologna: 59-60.

Aronne, G., Bonomi, C., Botarelli, L., Caterisano, R., Chiesura-Lorenzoni, F., Dal Monte, G., Menchetti, G., Puppi, G., Romano, B., Siniscalco, C., 2012. La rete dei Giardini Fenologici Italiani (GFI Network). In Atti del XV Convegno Nazionale di Agrometeorologia, Italian Journal of Agrometeorology, Patron Ed. Bologna: 63-64.

Beaubien, E.G., Freeland, H.J., 2000. Spring phenology trends in Alberta, Canada: links to ocean temperature. International Journal of Biometeorology, 44:53-59.

Chiesura Lorenzoni, F., 2002. Specie guida fenologicamente predittive del comportamento delle colture. In: Atti del convegno: Phenagri – Fenologia per l'agricoltura, 143-155.

Chmielewski, F.M., Rötzer, T., 2001. Response of tree phenology to climate change across Europe. Agricultural and Forest Meteorology, 108: 101-112.

Epifani, C., Alilla, R., Dal Monte, G., 2013. The Italian phenological database. In Atti del Convegno "Agroscenari: agricoltori, politiche agricole e sistema della ricerca di fronte ai cambiamenti climatici", Ancona 1-2 Marzo 2012. Italian Journal of Agrometeorology, Patron Ed. Bologna: 61-62.

Libertà, A., Girolamo, A., 1991. Geostatistical analysis of the average temperature fields in North Italy in the period 1961 to 1985. Séminaire CFSG sur la Géostatistique, Giugno 1989. Science de la Terre Sér. Inf. Nancy, 1-36.

Loague, K.M., Green, R.E., 1991. Statistical and graphical methods for evaluating solute transport models: overwiev and application. J. Contam. Hydrol., 7: 51-73.

Mariani, L., Alilla, R., Cola, G., Dal, Monte G., Epifani, C., Puppi, G., Failla, O., 2013. IPHEN - a real time network for phenological monitoring and modelling in Italy. International Journal of Biometeorology, DOI 10.1007/s00484-012-0615-x.

Meier, U., 2001. Growth stages of mono- and dicotyledonous plants. *BBCH*. Monograph, 2nd Edition. Federal Biological Research Centre of Agriculture, Germany.

Menzel, A., Fabian, P., 1999. Growing season extended in Europe. Nature, 397:659.

Menzel, A., Sparks, T.H., Estrella, N., Koch, E., Aasa, A., Ahas, R., Alm-Kubler, K., Bissolli, P., Braslavska, O., Briede, A., Chmielewski, F.M., Crepinsek, Z., Curnel, Y., Dahl, A., Defila, C., Donnelly, A., Filella, Y., Jatczak, K., Mage, F., Mestre, A., Nordli, O., Penuelas, J., Pirinen, P., Remisova, V., Scheifinger, H., Striz, M., Susnik, A., Van Vliet, A. J.H., Wielgolaski, F.-E., Zach, S., Zust, A., 2006. European phenological response to climate change matches the warming pattern. Global Change Biology, 12 (10): 1969-1976.

Miglietta, F., 1991. Simulation of wheat ontogenesis. II. Predicting dates of ear emergence and main stem final leaf number. Clim. Res., 1: 151-160.

Orlandi, F., Bonofiglio, T., Ruga, L., Sgromo, C., Sannipoli, V., Romano, B., Fornaciari, M., 2007. Phenological investigations of different winter-deciduous species growing under Mediterranean conditions. Ann. For. Sci., 64: 557-568.

Parton, W.J., Logan, J.A., 1981. A model for diurnal variation in soil and air temperature. Agric. Meteorol., 23: 205-216.

Porter, J. R. *et al.*, 1987. An analysis of morphological development stages in Avalon winter wheat crops with different sowing dates and at ten sites in England and Scotland. J. Agric. Sci. Camb. 109: 107-121.

Schaber, J., Badeck, F.W., 2005. Plant phenology in Germany over the 20th century. Regional Environmental Change, 5: 37-46.

Villani, G., Pratizzoli, W., Sacchetti, V., Botarelli, L., 2011. Analisi delle serie fenologiche delle specie del giardino di San Pietro Capofiume (Bologna). In Atti del XIV Convegno Nazionale di Agrometeorologia, Italian Journal of Agrometeorology, Bologna, 7-9 Giugno 2011. Patron Ed. Bologna: 135-136.

Wang, E., Engel, T., 1998. Simulation of phenological development of wheat crops. Agricultural systems, 58:1-24.

Walther, G.R., Post ,E., Convey, P., Menzel, A., Parmesan, C., Beebee, T.J.C., Fromentin, J.M., Hoegh-Guldberg, O., Bairlein, F., 2002. Ecological responses to recent climate change. Nature 416, 389-395